NOVEL TECHNIQUES FOR IMPROVED INDOOR POSITIONING AND LOCALIZATION USING HF RFID

By

Mohd Yazed Ahmad

A Thesis Submitted for the Degree of
Doctor of Philosophy

Faculty of Engineering & Information Technology,
University of Technology, Sydney
March 2013

CERTIFICATION

I certify that this thesis has not already been submitted for any degree and is not being submitted as part of candidature for any other degree.

I also certify that this thesis has been written by me and that any help that I have received in my research work, preparing this thesis, and all sources used, have been acknowledged in this thesis. In addition, I certify that all information sources and literature used are indicated in the thesis.

Signature of Candidate

----- -

(Mohd Yazed Ahmad)

DEDICATION

To my family members for their
patience and consistent support

ACKNOWLEDGEMENTS

ABSTRACT

This thesis investigates High Frequency Radio Frequency Identification (HF RFID) based positioning using a novel concept of multi-loop bridge reader antenna to localise moving objects such as autonomous wheelchairs in indoor environments. Typical HF RFIDs operate at 13.56 MHz and employ passive tags which are excited by the magnetic field radiated by the reader antenna. Positioning of moving objects using HF RFID systems derive location information by averaging the coordinates of detected passive floor tags by a portable reader antenna which are then recorded in the reader's memory and database. To successfully detect floor tags, the reader's antenna usually installed at the base of a moving object needs to be parallel to the floor. The magnetic field radiated by the HF RFID antenna is confined within its near field zone i.e., it is confined to a very close proximity of the antenna. This property of HF RFID helps to minimise interference to other appliances that may be present within the localisation area. Thus, HF RFID based positioning offers great potential benefit in providing location assistance in environments such as nursing homes, health care facilities, hospitals etc.

However, despite the significant developments that have occurred in this field, there still exist problems with positioning accuracies obtainable mainly due to the uncertainty of the reader recognition area (RRA) of the reader antenna, which has not been fully addressed in literature. This thesis aims to address this problem by proposing the concept of multi-loop bridge reader antenna so that the reader recognition area is divided into multiple sub zones and an error signal (bridge signal) in terms of the position of the tag will be generated that helps to reduce the position uncertainty.

The thesis starts with an investigation of the methods for creating multiple zones of RRA and the concept of bridge loop antenna from point of view of near magnetic fields. Different types of loop antennas for employing at the reader are electromagnetically analysed using both closed form solutions and numerical computations. The formation of reader recognition area (RRA) from different arrangements of loop reader antennas is also studied.

To ensure that proposed bridge antennas can perform in realistic, non-ideal indoor environments where they are affected by proximity of metallic objects etc, we proposed

methods of improvement. Equivalent circuits that reduce the computational complexity but can provide a broader understanding of the behaviour of bridge antennas have been formulated. This has lead to investigation of methods to minimise and/or eliminate the effect of metallic objects on the bridge signals.

Next, we investigate the applicability of the proposed bridge loop antenna for the localisation and positioning of an autonomous wheel chair resulting in a realistic implementation of HF RFID based positioning system. The system is then tested to localise an autonomous wheelchair in an indoor environment using a grid of passive floor tags. Novel algorithms are proposed to estimate the position and orientation of the moving object using bridge signals generated by the bridge antenna coupled with the available dynamic information of the wheelchair. A comparison of our experimental results with the published results in the literature revealed significant improvements achieved by our proposed methods over existing techniques for estimating both, the orientation and position. Further, we demonstrate that the proposed technique obtains accurate position and estimation using much lesser number of floor tags (increased sparcity) than any of the currently published method, thus, contributing to simplified and easily expandable tag infrastructure deployment.

We further extend the use of bridge loop antenna for situation when multiple tags are detected using the method of load modulation of the tags. When multiple tags present within the RRA of the bridge loop antenna, the resulting bridge signals incorporate information from all of the detected tags thus making it difficult to locate individual tags. To overcome this, we utilise states of the tag's load modulation to separate these bridge signals, which then allow us to utilise them to estimate instantaneous position and orientation of the moving object. We performed analysis using equivalent circuits, as well as computational electromagnetic modelling of realistic antennas, which are then compared with experimental measurements carried on prototype systems. The comparison showed good agreement which validate our proposed method.

Thus, the thesis incorporate contributions on various aspects of bridge loop reader antenna for HF RFID based positioning system. All full wave electromagnetic computations and simulations were carried by using a well known antenna design package "FEKO". All the key analyses, equivalent circuits, antenna models and

computational results for the proposed antennas and algorithms have been verified using extensive experimental campaigns to demonstrate the practical usefulness of the proposed methods. It is hoped that the findings in this thesis will result in newer efficient positioning systems in future.

Contents

List of Tables

List of Figures

List of Symbols

θ_β	θ_β is the angle between radial line r_β and the line along X_β-axis (see Figure 4-8)
θ_k	Heading of the object relative to the floor tags x-axis
ΔZ_m $m \in$ (Tag, Metal, Tag_Metal)	Change in impedance due to proximity of either or both tag and metal
C_{modul}	Capacitive load for modulation in a passive tag
d_{tag}	Inter tag separation distance
H	Magnetic field (A/m)
h_a	Separation between the plane of reader antenna and the plane of tag
h_m	Separation between the plane of reader antenna and the plane of metallic plate
Im(..)	Imaginary part
L	Length of the antenna
Loop-n $(n \in a, b, c, d)$	Notation for loop elements in a bridge antenna
M_{ij} $i \in (R,T,R',T')$ $j \in (R,T,R',T')$	Magnetic coupling between loop i and j R: reader loop, T: tag loop, R': image of reader loop, T': image of tag loop
P_a, $P_{c,d}$ and P_f	Points on the path of the object (PO_i) corresponding to the time flags of tag_i
Phs(..)	Phase component
POi	Path/trajectory of the moving object during the period of the presence of tag_i
Q	Quality factor
R_{modul}	Ohmic load for modulation in a passive tag
RRAn $n \in (1,2,3,4)$	Sub zones of RRA i.e. zone-1, 2, 3, or 4.
RRA-n $n \in (i, ii, iii)$	Type of reader recognition area, i.e. type-i, ii, or iii (see section 2.3)
S_{Rmodul}	Switch for load modulation of a tag
t_n $n \in (a, b, c, d, e, f)$	Time-Flag-of-Tag$_i$ a: when tag_i starts to appear in RRA1, b: tag_i in the middle of RRA1, c: RRA1 leaves tag_i, d: tag_i starts to apper in RRA2, e: tag_i in the middle of RRA2, f: RRA1 leaves tag_i
U_{Mij}	Potential due to magnetic coupling M_{ij}
V_β	Bridge potential signal i.e the potential signal between arm-1 and and-2
$V_{\beta1}$, $V_{\beta2}$	Signal at bridge arm-1, Signal at bridge arm-2
V_p	Voltage potential at a bridge source terminals (see Figure 3-14)

W	Width of the antenna
X_β, Y_β	X and Y axes cantered at a bridge antenna
$X_{(C\ or\ \beta)}$	The estimated position of the object carrying reader antenna C:conventional reader antenna, β: bridge reader antenna
X_{Cmodul}	Reactive impedance of capacitive load modulation
$Z_{n\ \ n\in\ (a,\ b,\ c,d)}$	Impedance of the loop elements in a bridge antenna
r_β	Radial distance between centre of RRA to the estimated tag position

List of Abbreviations

BP	Bridge potential
CW	Continuous wave
DBRLA	Dual bridge rectangular loop antenna
HF	High Frequency
IC	Integrated Circuit
MBRLA	Multi bridge rectangular loop antenna
MoM	Method of Moments
PC	Positioning Controller
RFID	Radio Frequency Identification Device
RRA	Reader Recognition Error
SBRLA	Single bridge rectangular loop antenna
SBTLA	Single bridge triangular loop antenna
TLB	Triangular Loop Bridge Reader Antenna

Chapter 1

Introduction and Overview

1.1 The importance of indoor positioning and localisation

Indoor positioning and localisation is useful in many new applications, which bring significant improvement to the quality of human life. The applications vary ranging from positioning of tagged items in manufacturing, and warehouses production, to the distribution and retailing, and more recently to the position and localisation to assist people with special needs such as elderly, disabled, etc. [1-7]. In all these applications, the key issue is to find the location and position of moving objects, vehicles or humans in indoor environments. The moving vehicles may range from service robots, autonomous vehicles such as wheelchairs, etc. Particularly for assisting and rehabilitation, these systems can provide new hope to people with special needs by allowing them to be independent in their day-to-day life activities. This area of study is becoming popular recently, driven mainly by the increasing demand as a result of increase in the number of elderly due to increased life expectancy worldwide as well as the genuine urge to use new developments in technologies for helping disabled people. The main driver behind these is the advancements in technologies such as in electronics, wireless communication, power devices, digital control, etc., where many interesting developments have occurred within the last decade. However, there are still many challenges that are faced in the adaptation of the technology for particular situations, which require further improvements. There is a large amount of published literature available in this area and the main focus of many of these reported studies is to realise a simple, cost effective and accurate indoor positioning and localisation system using wireless technologies [8-13].

There are many methods of independently obtaining location or position of a moving or static object. These can be classified by means of signal energy that is used for the measurement of position. Among the commonly used methods of positioning

and localisation include the use of mechanical rotation, ultrasound, radio frequency, infra-red, visual light, etc. Each of these categories can be further broken down into many sub categories depending on the methods of manipulating the signals that correspond to position of an object. Each method can offer certain advantages compared to the others and can suit certain applications better than the other. For use in assistive devices such as autonomous vehicles or wheelchairs, it is always desired to have a method that could offer a reasonable accuracy, reliable and easily operatable with low cost. One of the promising options is the use of radiofrequency wireless signals that employ electromagnetic waves. Generally a radio frequency (RF) based positioning system can offer accurate and reliable positioning accuracy. However, there many of radio frequency based positioning based positioning systems suffer from multipath propagation and affected by interference. So there is a need to explore radio frequency based technologies that do not suffer from multipath and can obtain the position information accurately.

In the category of RF based techniques, several technologies exist such as cellular communications, WLAN and WIFI (access points), Bluetooth, RFID, GPS, etc. GPS has become quite popular for outdoor applications, but it however fails in highly built-up areas or in indoor environments due to signal attenuation [14]. The RFID technology has gained much momentum recently for localisation and tracking, and it uses various frequency bands covering RF [15-17]. The low cost and ease of deployment is particular attractive for the use of the RFID technology for localisation especially for indoor environments. It has been reported that, the use of RFID technology can make possible for effective management of healthcare by minimising the common errors that can occur [7, 18, 19] which could save time, cost and resources. All these point towards advantages of employing RFID technology for health related applications.

With these advantages in mind, we mainly aim to investigate the use of RFID technology to obtain position information for locating and navigating autonomous vehicles such as wheelchairs in built-up indoor environments. We further note that due to its cost effectiveness and ease of system deployment, the RFID based localisation system can also be extended for outdoor environments.

1.2 Autonomous Wheelchair

Autonomous wheelchairs can offer a means to provide mobility to people with special needs. There exist various types of wheelchair systems, such as i) TAO Aicle Intelligent Wheelchair Robot [20], ii) the NavChair Assistive Wheelchair Navigation System [21], iii) the Hephaestus Smart Wheelchair System [22], etc. Most of these wheelchairs use multiple sensors to help localise themselves in various user environments. A typical autonomous wheelchair equipped with multiple sensors is illustrated in **Figure 1-1**.

THIS FIGURE IS EXCLUDED DUE TO COPY RIGHT

Figure 1-1: Typical autonomous wheelchair [20]

Typically employed sensors for positioning of autonomous wheelchairs/vehicles include GPS, Laser range sensor, visual camera, ultrasonic sensor, etc. Each of these sensors has limitations meaning that they may not be able to perform in all user environments. Recently, the use of RFID technology as means of obtaining position for localisation and positioning of autonomous wheelchairs/vehicles have become popular [12, 13, 20, 23-41]. The use of RFID helps to improve and overcome some of the limitations of the existing sensors. For positioning moving vehicles, HF RFID based systems offer advantageous solutions due to their relatively simple operation and lower cost.

1.3 RFID Technology

Radio frequency identification RFID is a non-contact type technology based on principles of radar and wireless communication that uses electromagnetic waves to transfer data from a reader to a tag. RFID system typically consist of two main parts: i) the transponder typically known as tag, and ii) the interrogator, also known as reader. Usually, tags/transponders are attached/embedded to objects for the purpose of identification and tracking, with reader/interrogator sends the probing signals. In general, the transponder can be either active or passive. Active tags have their own power source, while passive tags do not require their own power source, which derive their excitation energy from the radiated/induced electromagnetic fields emanated from the reader antenna. Hence, passive tags are more popular and lower in cost mainly because no batteries are needed within the tags. Further, without the need of a battery, passive tags can be made much more compact, thinner and flexible which contribute to its durability, therefore they are used in various environments including as floor tags.

RFID technology can be categorised based on its frequency band of operation, which are: i) Low frequency (LF) RFID, ii) High frequency (HF) RFID, iii) Ultra high frequency (UHF) RFID, and iv) Ultra wideband (UWB) RFID. The frequency bands that are typically used by RFID technology is illustrated in **Figure 1-2**.

THIS FIGURE IS EXCLUDED DUE TO COPY RIGHT

Figure 1-2: Frequency bands for typical RFID [42]

At lower frequency bands, viz., LF and HF, inductive coupling method is typically utilised as means of communication, while at higher frequency starting from UHF,

radiative coupling is generally used. From the point of view of indoor localisation, inductive coupling, especially for HF RFID, can offer relatively better localisation accuracy achievable with much lower interference to the surrounding objects [43]. The main reason is that, this technology uses magnetic field, which is confined to areas closer to the reader antenna, and when a tag is placed within its close proximity to the reader antenna, it gets detected. These aspects, along with simple methods to deploy and operate as compared with other RFIDs, make HF RFID more popular for use in the localisation of most autonomous moving vehicles/robots in indoor environments [8, 10-13, 20, 23, 44]. In addition, HF RFID has also gone through many significant technological improvements [45-50].

Working principle of a typical HF RFID system that uses inductive coupling can be described by considering schematic diagram as shown below.

THIS FIGURE IS EXCLUDED DUE TO COPY RIGHT

Figure 1-3: Inductive coupling with load modulation [51]

Inductive coupling in HF RFID system is similar to the magnetic field induction in a transformer. Both the reader and tag antennas employ loop coil antennas which act analogous to primary and secondary coils of a transformer respectively. Both the loop antennas are tuned to resonate at the operating frequency of 13.56 MHz. When an alternating current flows in the reader antenna, it induces magnetic field 'H', to the tag antenna from which it receives signals. In other words, the tag receives energy from the reader by means of transformer action and the magnetic energy gets attenuated quickly as tag moves away from reader antenna. Message can be sent from the reader to the tag by varying the magnitude of the current in the reader coil to correspond to the particular message to be transferred. The message is relayed to the tags through the induced magnetic field from the reader coil.

The reader receives information from the tag by letting steady alternating current in its coil so that steady alternating magnetic field is induced near its coil. When a tag is coupled within this field, information can be transferred to the reader by varying the impedance using tag's load modulation in such a way that any slight variation occurring in the net magnetic fields will then be relayed to the reader through the appropriate changes in the induced current. The resulting changes in impedance due to switching sequence in the tag's load modulation is therefore detectable by the reader in the form of variation of the induced current in its loop antenna. Hence, information can be transferred from the tag by varying the switching sequence in the tag. This is how tag's load modulation works in the HF RFID[51].

Types of modulation techniques and protocols for sending and receiving information, to and from a reader and a tag are generally specified by an international standard. This is important to ensure that both readers and tags are compatible even if they are manufactured by different manufacturers. Typical standards used for HF RFID are ISO14443 Type-A/Type-B and ISO15693 [31, 32] as indicated in the **Figure 1-4**. The figure also indicates the key protocols as well as the illustration of the signals from reader to tag, and from tag to reader.

THIS FIGURE IS EXCLUDED DUE TO COPY RIGHT

Figure 1-4: Standards and the key protocols used with HF RFID [52]

In this thesis, we utilise the most commonly employed standard ISO15693.

1.4 RFID for positioning

Traditional positioning methods use dead reckoning systems in which the measurement data is obtained either from wheel encoders or inertial measurement units [53, 54]. However, for moving objects, the dead reckoning technique accumulates errors over the distance travelled which results in deterioration of the estimation of position and orientation [55, 56]. Limitations of dead reckoning systems are typically compensated by using information from additional sensors such as cameras, ultrasonic sensors, lasers, etc. [23, 57, 58]. However, in some situations the deployment of sensors can be constrained due to special requirements such as line of sight, higher illumination levels etc., which may be difficult to ensure in all the user environments [59, 60]. In addition, use of additional sensors may also lead to increases in the complexity of positioning algorithms.

Processing Controller   RFID Reader   Reader Antenna   Passive tags
& RFID Database

Carried by the vehicle/moving object   Deploy as floor tags

(a)
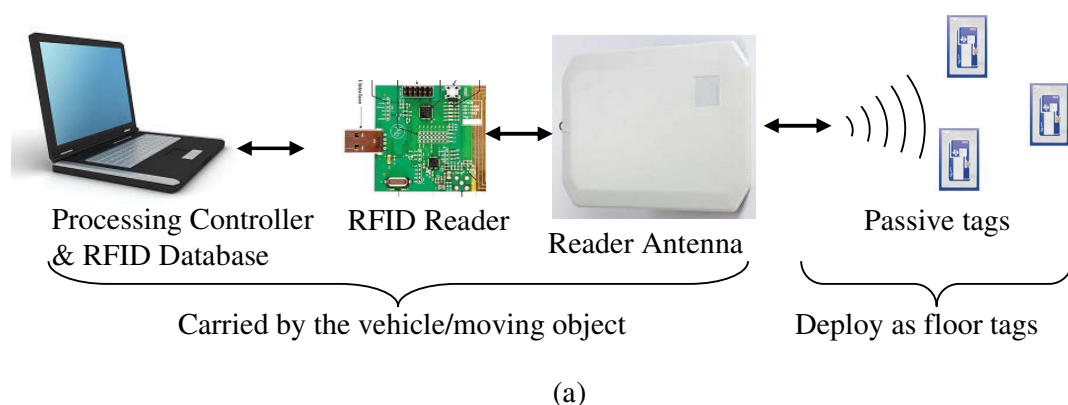
THIESE FIGURES ARE EXCLUDED DUE TO COPY RIGHT

(b)   (c)

Figure 1-5: HF RFID for positioning

    (a) Key components of HF RFID system

    (b) A vehicle carrying the reader moving on a floor tags [11]

    (c) Reader recognition area on the floor tags [23]

1.4.1 Why HF RFID?

The radio-frequency identification (RFID) technology can potentially offer simple, cost-effective and reliable means for localisation, positioning and tracking of autonomous moving vehicles such as wheelchairs, robots etc., [12, 26, 61-63]. Typical RFID system for positioning of moving vehicles is illustrated in Figure 1-5. For such applications, the HF RFID can offer relatively better accuracy due to utilisation of near magnetic fields, which are confined to the close proximity of reader's loop antenna, and requires that tags be located in its close proximity. Since the fields are confined to relatively smaller areas, less interference will caused to any other sensitive devices that may be present in the user environments, thus making it suitable to be used in any environment such as healthcare facilities, hospitals, nursing homes, etc. Also, since the frequency used by HF RFID is only 13.56MHz, its signals can penetrate through environments that can be highly humid, wet etc. [64, 65]. The above mentioned benefits of HF RFID have led us to consider it for the applications considered in this thesis.

Key components of a typical HF RFID based system for positioning a moving object is indicated in Figure 1-5. Such positioning system utilises tags placed on floors on which the reader moves with its antenna usually fixed to the base of the moving object. The area underneath the antenna having sufficient level of magnetic field to interrogate tags is known as reader recognition area (RRA), marked with dotted circular line (see Figure 1-5 (c)). The Processing Controller (PC) containing "RFID database" records the information of all tags, and as soon as the tags fall within the reader recognition area, the reader detects the tags and their positions are retrieved from the RFID database. The Unknown position of the object is calculated with respect to the retrieved coordinates of the detected tag(s).

1.5 Limitations of Existing Methods With HF RFID Localisation

In spite of ample available research on the use of HF RFID for localisation of autonomous moving vehicles, there however, are still some limitations that require improvement. The main problem that remains fully unsolved is the uncertainty that results in reader recognition area (RRA) [12, 13, 23]. Whenever a tag is present within

RRA, the system cannot deduce the exact location of the detected tag, thus the position estimation of the moving object has uncertainty as illustrated in **Figure 1-6**. Referring to the **Figure 1-6**, the estimated position of the reader antenna can vary at an instant when it detects tagA. Since the reader antenna is fixed to a moving object, the estimated position of the object can also vary viz., either at P, Q, R, or S, thus contributing to the positioning uncertainty.

Most of HF RFID based positioning system attempt to overcome this problem through indirect methods, that is, either by increasing the tag density or the arrangement of tags on the floor [11, 66-69], or utilisation of motion dynamics of a moving object [11, 13, 25], use of multiple reader antennas with multiple readers [70], or use of additional sensors [20, 23], etc. However, these indirect methods cannot fully reduce the uncertainties.

THIS FIGURE IS EXCLUDED DUE TO COPY RIGHT

Figure 1-6: Uncertainty in reader recognition area [12]

In view of the significance of HF RFID positioning system, in this thesis, we describe methods to reduce uncertainty of reader recognition area by proposing a novel bridge loop reader antenna. The proposed bridge reader antenna can generate a bridge potential signal (also known as error signal) as a function of the position of the floor tags with respect to the boundaries of its reader recognition area (RRA). Thus, the extra information in the form of error signal helps to reduce uncertainty of reader recognition area.

1.6 Current Issues and challenges

1.6.1 Uncertainty within reader recognition area

The main issue associated with HF RFID based localisation is the uncertainty due to reader recognition area (RRA). A thorough literature search shows that, methods to overcome this limitation are not fully investigated. In this thesis, we investigate novel approaches to directly overcome this limitation using the concept of bridge potential signals.

1.6.2 High tag density

Use of higher tag density on the floors are typically employed to reduce position uncertainty. However, increasing the tag density can increase the infrastructure cost etc. This can be avoided if the system is capable of obtaining accurate position estimation even with sparsely placed floor tags. In this thesis, we offer methods to obtain position and orientation of objects with sparsely placed floor tags which require much lesser number of tags and thus simplifying the infrastructure and installation.

1.6.3 Metallic environment

Reader antenna is placed at the base of a moving object to face the floor tags that are typically installed on the floor. The presence of metallic objects from the structure of the moving object as well as the metallic rods placed inside concrete floors etc may potentially create interference to the performance of the induced magnetic fields from the reader antenna. We investigate methods to minimise the effect of metallic objects on bridge potential signal.

1.6.4 Localisation in the absence of RFID data

When RFID is used for localisation, the information from RFID reader [16, 17] is crucial. This is obtained through reader(s)-tag interrogation. However, due to some reasons at some locations when tags are not present the position and location of the reader may be unknown. In such a scenario, other ways of obtaining position information is required in order to keep track the object thus helps navigation. We will investigate as to how the object dynamics can be obtained from readily available wheel encoder that can be utilised along with recent RFID measurements to obtain position as well as orientation of an autonomously moving object.

1.6.5 Instantaneous position and orientation

In certain scenarios, it is important to obtain instantaneous position and orientation that is derived solely from RFID information. We propose a technique based on tag's load modulation to achieve this.

1.7 Aims and Objectives:

The aim of this study is to develop methods of improving localisation in indoor environments using HF RFID based system to localise and navigate autonomously moving object such as an autonomous wheelchair etc in indoor environments. To achieve this aim, we focus on the following objectives:

i. Investigate a novel technique to manipulate reader recognition are (RRA) of HF RFID reader antenna to reduce uncertainty typically faced by HF RFID based positioning system.

ii. To investigate novel HF RFID reader antenna capable of providing signal useful to improve the positioning accuracy with reduced floor tag density leading to simple infrastructure.

iii. To investigate techniques to increase reliability and minimise interference due to proximity of metallic objects on the proposed reader antenna, so it can be useful in any general indoor environments.

iv. To develop positioning algorithm that utilises signal from the proposed reader antenna, so that it improves the position and orientation estimations.

v. To further improve the positioning algorithm by using the states of tag's load modulation, to allow estimation of the instantaneous position and orientation of a moving object.

vi. Validate the proposed concepts, computational analyses, antenna models, and algorithms through series of experimentations.

1.8 Brief description of methodology

We propose methods of generating multiple RRA zones to reduce uncertainty on the location of the detected tag with respect to the reader antenna. We achieve the RRA separation by using the concept of bridge loop antenna that uses multiple loop antenna elements arranged in such a way it can provide bridge potential (error signal) as the function of tag position with respect to the antenna. Analysis due to interference of metallic object is then performed to ensure the proposed concept of bridge antenna will be able to perform within metallic environments making it more realistic. Equivalent circuits are formulated to assist with analyses which then conformed by realistic electromagnetic simulations and later, measurements made on designed prototypes. An overall, practical HF RFID based positioning system is then described that uses novel algorithms for the estimation of position and orientation of a moving vehicle. This system and the algorithms are investigated using experimental prototype to localise an autonomous wheelchair with sparsely placed floor tags. The performance of the proposed system is compared with data derived from recent published literature. The above system and the algorithm are further improved by investigating the use of tag's load modulation so that the system is able to provide instantaneous position information when multiple tags are present. In addition, novel algorithms capable to estimate position and orientation instantaneously solely with HF RFID data when multiple tags are detected is proposed. All the proposed techniques are verified using measurements from designed prototypes and full wave electromagnetic simulations.

1.9 Organisation of this thesis

This thesis presents techniques to improve indoor positioning and localisation using HF RFID. This thesis is organised as follows:

Chapter 1: This chapter introduces motivations and briefly reviews the current state of the art to highlight the potential gaps in knowledge, the associated problems and the shortcomings in the current literature. It then lists the aims and objective of this thesis, and then briefly describes the methodology and the organisation of this thesis.

Chapter2: The concept of bridge antenna is introduced in this chapter. This chapter starts with defining the reader recognition area (RRA), and presents methods of characterising it and then explains as to how uncertainty can be reduced through manipulation of the RRA using the concept of bridge antenna. The rest of the chapter then describes the design and the performance of various types of bridge antennas. Measurements that are performed on a bridge antenna prototype are reported to validate the predicted results.

Chapter3: This chapter first describes the effects of proximity of metallic objects on the performance of the bridge antenna. To analyse the effects, approximate equivalent circuits are introduced that can help with characterising the behaviour of the bridge signals due to the interference from metallic objects. The analysis initially uses simplified models, but later obtains accurate prediction using full wave electromagnetic modelling. Methods to minimise the effects of the metallic object interferences are then proposed. The proposed techniques are validated using realistic electromagnetic simulation models as well as experiments on prototypes.

Chapter4: This chapter describes HF RFID based positioning system using the proposed concept of bridge antenna. It proposes location and orientation algorithms which use information from bridge antenna along with the available wheel encoder from the vehicle. The algorithms are tested to localise an autonomous vehicle in indoor environments. Performance for location and orientation estimations between the systems using a conventional antenna and the one with a bridge antenna are then compared. The performance comparisons over the existing methods reported in recent literature are also included.

Chapter5: This chapter extends the propose HF RFID based positioning system to effectively utilise the bridge signal when multi tags are detected. The equivalent circuit proposed in chapter-3 is modified to analyse the effect of tag's load modulation. Technique to separate the bridge signal is then presented. Algorithm to estimate position and orientation using the bridge signals from multiple tags are then proposed. Experimentation is included to verify the techniques to separate the bridge signal.

Chapter6: This chapter summarises the overall chapter, highlight the key contributions, indicate the potential future research and then conclude the thesis

1.10 Publications resulted from this thesis

Peer reviewed publications resulted from this thesis are listed below

Academic journals:

[1]   M. Ahmad and A. Sanagavarapu, "Novel Bridge-Loop Reader for Positioning with HF RFID under Sparse Tag Grid," *IEEE Transactions on Industrial Electronics,* 2013. (Future Issue)

[2]   M. Y. Ahmad and A. S. Mohan, "Multiple-bridge-loop reader antenna for improved positioning and localisation," *Electronics Letters,* vol. 48, pp. 979-980, Aug. 2012.

Conferences:

[3]   M. Y. Ahmad and A. S. Mohan, "Multi-Loop-Bridge Antenna for Improved Positioning Using HF-RFID," in *IEEE Int. Sym. on Antennas and Propag USNC-URSI*, Chicago, Illinois, 2012. pp. 1-2

[4]   M. Y. Ahmad and A. S. Mohan, "Multi-loop Bridge HF RFID Reader Antenna for Improved Positioning," in *Asia Pacific Microwave Conference*, Melbourne, 2011, pp. 1426-1429.

[5]   M. Y. Ahmad and A. S. Mohan, "Techniques to Improve RFID Reader Localisation for Indoor Navigation," *Asia Pacific Symposium of Applied Electromagnetics and Mechanics*, 2010.

[6]   M. Y. Ahmad and A. S. Mohan, "RFID reader localization using passive RFID tags," in *Asia Pacific Microwave Conference*, Singapore, 2009, pp. 606-609.

Chapter 2

The Bridge Loop Reader Antenna for HF RFID

2.1 Introduction

Reader antenna acts like a transducer that converts electrical signals from the reader into electromagnetic fields that are radiated into surrounding space so that passive tags is energised to respond to the reader. In the case of HF RFID Reader, mostly loop antennas are used. The loops radiate magnetic fields, which are usually confined to areas close to the reader antennas. The region at which the level of magnetic fields radiated by a reader antenna is sufficiently large to be able to energise tags located within its proximity is denoted as the reader recognition area (RRA). The dimension of the RRA depends directly on the strength of the near magnetic fields radiated by the reader loop antenna, and the sensitivity of the tag. The use of conventional loop reader antennas can only detect the presence of a tag which lies anywhere within the RRA. The uncertainty may also increase with the increase size of RRA [8, 12, 13]. To overcome this, denser tags are typically used [9, 11]. Other approaches such as the use of multiple readers [70], additional sensors [23] and host of other alternatives [11-13, 71, 72] have also been proposed. In this thesis, we propose a bridge signal concept using loop antennas to overcome the uncertainties due to RRA. The proposed approach splits the RRA into sub zones that are identifiable using the polarity of the bridge signal. The location can be further refined by monitoring the changes within bridge signal which are directly correlate-able to the change in the position of tag.

This chapter introduces the concept of the Bridge-loop antenna and derives all the necessary design parameters under ideal environment. We start with an electromagnetic modelling and simulation to investigate the behaviour of magnetic fields, RRA and bridge potential and later validate them using experimental prototype of bridge antennas. Later, many more simulation models and experimental prototypes of bridge antennas are presented to parameterize their performance (i.e. magnetic fields and

bridge signals). The advantages of the proposed method are highlighted. It will be demonstrated that the proposed method is not only offering a novel way of improving positioning accuracy, but also reduce the density of tags for indoor positioning system, using HF RFID.

Our contributions in this chapter include: i.) Characterisation of different shapes of loop antennas to investigate their corresponding RRAs so as to choose the appropriate shape for current application; ii) Methods of selection of size and shape of RRA depending on the desired level uncertainty allowable in any HF RFID based positioning system; iii) Manipulation of RRA by establishing multiple zone RRAs to further reducing uncertainties; iv) Introduce the concept of novel bridge antenna in order to achieve multiple zone RRAs; v) Investigate the different types of bridge antennas; and vi) Both simulation and experimental results are presented to validate and demonstrate the usefulness of the proposed concepts.

This chapter is organised as follows: section 2.2 describes closed form expression for magnetic fields induced from a reader loop antennas for the purpose of comparison with simulation. In section 2.3 the definition and characterisation of RRAs for different types of loop antennas are included, while section 2.4 presents methods to manipulate the RRA to reduce uncertainties. The concept of bridge antenna is then introduced in the section 2.5. and a practical version of bridge antenna is introduced. In section 2.6, different types of bridge antennas are proposed whereas in section 2.7 simulation and experimental setup are described to evaluate the performance of the proposed bridge antennas. Results are then provided in section 2.8, and finally, in section 2.9 the work presented in this chapter is summarised.

2.2 Magnetic fields of a loop antenna

Loop antenna is the basic antenna element of a reader antenna for HF RFID. All HF frequencies loop antennas have many advantages over other types of antennas mainly for application involving magnetic fields. Here we will examine magnetic fields produced by a standard circular loop antenna at close-in distance. This is an essential parameter that will be used to explain concepts and variables in the later sections, and will also be utilised to validate the results obtained from electromagnetic simulations.

Consider an electrically small metallic loop located using a standard coordinate system as depicted in **Figure 2-1**. The source point and the field/observation point are denoted using spherical coordinates as (r' = a, θ' = π/2 , φ') and (r, θ, φ) respectively. We use prime to indicate parameters associated with the source point. The circumference 'S' of the loop is considered to be smaller than one-tenth of wavelength i.e. S <λ/10. Under such a condition, the current 'I(φ)' throughout the loop can be considered constant [73]. We denote the constant current as I_0. The resulting magnetic fields (H-fields) due to a constant current I_0 flowing in such a loop are well known and are derived elsewhere in the literatures [74, 75]. However, we briefly present the analysis here mainly with an aim to obtain magnetic fields at distances very close to the loop. The H-fields radiated by the loop anywhere can be written as [76],
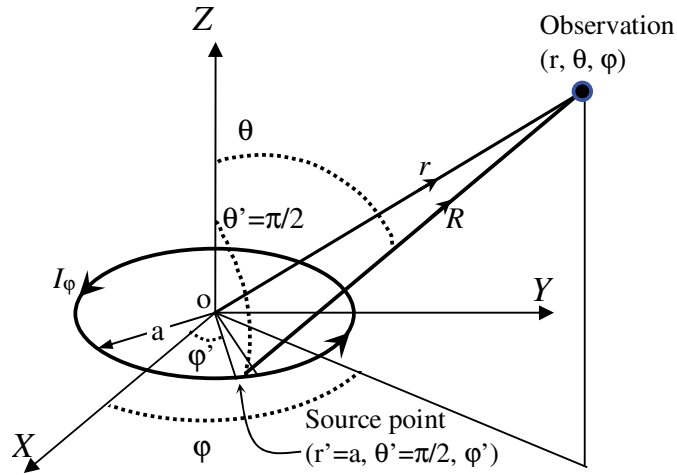
Figure 2-1 Geometry of a loop antenna

$$\mathbf{H} = \iiint_V \nabla \times \overline{\mathbf{G}}_{EJ0}(r,r')\mathbf{J}(r')dV'. \qquad (2.1)$$

Where $\overline{\mathbf{G}}_{EJ0}(r,r')$ is the dyadic Green's function [76, 77], and the term *J(r')* is a volumetric current density on the loop. Considering electrically small loop, thus constant current ($I_\varphi = I_0$), and following the procedure described in [76], the magnetic field produced by the loop can be derived using dyadic Green's function in spherical harmonics as

$$\begin{bmatrix} H_r^> \\ H_r^< \end{bmatrix} = \frac{ik_0^2 a I_0}{2} \sum_{n=1}^{\infty} (2n-1)\frac{dP_n(0)}{d\theta}P_n(\cos\theta)\frac{1}{k_0 r}\begin{bmatrix} h_n^{(1)}(k_0 r)j_n(k_0 a) \\ h_n^{(1)}(k_0 a)j_n(k_0 r) \end{bmatrix}, \qquad (2.2a)$$

$$\begin{bmatrix} H_\theta^> \\ H_\theta^< \end{bmatrix} = \frac{ik_0^2 a I_0}{2} \sum_{n=1}^{\infty} \frac{(2n+1)}{n(n+1)} \frac{dP_n(0)}{d\theta} \frac{dP_n(\cos\theta)}{d\theta} \frac{1}{r} \begin{bmatrix} \dfrac{d[rh_n^{(1)}(k_0 r)]}{d_0 dr} j_n(k_0 a) \\ \dfrac{d[jn(k_0 r)]}{k_0 dr} h_n^{(1)}(k_0 a) \end{bmatrix}, \quad (2.2b)$$

$$\begin{bmatrix} H_\varphi^> \\ H_\varphi^< \end{bmatrix} = 0. \quad (2.2c)$$

The term $h_n^{(1)}(..)$ and $j_n(..)$ in (2.2) are the spherical Hankel and spherical Bessel functions of the first kind. The term $P_n(\cos\theta)$ is the associated Legendre function. The notation '>' and '<' in the above expressions represent the fields evaluated in the region r > a, and r < a respectively. As for the region 'r = a', the fields are obtained through interpolation using values near the region.

For r>>a, and considering observation along r with θ=0, and retaining only the first term in the summation (2.2) i.e. n=1, it can be shown that the above formulas reduce to the well known far field expression given below in (2.3). It demonstrates that the use of the first term n=1 is sufficient enough when evaluating fields far away from the antenna (r>>a) because of the contribution of higher order terms at this region is almost negligible [78].

$$H_r^> = \frac{ia^2 I_0}{2r^3} \quad (2.3)$$

The expressions in (2.2 a-c) are exact closed form solutions which are obtained analytically. Closed form solutions are usually desirable for loops having regular shapes viz., circular loops etc. For loops having arbitrary shapes, currents can be derived using method of moments (MoM) [73]. MoM uses integral equation formulation of Maxwell's equations to obtain currents and fields of any antenna [73]. In view of this, we use the commercially available MoM package "FEKO" [79, 80] to perform numerical modelling and simulation of antennas and fields in this thesis [76, 81-83].
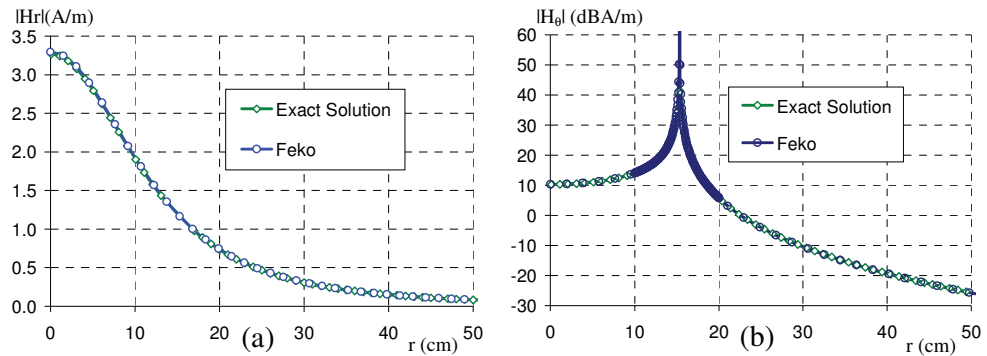
Figure 2-2: The H-fields of the loop antenna over observation distance
(a) H_r with $\theta = 0°$, and (b) H_θ with $\theta = 90°$

The magnetic fields are first computed using closed form expression of (2.2 a-b) assuming I_0=1Ampere are plotted in **Figure 2-2** (a-b). For the sake of comparison, the corresponding field components are also computed using FEKO and they are plotted in the same figures. The close agreement between closed form results and FEKO results serve to validate the computational results obtained by FEKO.

The results in **Figure 2-2** (a-b) indicate that magnetic fields produced by a loop antenna decay rapidly with distance. Results obtained using FEKO are in a good agreement with exact results obtained using 2.2(a-b). The advantage of FEKO simulation tool is that it allows arbitrary shaped loops as well as any scatterers and obstructions to be modelled accurately for which deriving closed form expressions can be extremely difficult. Since we have validated the FEKO results with closed form exact results, we will henceforth use FEKO for the design and analyse loops of different shapes and sizes in this thesis.

2.3 Reader recognition area (RRA)

2.3.1 Definition

Reader recognition area (RRA) can be defined as the region within which the level of magnetic fields produced by the reader antenna is sufficiently large to be able to interrogate tags. To define RRA, let us assume that the tags are located on a floor whose plane is parallel to the plane of the reader loop antenna as illustrated in **Figure 2-3**. Under such conditions, the z-component of magnetic field (H_z) radiated by the loop significantly contributes to energise the floor tags. Generally, the tag antennas are much smaller than the reader antenna. The reader recognition area (RRA) can be determined

by examining the magnitude of H_z throughout the plane where tags are located (tag plane) to determine whether it is higher than a given threshold value usually specified by the manufacturer of the floor tags.
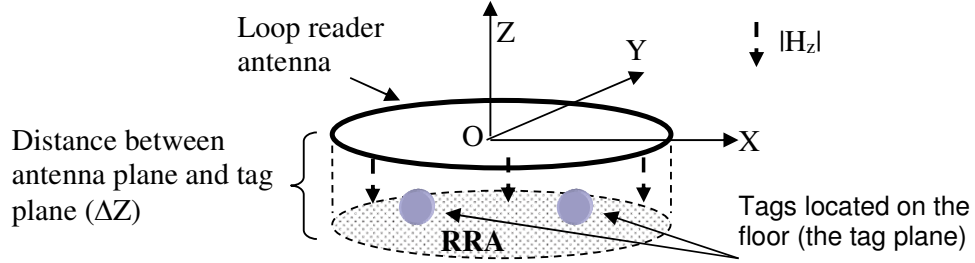
Figure 2-3: Illustration of RRA for typical HF RFID reader antenna

To understand how RRA is related to the parameter/geometry of the reader antenna, we will examine the RRA using magnetic fields produced by a loop antenna as explained previously in section 2.2. The expressions for magnetic fields given in (2.2 a-c) are derived using spherical coordinates. The corresponding values of magnetic fields in Cartesian coordinates can be obtained by using the following spherical to Cartesian coordinate transformation:

$$\begin{bmatrix} A_x \\ A_y \\ A_z \end{bmatrix} = \begin{bmatrix} \sin\theta\cos\varphi & \cos\theta\cos\varphi & -\sin\varphi \\ \sin\theta\sin\varphi & \cos\theta\sin\varphi & \cos\varphi \\ \cos\theta & -\sin\theta & 0 \end{bmatrix} \begin{bmatrix} A_r \\ A_\theta \\ A_\varphi \end{bmatrix} \qquad (2.4)$$

The Z-component of magnetic fields i.e. Hz is obtained by applying the above transformation, given by

$$H_z = H_r cos\theta - H_\theta \sin\theta , \qquad (2.5)$$

which helps to obtain, the magnetic fields induced on the tag plane. Assume that the tag plane is located at a plane 5cm below the plane of loop antenna. The H-field on this plane along x-axis is computed using (2.5) and result is plotted in **Figure 2-4** (a). We have also obtained H_z value using FEKO which is also included in the same figure below.
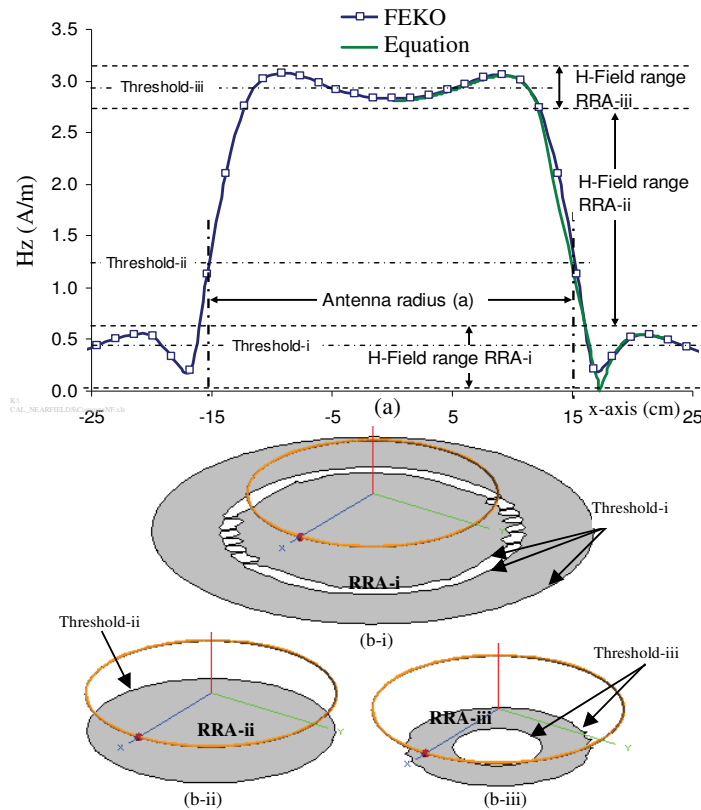
Figure 2-4: The Magnetic fields on the tag plane at z=5cm

(a) taken along x-axis, (b-i to b-iii) overall plot corresponding to type of RRA.

Results in **Figure 2-4** (a) highlight that the reader recognition area can be categorised into three types: RRA-i; RRA-ii; and RRA-iii; and they are shown in **Figure 2-4** (b-i to b-iii). These variations in RRA occur due the different levels of tag sensitivities as well as the magnetic fields produced by the reader antenna. In a normal operation, RRA-ii is always desired because it is more stable and provides more consistent detection area. This type of RRA can be typically achieved by adjusting the amount of input power to the reader so that the appropriate amount of current is supplied to the radiating loop reader antenna.

Comparison between results obtained using both FEKO and the closed form expressions show good agreement, as can be observed in **Figure 2-4** (a) which once again clearly confirm the accuracies obtainable using FEKO simulations. This will helps us justifying use of FEKO for computing the electromagnetic characteristics of reader antennas in this thesis.

The separation distance between the plane of the tag and the plane of the reader antenna may not always be fixed at a constant value. Therefore, it is important to

examine RRA characteristics when the separation distance is varied. In Figure 2-5, the plots of magnetic fields at different separation distances from the initial tag plane are shown. Results for different dimensions of reader loop antennas (electrically small) are also included in the plot. In this plot, the distances between reader antenna and tag plane are varied within ±20% of the initial reference distance, of h_{tag_plane} = 5cm.
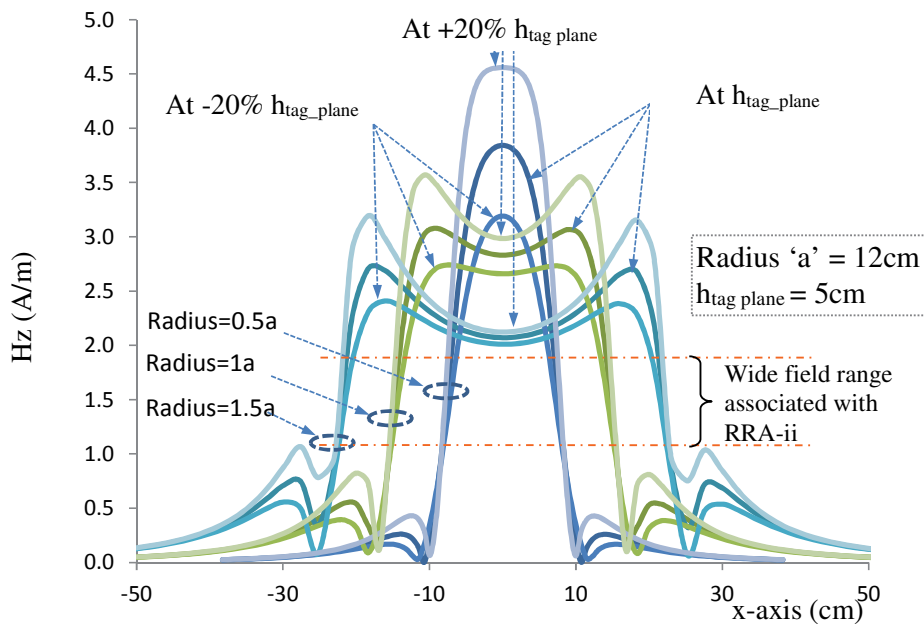
Figure 2-5: Magnetic fields at different separation distances from the initial tag plane

From the results shown in **Figure 2-5**, it can be seen that even for a variation of h_{tag_plane} distance within ±20% of its reference value, the antenna is still able to produce comparable reader recognition area, especially for the RRA-ii indicated in **Figure 2-4** (b-ii). The size of RRA of this type does not change significantly as can be seen from the above plot. This characteristic is important to ensure that the region of tag detection and its boundary are consistent. The pattern of RRA-ii holds irrespective of whether the size of reader antenna is smaller or larger as shown in **Figure 2-5**. Another important characteristic that can be deduced from this investigation is that, the size of RRA is related to dimensions of the loop. If one desires to have larger RRA, a larger sized loop needs to be considered and vice versa. However, one must ensure that the loop is still can be considered electrically small that current along the loop to be almost constant.

2.3.2 RRA for different loop geometries
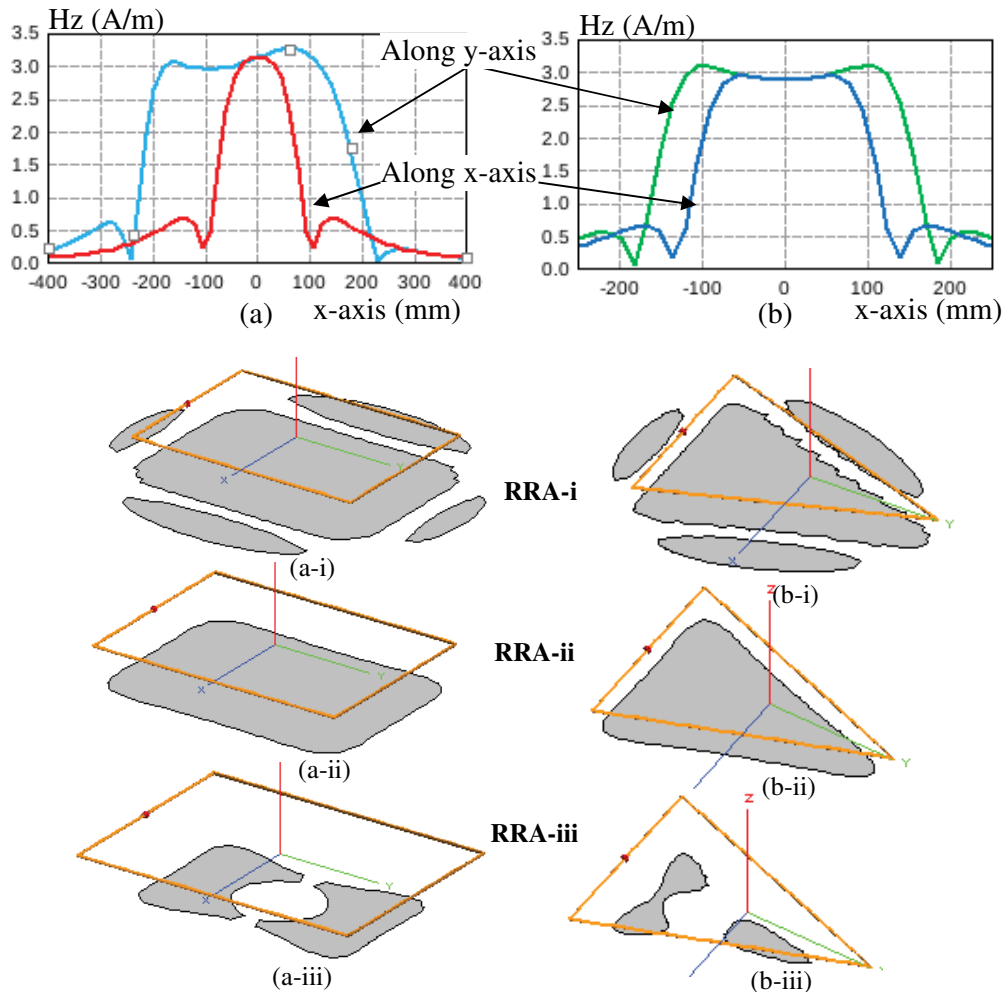
Figure 2-6: Computed magnetic fields and the RRAs for
(a) rectangular loop, and (b) triangular loop.

Results given in the previous section indicate that the size of RRA that is formed closer to the loop reader antenna can be influenced by the geometry of the antenna. For some applications with space constraints, reader antennas may have to be designed to have non-circular shapes so as to fit it into a certain limited space. We consider the two common shapes viz., i) rectangular and ii) triangular loops to investigate whether loop shape at all influences the resulting RRA. To achieve this, we have used FEKO simulations to compute magnetic fields for triangular and rectangular loops to obtain their corresponding RRAs at h_{tag_plane}=5cm which are shown in **Figure 2-6**.

The results in **Figure 2-6** reaffirm that the preferred RRA-ii mode is consistently produces recognition area that closely resembles the geometry of the radiating loop. For

a given tag and reader, it is possible to obtain this RRA mode because the input current fed to the loop can be easily adjusted at the reader. The adjustment need not to be too accurate because once the tag threshold value is set closer to the central value of the H-Field for RRA-ii range, any slight change does not significantly vary the size of the RRA as is readily indicated in **Figure 2-5**.

To this point, we have established the RRA mode that is useful for use with different loop antennas. Utilisation of this mode of RRA for applications and methods of improvements will be highlighted in the next section.

2.4 Manipulation of RRA for positioning

2.4.1 Positioning Uncertainty due to the size of RRA

Typical HF RFID based positioning of a moving object utilising floor tags is illustrated as in **Figure 2-7**. The object to be localised typically is equipped with a HF RFID reader whose antenna is placed at the base of the moving object. Passive tags are installed within the area to be localised and their positions are known. Whenever the reader recognises the tag(s) that are located within its recognition area (RRA), the object position can be estimated with respect to known tag position. Typically, position is estimated either by averaging all the coordinates of the detected tag(s) or averaging of minimum and maximum coordinates of the detected tag(s) [11, 23] when employing conventional RFID reader antenna. Other methods such as nearest neighbour approximation, probabilistic methods, etc. have also been proposed [71, 72].
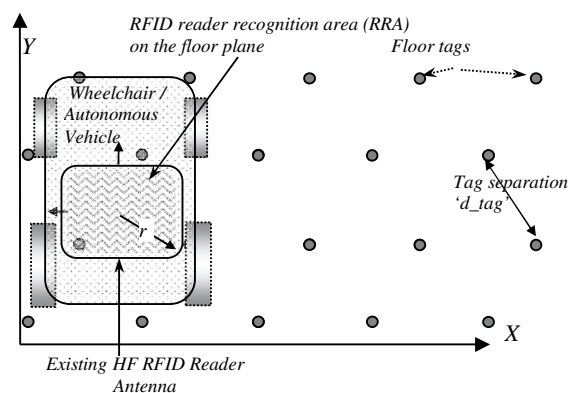
Figure 2-7: Positioning using HF RFID with floor tag

The common limitation suffered by all these techniques is that their localisation uncertainty depends on the density of the tags on the floor and the size of reader recognition area (RRA). In general, larger reader recognition area allows lesser tag density but the obtainable positioning accuracy may have to be compromised as illustrated in **Figure 2-8**. In this figure, the maximum error due to a reader antenna that has larger RRA (Error_B) is obviously higher than that of the smaller antenna having smaller RRA (Error_A). However, the antenna with large RRA may allow tags to be placed sparsely on the tag plane.
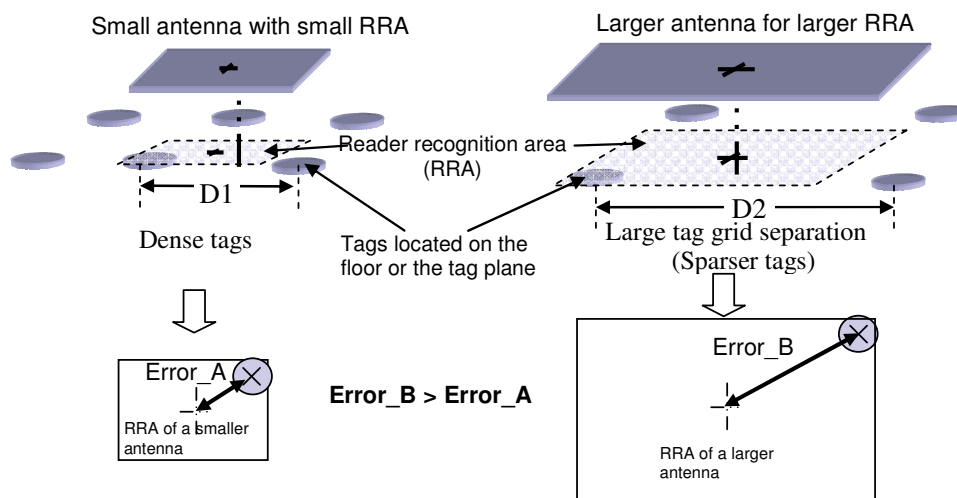
Figure 2-8 Size of RRA and tag density

To overcome some of these problems, various methods have been proposed in the literature. Han, et al. [11] used densely arranged triangular grid pattern of floor tag arrangement and proposed orientation-estimation algorithm based on motion continuity. Another method to obtain optimal recognition area for RFID based system is available in [72]. Park and Hashimoto [12] initially used tag's coordinates with trigonometric functions to localise an autonomous mobile robot but later improved their system by including the tag read time [13].

Methods of using additional sensors have also been proposed, for example, Choi, et al. [23] employed nine units of ultrasonic sensors installed on the front side of a moving object to improve localisation. For detecting tags, the recognition area of the reader antenna plays an important role. Attempts to improve the read range of HF RFID reader antenna have also been reported in [84, 85]. However, methods are required, that can gainfully manipulate the recognition area of the reader antenna to improve

positioning and localisation even when the tag grid separation is large. Such methods, to the best of our knowledge, have not been attempted in the open literature.

2.4.2 Forming RRA with multiple zones to reduce uncertainty

To overcome localisation uncertainty, multiple-loop reader antenna can be employed so that its recognition area can be bifurcated into multiple zones. Such multiple recognition zones allow the system to have additional information to indicate as to which of the zones (thus their corresponding loops) are closer to a detected tag(s) thereby helping to improve positioning. This concept is intuitively illustrated in Figure 2-9 below. As can be seen, the magnitude of the error reduces when RRA has multiple zones.
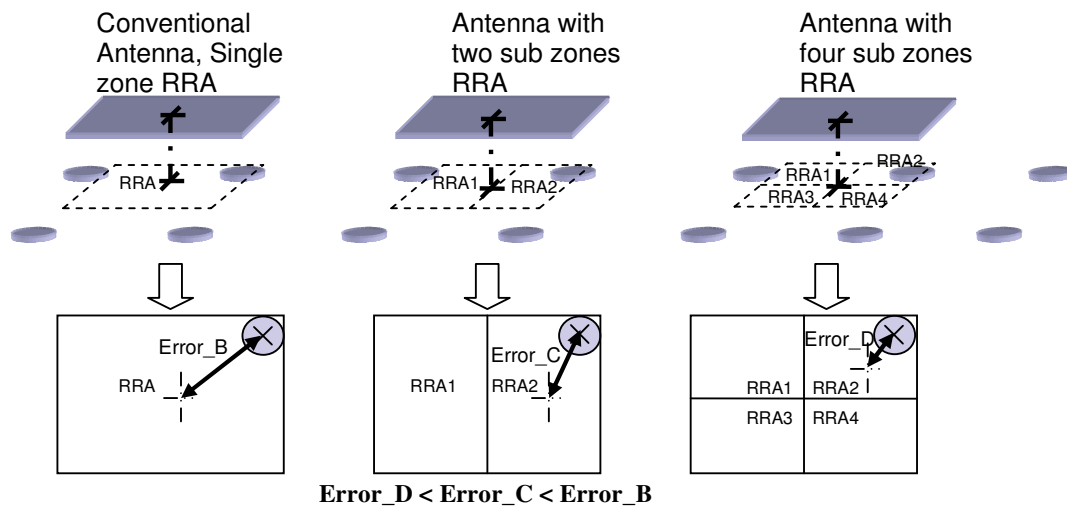
Figure 2-9 Effect of multiple zones to the positioning accuracy

In general, multiple recognition zones can be achieved either by connecting multiple antennas to multiple readers, or alternatively using electronic switching techniques [51, 52]. The former approach requires more than one reader, which can be expensive and is usually not desirable. The latter approach may degrade read performance due to losses in switching. To overcome these problems, we propose a novel bridge-loop configuration [86-89] to form multiple RRA zones.

Before we discuss on the concept of the bridge antenna it is important to first discuss its key features, viz., i) Bifurcating of RRA into multiple zones using multiple loops, and ii) Change in loop impedance due to proximity between reader antenna and tag antennas. These two features will be discussed below.

2.4.3 Arrangement of multiple loop antennas to bifurcate the RRA to form multiple zones

RRA can be bifurcated into multiple zones by employing multiple loops antennas. Two important requirements need to be ensured to gain advantages when employing multiple loop antennas to obtain multiple RRA zones:

i)   The loops and their excitation must be arranged in such a way, the resulting total magnetic fields be along the same direction to add constructively to produce magnetic fields comparable to a single loop antenna.

ii) A method to recognise as to under which of the zones, the detected tag is located.

Consider that the floor tags are placed sparsely in a rectangular grid (see **Figure 2-7**) which mean, at any instance of time, only one tag may be present within the RRA of the reader loop antenna.

Let us first analyse as to how the above mentioned first requirement can be achieved. Consider a single loop as well as two loop antennas having similar outer dimensions as depicted in **Figure 2-10** (a-b). The two loop antenna is arranged and exited in such a way that at any instant of time, the currents can be considered approximately constant and flow along all the edges of the antenna in a direction same as the single loop antenna as illustrated in the **Figure 2-10** (a-b). This configuration allows the total net magnetic fields at the tag plane to be approximately equal to that of a single loop antenna. Thus, they both produce a comparable RRA.

(a)   (b)
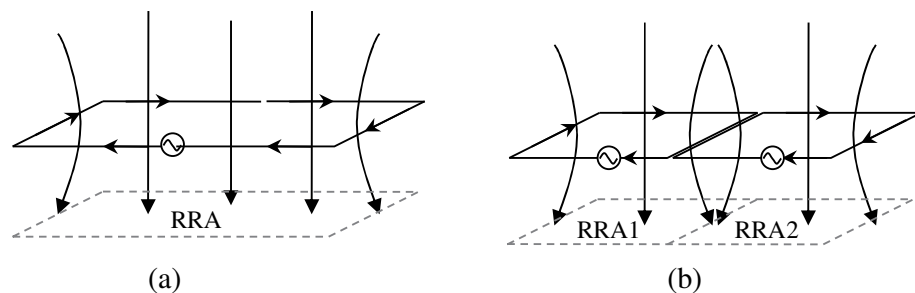
Figure 2-10: RRA of single loop and multi loops

As for the second requirement is concerned, the loop antenna must be able to recognise the location of the tag with respect to the RRA. This can be obtained depending on the method used to connect and energise the loop. For example, when using multiple readers, the location of a tag can be recognised by examining data from

both the readers. When switches are used with a single reader, the information from switching controller and the reader have to be examined. This process of identification can be performed by an algorithm that runs at the processing controller, which controls the reader(s) and/or switches.

An alternative way of achieving the similar goal is by connecting the loops in a serial fashion using a single reader. The proximity of the detected tag with respect to the RRA of either the first loop or the second loop can be determined by examining the potential difference at the two loops. This potential difference can be obtained by using a differential circuit. This technique can be work well because the change in impedance of the loops occurs due to the presence of a tag. This is a result of the magnetic field coupling, which occurs between the tag and the reader loop. Thus, obtaining multiple RRA zones using multiple loops can be made useful.

2.4.4 Effects of proximity between reader antenna and the tag

Interaction or coupling between a reader antenna and the tag modifies the impedance of both the antennas [42, 51]. This property is important because it can be utilised to identify the degree of proximity between the tag and the reader antenna.

Let us examine the changes in the impedance of a loop reader antenna due to the presence of a tag placed at some close distance from it. We assume both the tag and the reader antennas are placed on planes that are parallel to each other. The tag antenna is usually four or five times smaller that of the conventional reader antenna and both the antennas are assumed to be circular loops. This arrangement is illustrated within **Figure 2-11**. Using FEKO, we compute the current, magnetic field, and the resulting impedance of the single loop reader antenna when a tag antenna is moved along a line that is perpendicular to the centre of the reader antenna. The change of the impedance as a function of the separation distance is plotted in **Figure 2-11**. The plot confirms that the proximity of a tag influences the impedance of the reader antenna. This characteristic can be utilised to recognise location of a tag with respect to the loop reader antenna.

Now let us arrange two loop elements to form dual loop reader antenna as previously shown in **Figure 2-10** (b). When a tag is present directly underneath any of the loops, the impedance of both the loops will change, but the loop that is closer to the

tag will experience different change from the one that is not closer to it. Thus, there will be a potential difference between both the two loops. Interestingly, this potential difference will change as a function of the location of the tag. By examining this difference signal, the location of the tag can be determined whether it is underneath the first loop or the second loop, in other words, whether the tag is within RRA1 or RRA2. This is the basis in forming the proposed bridge antenna.
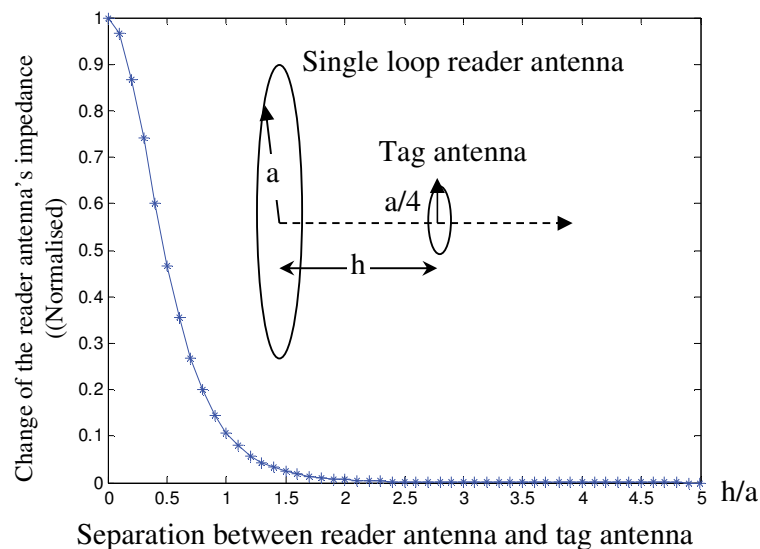
Figure 2-11: Change of impedance over separation between the tag and the reader's antenna

2.5 The concept of bridge-loop antenna

It is shown in the previous section that multiple RRA zones can be obtained by connecting two loops in series and feeding them from a single reader. The two loops are arranged so that their magnetic fields are induced over physically two different areas and there is no intersection. The location of the detected tag can be identified by examining the change in the impedance of the loops. However, the change in the impedance cannot directly be obtained in practice easily. This problem can be overcome by arranging all multiple loop antennas in a Wheatstone bridge configuration, which will be discussed further below.

2.5.1 Concept

A Bridge-loop antenna is an antenna that has multiple loop antenna elements connected in a Wheatstone bridge configuration so as to produce magnetic fields in such a way that two or more distinct recognition areas (RRAs) are formed. In general, its working is similar to a conventional loop antenna, but has an additional feature in the form of bridge potential signal, produced from the bridge circuit when a tag is present in close proximity to any of the loop elements. This is possible due to the magnetic coupling between the tag and the near by loop elements of the reader antenna which in turn, creates an imbalance in the bridge to cause bridge potential signal to develop in the bridge arms. This signal provides additional information to identify the location of the tag with respect to the antenna and can be very useful for localisation applications.

The use of bridge antenna assumes the following:

i) The loop antenna elements are electrically small i.e. the total loop length 'S' between source terminals is much smaller to the wavelength 'λ' of the operational frequency (S<λ/10). Therefore, the current in the loops can be considered uniform to obtain constructive radiated magnetic fields at close distance.

ii) Both the reader and tag antennas are assumed to resonate at the same operating frequency. Whenever tags are present within the proximity of the bridge reader antenna, coupling effects between the tag and the loops can cause changes in the impedance of the loop elements.

With the above assumptions, it is possible to arrange multiple-loops in a bridge form, which will be explained in the next section.

2.5.2 Working principles of a bridge-loop antenna

Working principle of a bridge-loop antenna is best explained by considering its basic form, which employs a single bridge as illustrated in **Figure 2-12** (a-b). The loop elements of the antenna are configured in such a way that they represent the four arms of the Wheatstone bridge with complex impedances Z_n, (n = a, b, c, d..) as schematically shown in **Figure 2-12** (c), where Z_n represents series resistive and inductive component of nth loop.
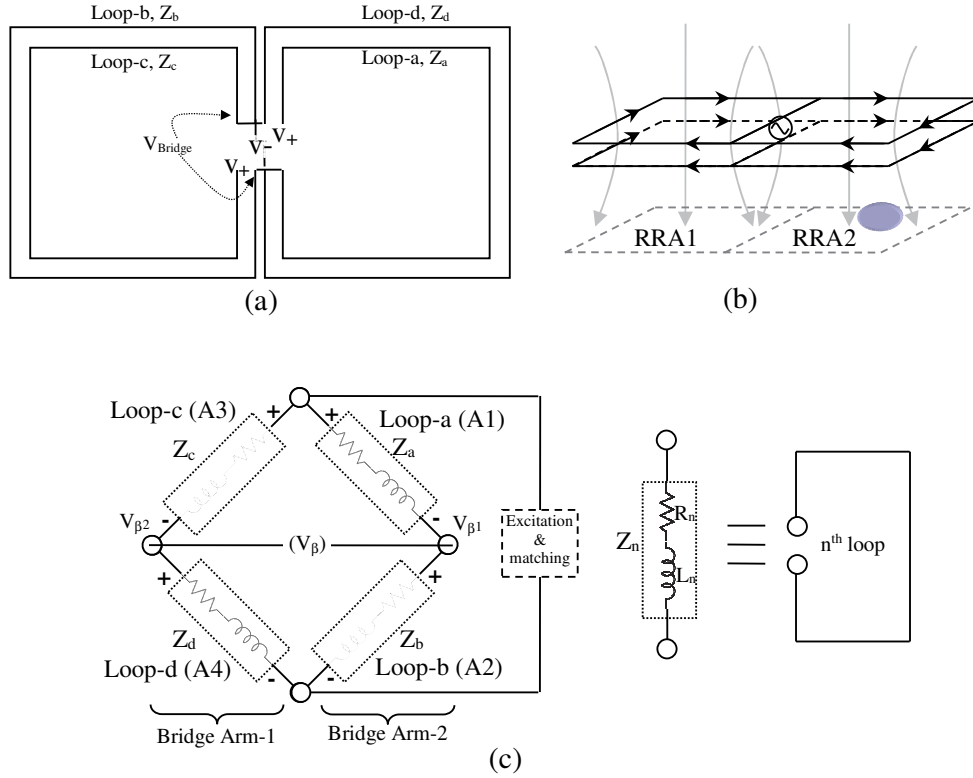
Figure 2-12: Loop connections in a bridge form.

If a passive tag presents directly under one of the loops, then a change in impedance (ΔZ) is created to cause an electric potential (V_β) to be developed at the bridge terminals. The resulting potential is given by

$$V_\beta = (\frac{Z_b \pm \Delta Z_b}{(Z_a \pm \Delta Z_a) + (Z_b \pm \Delta Z_b)} - \frac{Z_d \pm \Delta Z_d}{(Z_c \pm \Delta Z_c) + (Z_d \pm \Delta Z_d)})(V_+ - V_-), \qquad (2.6)$$

The terms Z_n and ΔZ_n represent the initial impedances and their corresponding small changes respectively. All these impedances are associated with the loop elements at bridge arm-1 and bridge arm-2. The terms V_+ and V_- are the potentials at the bridge source terminals. These parameters are indicated in **Figure 2-12** (c).

The first and the second terms of the impedance ration in (2.6) are the transfer functions of arm-1 and arm-2. They can be represented by $H_{\beta1}$ and $H_{\beta2}$, where

$$H_{\beta1} = \frac{Z_b \pm \Delta Z_b}{(Z_a \pm \Delta Z_a) + (Z_b \pm \Delta Z_b)}, \qquad (2.7)$$

$$H_{\beta 2} = \frac{Z_d \pm \Delta Z_d}{(Z_c \pm \Delta Z_c) + (Z_d \pm \Delta Z_d)}. \qquad (2.8)$$

Assume that all the elements of the bridge loops are identical where $Z=Z_a=Z_b=Z_c=Z_d$. When a tag present within loop region-1, we have:

$$H_{\beta 1} = \frac{Z}{2Z \pm \Delta Z}, \qquad (2.9a)$$

and

$$H_{\beta 2} = \frac{Z \pm \Delta Z}{2Z \pm \Delta Z}. \qquad (2.9b)$$

On the other hand, when a tag present within loop region-2, we have:

$$H_{\beta 1} = \frac{Z \pm \Delta Z}{2Z \pm \Delta Z}, \qquad (2.10a)$$

and

$$H_{\beta 2} = \frac{Z}{2Z \pm \Delta Z}. \qquad (2.10b)$$

Note that, the transfer function of bridge arm-1 ($H_{\beta 1}$) and the transfer function of bridge arm-2 ($H_{\beta 1}$) can change with the location of the tag because the transfer functions depend on the input impedance of the loop elements involved.

Consider an excitation in the form of a sinusoidal input of $V_{in} = A \, cos(\omega t + \theta)$ is applied to the bridge, where 'A' is magnitude of the input signal, ω is the radial frequency in rad/sec, and θ is the phase shift in degree of the input signal. This excitation represents a pure sinusoidal signal from a RFID reader under steady continuous wave (CW) period which occur during initialisation stage of a reader-tag interrogation [51]. Because the bridge signal is taken during a steady CW period, any signal variation/distortion due to modulation will not affect the bridge signal.

The potentials at both the bridge arms can be obtained by considering magnitudes and phases of the transfer functions of both the bridge arms and multiplying them with the CW input signal as given by:

$$V_{\beta 1} = A \, | H_{\beta 1} | \cos(\omega t + \varphi_{H_{\beta 1}}), \qquad (2.11)$$

and

$$V_{\beta 2} = A \, | H_{\beta 2} | \cos(\omega t + \varphi_{H_{\beta 2}}). \qquad (2.12)$$

The resulting bridge potential is:

$$V_{\beta} = A\left(| H_{\beta 1} | \cos(\omega t + \varphi_{H_{\beta 1}}) - | H_{\beta 2} | \cos(\omega t + \varphi_{H_{\beta 2}})\right) \qquad (2.13)$$

These are some of the advantages of using the bridge configuration as compared to serially connecting the loops. The bridge configuration reduces the effect of

interferences and increase sensitivity [90] in the signal potential that helps to detect the location of a tag as compared to the dual loop antenna discussed previously in section 2.4.

2.5.3 First experimental prototype: Bridge antenna version-1
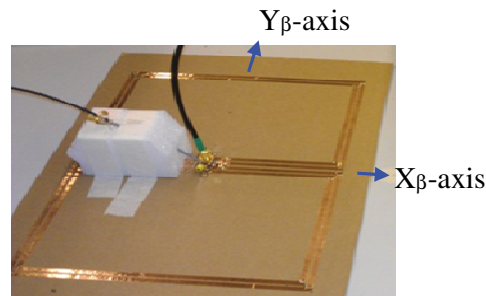
Figure 2-13: The first prototype of the bridge antenna

To quickly realise the feasibility of the concept of the bridge-loop antenna, we first designed and fabricated a prototype, which we call bridge antenna version-1. The loops of this version-1 bridge-loop antenna are arranged on a flat single layer substrate, the feeding and terminals are located at the centre of the antenna. We utilise adhesive copper tape to form the conducting loop elements in the prototype which is illustrated as in **Figure 2-13**. A commercially available reader and a passive tag from Texas Instruments are utilised in the experimentation. We have first modelled the configuration using FEKO in which the power level for antenna excitation is set to be similar to the one produced by the commercial reader, and the tag is modelled electromagnetically using a geometry similar to the actual tag.

We determine the RRA of the antenna by comparing the measured results from prototype version-1 and the computed results using FEKO. The magnetic fields along X_β and Y_β axes at a plane that is parallel to the plane of the reader antenna which lies below the antenna at z=-6cm. We denote this plane as the "tag plane". Both the measured and the calculated results are shown in **Figure 2-14**.
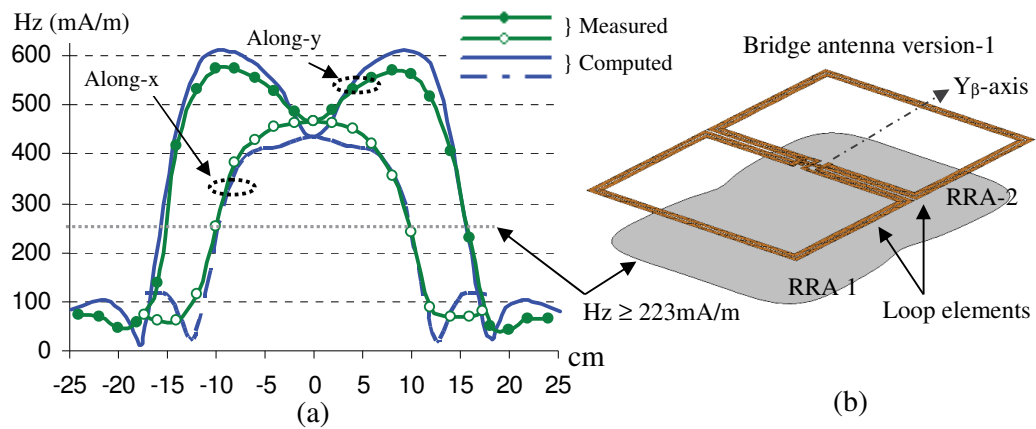
Figure 2-14: Magnetic fields, and RRA of the reader antenna

Experimental and measured results indicate that the level of magnetic fields induced by the bridge antenna is sufficient to energise any standard HF RFID tag. The comparison between measured and FEKO simulation results indicate a good agreement. This provides additional confidence that the FEKO models can be employed to obtain reliable prediction of the magnetic field performance of the bridge-loop antenna.

We therefore use the FEKO to calculate the overall magnetic field on the tag plane to estimate the RRA of the antenna. The RRA type-ii as explained in the previous section is considered here because of its stability and consistency. The magnetic field threshold is chosen to be 223mA/m which is the typical value of magnetic field required by the chosen tag as per manufacture's specification [91]. The results of this simulation is included in **Figure 2-14** (b) which show agreement with our initial assumption that the shape of the RRA-ii is similar to the outer dimensions of the antenna created it.

We also examine the variation of the magnitude of bridge signal V_β produced by the antenna due to variation in the positions of the detected tag. For this, the tag is positioned on a plane (tag plane) parallel to the plane of the antenna. Bridge signal is computed and measured using the prototype when the tag moves crossing the Y_β-axis on the tag plane right below the loop antenna. Both the FEKO calculation and the measured results are plotted in **Figure 2-15** (a) for comparison.
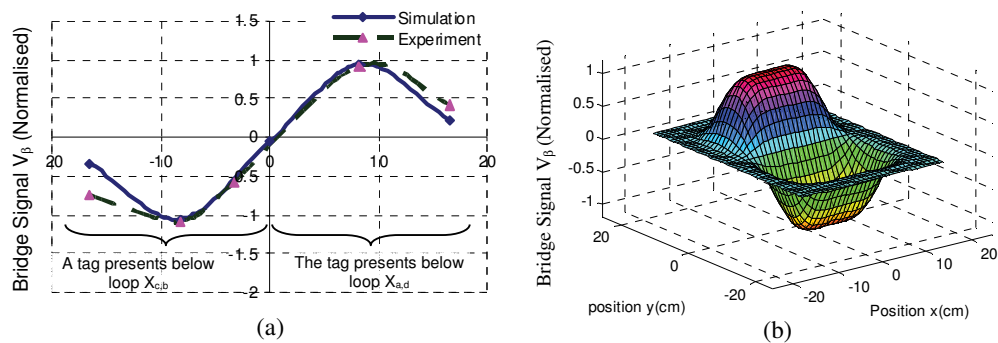
Figure 2-15: The variation of bridge signal V_β of the bridge antenna version-1
(a) along Y-axis, and (b) Surface plot to indicate the overall changes in the bridge signal

The comparison of the bridge signal V_β shows a very good agreement between simulation and measured results. To evaluate the overall bridge signal pattern, we compute the overall variation signal pattern when the tag is positioned in any location within the tag plane. The result is shown in **Figure 2-15** (b). Both the results in **Figure 2-15** (a) and (b) indicate that the concept of the bridge potential from the bridge-loop antenna can provide a means to find the position of the detected tag. This feature can be utilised for positioning and localisation of a tag as well as the reader antenna itself.

2.6 Different Types of Bridge Loop antennas

The results shown in the previous section have motivated us to further investigate the concept of bridge loop antenna. The loops used for the bridge antenna can be printed on multiple layered substrates so that the magnetic field pattern and hence the RRA can be further improved. Also, the shape of the loops can be modified to obtain additional features for the bridge potential that can enhance the capability to localise a tag or the reader. Further, a number of bridges can be added using extra loops to further compartmentalise the RRA into smaller zones so that its ability to recognise the location of a tag can be further enhanced. These attempts are described below. In general, bridge-loop antennas can be classified depending on the number of bridges and the shape of the loop elements. The following three types of bridge antennas are further proposed and evaluated in this chapter:

      i) Single-bridge with rectangular shaped loops antenna (SBRLA)

      ii) Single-bridge with triangular shaped loops antenna (SBTLA)

iii) Multiple-bridge with loop elements antenna (DBRLA), in which the shapes of the loops can be either rectangular or triangular.

In this section, firstly we will analyse the above antennas using electromagnetic analysis based on thin wire loop approximation. The overall current flowing in the loop, and the resultant magnetic fields and the corresponding RRAs having multiple zones will be described using the thin wire electromagnetic models of loop elements. We then employ realistic models of the bridge antenna, which will be analysed using FEKO and later used in experimental prototypes. The dimensions, the geometries, and the expected RRA are indicated in the models.

We assume RRA type 'ii' (RRA-ii) for all the antennas. The RRA-ii is previously defined in section 2.3. The RRA is considered to be formed on a plane that is parallel to plane of the bridge loop antenna. The loop elements will be denoted by letters (a, b, c, d, …) or by combination of capital letters with numbers (A1, A2, A3, …). These notations will be used: either to describe approximate models or to describe the arrangement of the loops in realistic models especially when it involves multiple bridges.

2.6.1 Thin wire models of bridge antennas

Here we define thin wire as a conductor having radius much smaller than the wave length, illustrated in Figure 2-20. Thin wire is used to represent the ideal case scenario and also to facilitate in simplifying our explanations. It is therefore much convenient to indicate the arrangement of the bridge-loop elements, the direction of current in the loop, and the illustration of the radiated magnetic fields from the loop element.

2.6.1.1 Single-bridge-rectangular-loop antenna (SBRLA)

This bridge antenna includes a single bridge formed with rectangular loop elements. The **Figure 2-16** (a) indicates how thin wire loop elements are arranged and connected in a bridge form. The excitation and bridge signal terminals are located at the centre of the antenna.

This configuration allows current in the loops to flow in a direction so as to produce constructive uniform magnetic fields for creating the overall RRA as illustrated in **Figure 2-16** (b). The overall dimensions of so formed RRA would be comparable to the size of a single loop antenna.

The overall RRA can be zoned into two smaller RRAs viz., RRA1 and RRA2. The bridge signal will vary with the tag location with respect to RRA zones. The advantage of smaller RRA zones is that it would help to reduce the uncertainty and errors in positioning and localisation. These aspects will be further discussed in the coming sections.
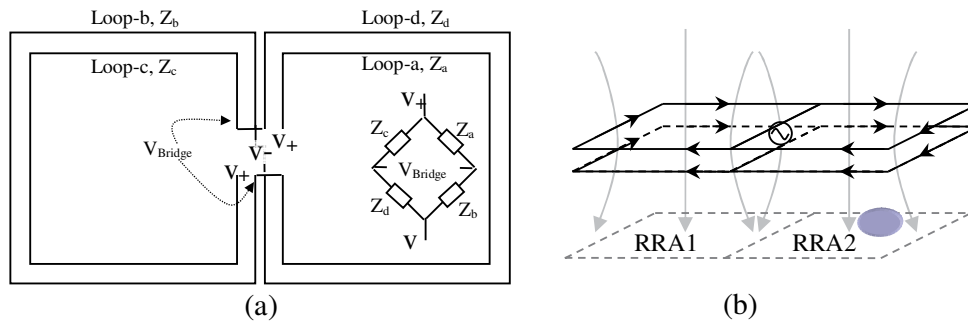
Figure 2-16: Schematic for Single-bridge-rectangular-loop reader antenna
a) Loop shape, and arrangement, (b) Direction of currents, magnetic fields and RRA zones of the antenna.

2.6.1.2 Single-bridge-triangular-loop (SBTLA)

This antenna is quite similar to the previous antenna except that the shape of the loop elements is triangular. Loop arrangement and their connections are shown in **Figure 2-17** (a), whereas the direction of the current flow in the loop as well as the resulting magnetic field and the RAA are illustrated in **Figure 2-17** (b).

Although, the loops are in triangular shaped, but when triangular loops are joined, the outer boundary becomes rectangular and hence the overall RRA will be comparable to that of rectangular shaped antennas as shown in **Figure 2-17** (a). The two resultant zoned RRAs of this antenna are triangular shaped (RRA1 and RRA2). Thus, this antenna can provide unique pattern of the bridge signal when a tag moves across its RRA zones at different point. In particular, this antenna can produce variations of the bridge potential to correspond two directions (vertical and horizontal) with respect to the placement of the tag. This aspect will be discussed further in section 4.2 in chapter-4.
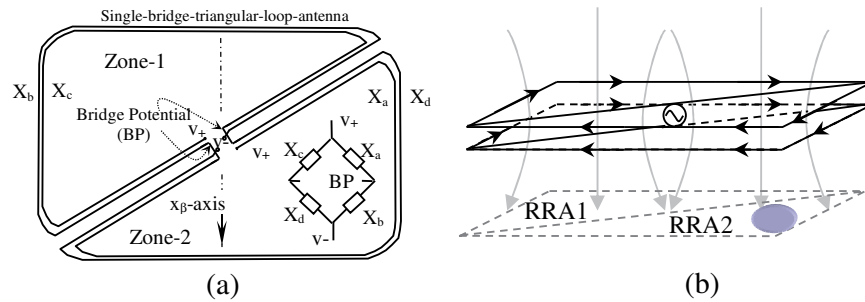
Figure 2-17: Schematic of Single-bridge-triangular-loop reader antenna

(a) Loop shape, and arrangement, (b) Direction of currents, magnetic fields, and RRA zones of the antenna.

2.6.1.3 Generalized form of bridge loop antenna (Multiple-bridge-rectangular-loop)

The concept of bridge antenna can be extended to include multiple bridges so that the overall RRA can be divided into many possible zones by increasing the number of bridges. **Figure 2-18** illustrates schematically the arrangement for N-bridges. The loops in each bridge can have any shape but here we consider their shape to be rectangular so that their performance can be compared and also the ease of fabricating on experimental prototype. Loop arrangement for each bridge is illustrated in **Figure 2-18** (a), which shows that the connections can be repeated and rearranged appropriately to obtain the desired RRA zones.

This type of bridge antenna is suitable if one desires to have much smaller sub zones of RRA especially when the overall RRA is relatively large. To demonstrate the above concept, we consider two bridges with rectangular shaped loop elements. We call this antenna as dual-bridge-rectangular-loop antenna (**DBRLA**). Loop arrangement for each bridge is quite similar to that of a single-bridge-rectangular-loop antenna as shown in **Figure 2-16**. However, the loops for the second bridge (Bridge-B) may have to be rearranged so that the centre line that divides the overall RRA of this bridge antenna is orthogonal to its counterpart from the first bridge (Bridge-A) as illustrated in **Figure 2-19** (b). The letters 'A' and 'B' are used to denote parameters associated with first bridge (bridge-A) and second bridge (bridge-B) respectively.
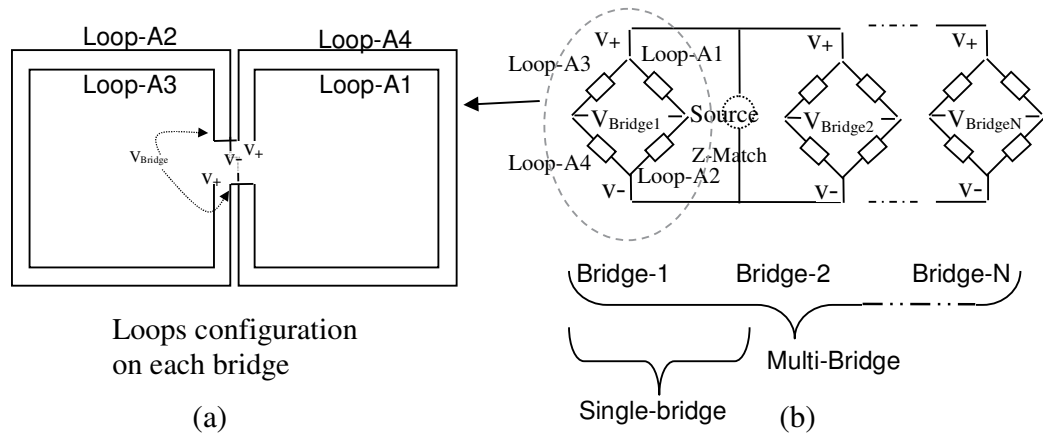
Figure 2-18: Schematic of Multiple-bridge-rectangular-loop antenna
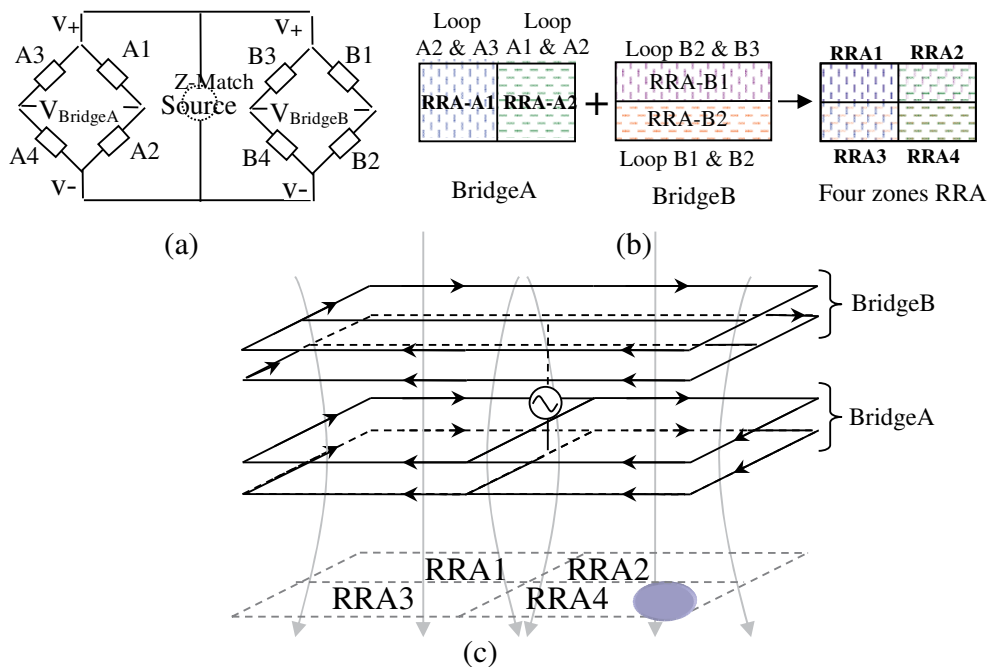
Figure 2-19: Schematic of dual dual-bridge-rectangular-loop antenna (DBRLA)

(a) Connections of the loop elements in dual bridges, (b) Formation of RRA of the antenna,

(c) Direction of currents, magnetic fields, and RRA of the antenna.

Letting the loop elements associated with each of the two bridges to overlap orthogonally, would lead to four distinct regions of RRA as illustrated in **Figure 2-19** (b). The direction of currents in the loops, the resulting magnetic fields, and the resulting RRA is illustrated in **Figure 2-19** (c). This arrangement demonstrates that the concept of bridge antenna can be extended to make further splits of the overall RRA into relatively smaller sub-zones. The creation of smaller sub zones of RRA further

reduces positioning uncertainties and thus errors are minimised. This antenna then is suitable for dividing a relatively large overall uniform RRA into smaller sub-zones, which may have applications in the areas of smart table etc. Next, we will describe realistic models of the above mentioned bridge loop reader antennas.

2.6.2 Realistic models for the bridge loop antennas

Instead of using thin wire models as explained in the previous section, we have modelled metallic strips with finite thickness and width in FEKO so as to closely simulate the conducting elements used for prototyping the bridge antennas. Conducting strip is chosen because it is easier to fabricate loop elements on the surface of any thin supporting substrates. Further, when we form loops on multiple layers, this approach helps to minimise the overall thickness of the antenna. Compact bridge antenna is desirable to ensure its physical structure does not interfere with the operational environment of the device to which the antenna is attached.

Thin wire element and the metallic strip can be considered almost equivalent electrically at the frequency of 13.56MHz, however when they are placed in multiple layers, their impedance can be different. This is examined through FEKO simulations considering the geometry in Figure 2-20 with (the length of both the conductors $l_{conductor}$ = 1m, the wire radius R_W = 2.4mm, and Strip width R_S = 4.8mm). FEKO results presented in the Table 2-1 indicate that the impedances between the wire conductor and the metallic strip are not similar especially under multiple layers substrate. Therefore, when simulating the antenna in FEKO, it is important to use the conductor geometry that is similar to the one used in prototyping the bridge antenna (which in this case is metallic strip), so that performance of the actual bridge antennas can be closely evaluated.

Another important aspect in the design of bridge antenna is that, it is important to ensure that the loop elements at the bridge arms have the same impedance mainly to ensure balancing the bridge and minimise the offset in the bridge signal V_β as indicated in section 2.5.2. This can be achieved by ensuring identical dimensions for the loops and utilise symmetrical arrangements. The physical geometries of realistic models for bridge loop antennas are presented below.
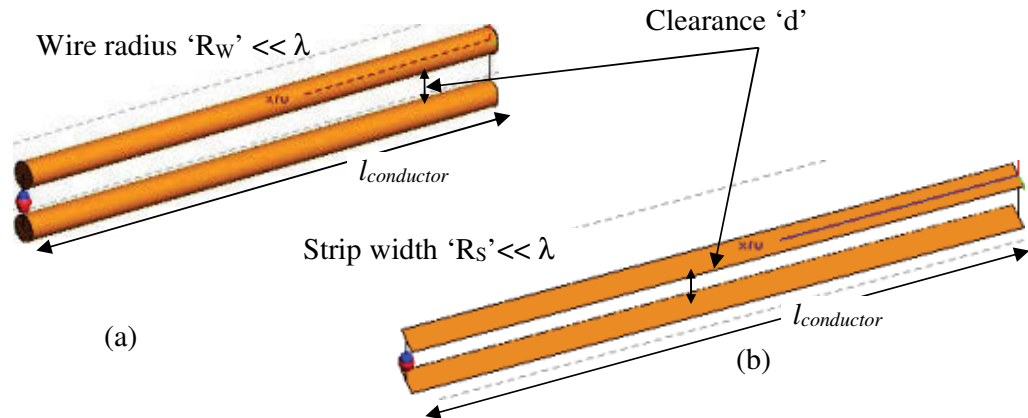
Figure 2-20 Illustration of thin wire and strip wire

Table 2-1: Comparison between the inductance of thin wire and the inductance of strip conductor

Type of conductors	Inductance at separation 'd'	
	d=100mm	d=5mm
Thin Wire	1.7891 uH	0.58376 uH
Strip Wire	2.1133 uH	0.94662 uH
Difference	18%	62%

2.6.2.1 Loop arrangement for Single-bridge-rectangular-loop antenna (SBRLA)

In a single bridge loop antenna, four loops made of metallic strips are utilised to represent the four arms. The upper left and the bottom right arms are combined to produce constructive magnetic fields for the first RRA (RRA1), and similarly for the second RRA (RRA2), which is created by the magnetic fields of other two loops of the bridge. Each of the two loops has to be co-located or placed close together. One of the best ways to achieve these is to stack the loops so that they are arranged in different layers with air/substrate in between. Physical arrangement for realistic model of this antenna is illustrated in **Figure 2-21**.
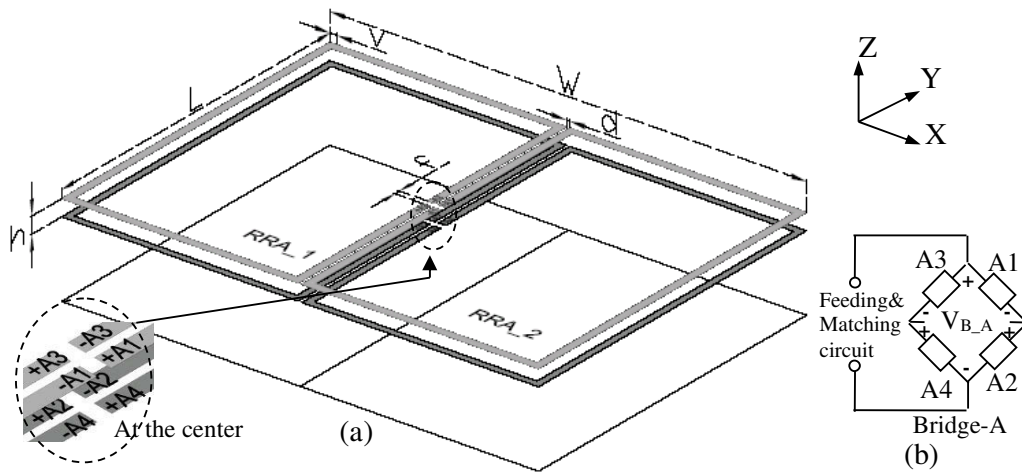
Figure 2-21: Physical loop arrangement for realistic model of single-bridge-rectangular-loop antenna

2.6.2.2 Loop arrangement for Single-bridge-triangular-loop antenna (SBTLA)

Triangular loop arrangement is quite similar to the rectangular one except that each of the loops takes a triangular shape. The physical model of this antenna is shown as in **Figure 2-21**.
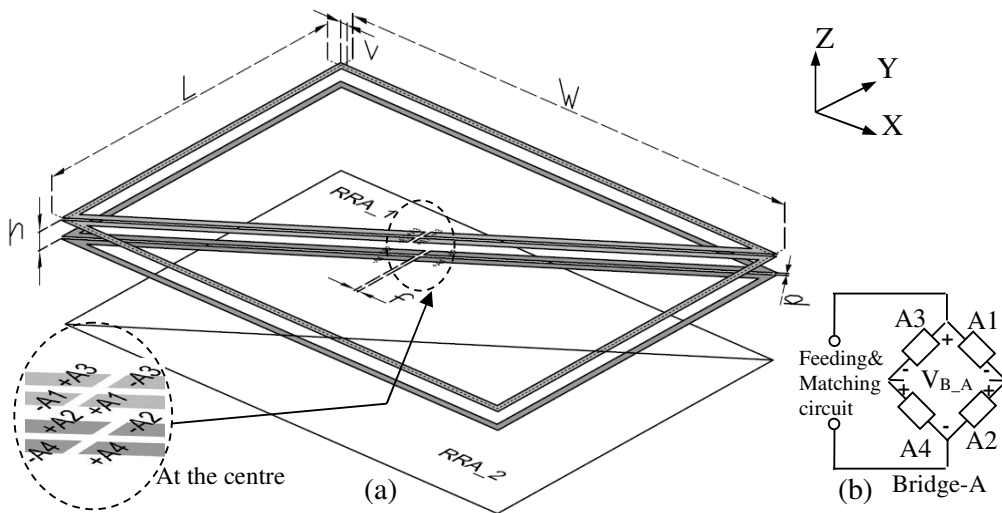
Figure 2-22: Physical loop arrangement of single-bridge-triangular-loop antenna

2.6.2.3 Loop arrangement for Double-bridge-loop antenna (DBRLA)

This antenna can be considered as an extension of the SBRLA. It utilises two bridges to create smaller RRA. The physical arrangement for the realistic model of this antenna is illustrated in **Figure 2-23**.
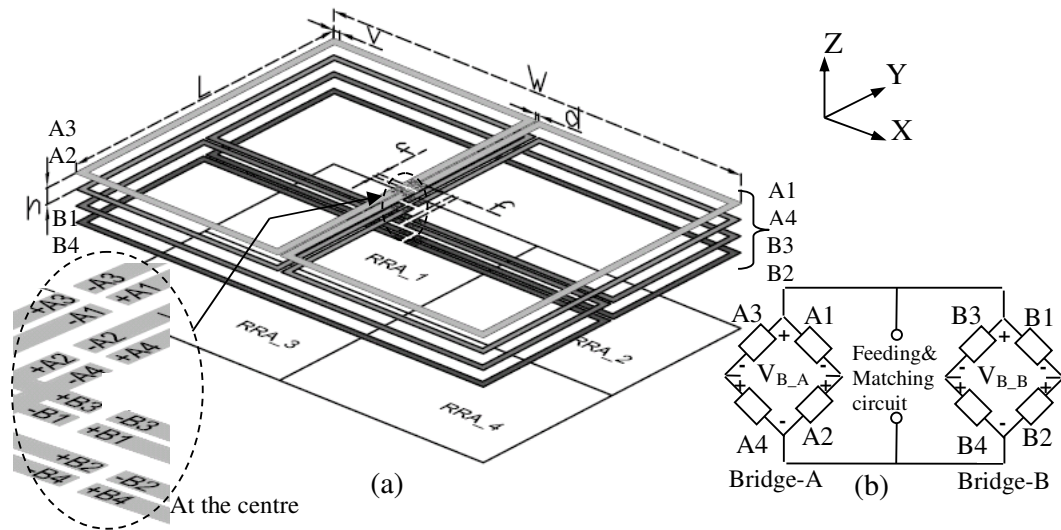
Figure 2-23: Physical loop arrangement of dual-bridge-rectangular-loop antenna

2.6.3 Realistic model parameters

We choose a common outer dimensions for all the antennas so that a proper comparison can be made. Detailed dimensions of the antennas are tabulated in **Table 2-2**.

Table 2-2: Dimensions of the prototype antennas

Types*	Width (W) mm	Length (L) mm	Track Width mm	Track Clearance mm	Other parameters mm
SBRLA	320	230	4.8	1.2	-
SBTLA	320	230	4.8	1.2	h=3
DBRLA	320	230	4.8	1.2	h=3

* SBRLA: Single-bridge-rectangular-loop
   SBTLA: Single-bridge-triangular-loop
   DBRLA: Double-bridge-rectangular-loop

2.6.4 Impedance matching and quality factor

Proper impedance matching is necessary to maximise the magnetic field produced by the antenna. This is achieved by making sure that the antenna resonates at the proper operating frequency. One can employ any of the available methods of antenna tuning and impedance matching [84, 85]. In this thesis, a method employing three-element matching with series parallel configuration [84] is used as shown in **Figure 2-24**.
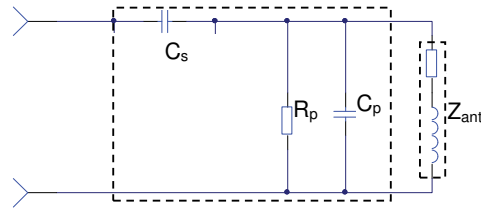
Figure 2-24: Three-element matching

The chosen tuning approach provides flexibility for wide range of sources and it allows quality factor 'Q' to be specified. Depending on the target application, 'Q' should be chosen to allow appropriate bandwidth required for modulation [84, 85]. The modulation requirements for commercially available RFID system are in general specified by ISO standards. For HF RFID that operates under vicinity-coupling (i.e. range up to 1m) is covered by ISO15693 standard. The standards unify all the requirements for RFID manufacturers so that RFID readers and tags are compatible with one another. Thus, any standard reader can interrogate tags made by different manufacturers. Our antenna is designed to be compatible with this widely used standard, ISO15693. This standard specifies the modulation requirements for both, down-link (i.e. from reader to tag) and up-link (i.e. from tag-to reader). Under this standard, information from a tag to a reader is modulated using a sub carrier of 423 kHz through either ASK or FSK. This may require a bandwidth of $2 \times 423\,\text{kHz} = 846\text{kHz}$ [51, 92, 93]. On the other hand, the bandwidth requirement for modulating data from the reader to the tag is much lower [92] that the minimum bandwidth for the system is constrained by the tag modulation. For this reason, we will only consider the bandwidth requirement by the modulation of the tag as specified by the standard.

Quality factor 'Q' of an antenna is related to the bandwidth 'BW' and the centre frequency 'f_0' by

$$Q = f_0 / BW , \qquad\qquad (2.14)$$

Using the bandwidth limit as specified by the standard which is about 846kHz, we obtain the maximum allowable quality factor $Q = 16$. Use of a larger Q will give higher level of magnetic fields but the bandwidth for modulation will be scarified and will potentially degrade the performance of the RFID system [51]. The selection of Q is therefore, has to be properly chosen to be within an appropriate range to balance between the radiated magnetic fields and the bandwidth for modulation. In this thesis,

the bridge antennas equipped with a standard reader is set to provide quality factor within the rage of ($8 \leq Q \leq 16$).

Knowing the quality factor, we are now one step closer to obtain the matching elements for the antenna. Consider the circuit in **Figure 2-24**, and assuming the loop resistance is very low, the antenna can be considered to have a parallel resonance configuration. The quality factor 'Q' of the antenna is therefore related with the parallel resistance 'R_P' and the loop inductance 'X_L' by

$$Q = R_P / X_L. \tag{2.15}$$

and hence 'R_P' can be calculated using the above equation. Next we can proceed to find C_P and C_S. We use smith chart in Figure 2-25 to help with our explanation.
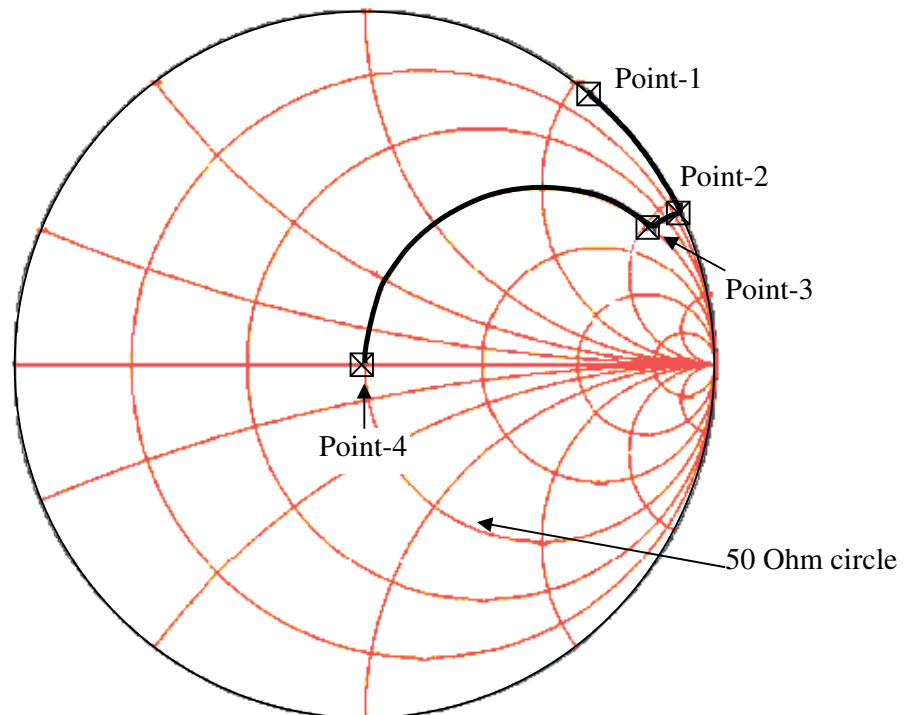
Figure 2-25: Smith chart indicating the matching elements and the impedance lines for matching the antenna using three-element match.

Referring to Figure 2-25, point-1 indicates the impedance of the antenna, point-2 is the impedance point after the inclusion of the parallel capacitance 'C_P', and points-3 and 4 are the impedances after inclusion of 'R_P' and 'C_S' respectively. The value of C_P is chosen so that the resulting impedance lie on the 50 Ohm circle when the antenna connected to the parallel circuit components (R_P and C_P). Finally, C_s is chosen to bring

the impedance closer to the purely resistive 50 Ohm point that is located at the centre of the Smith chart. In other words, the impedance of C_s is chosen to be the conjugate of impedance at Point-3. By putting these statements into mathematical expressions, we can calculate C_P and C_S. We firstly calculate C_P using the parallel impedance

$$Z_{Parallel} = R_P \parallel C_P \parallel L_{ant}$$
$$= \frac{L_{ant}R_P}{\left(j\omega L_{ant} - \dfrac{j}{\omega C_P} \right)\left(R_P + \dfrac{L_{ant}}{j\omega L_{ant} - j(1/\omega C_P)} \right)C_P} \tag{2.16}$$

To bring the parallel impedance $Z_{parallel}$ impedance on to the 50 Ohm circle in the Smith chart, the real component of $Z_{parallel}$ must equal to 50 Ohm, hence we can write

$$\mathrm{Re}\left[\frac{L_{ant}R_P}{\left(j\omega L_{ant} - \dfrac{j}{\omega C_P} \right)\left(R_P + \dfrac{L_{ant}}{j\omega L_{ant} - j(1/\omega C_P)} \right)C_P} \right] = 50, \tag{2.17}$$

$$\frac{L_{ant}^2 R_P}{(R_P^2 + \dfrac{L_{ant}^2}{(\omega L_{ant} - \dfrac{1}{\omega C_P})^2 C_P^2})(\omega L_{ant} - \dfrac{1}{\omega C_P})^2 C_P} = 50,$$

solving for C_P, then we have

$$C_P = \frac{10L_{ant}R_P^2\omega^2 \mp \sqrt{2}\sqrt{-50L_{ant}^4 R_P^2\omega^6 + L_{ant}^4 R_P^3 L^4 R^3\omega^6}}{10L^2R^2\omega^4}. \tag{2.18}$$

Next, the C_S is calculated using the conjugate of the $Z_{parallel}$

$$\omega C_S = -\mathrm{Im}\left[\frac{L_{ant}R_P}{\left(j\omega L_{ant} - \dfrac{j}{\omega C_P} \right)\left(R_P + \dfrac{L_{ant}}{j\omega L_{ant} - j(1/\omega C_P)} \right)C_P} \right], \tag{2.19}$$

solving for C_S in (2.19), we obtain the following expression

$$C_S = \frac{L_{ant}R_P^2}{(R_P^2 + \dfrac{L_{ant}^2}{(\omega L_{ant} - \dfrac{1}{\omega C_P})^2 C_P^2})(\omega L_{ant}^2 - \dfrac{1}{\omega C_P})C_P}. \tag{2.20}$$

The above procedures are employed when matching the proposed bridge antennas.

2.7 Simulations and experimentations to evalutate the bridge loop antennas

The aim of this section is to evaluate the performance of all the proposed bridge loop antennas in term of their return loss, radiated magnetic fields and corresponding bridge signals. Note that, our previous analysis on bridge antenna version-1 (in section 2.5.3) indicated that, FEKO calculation can provide accurate results that agree with the measurements. In this section, we therefore, will firstly calculate the performance of the proposed bridge antennas using FEKO, and later the measurement will be performed on the prototype of a dual-bridge-rectangular-loop reader antenna (DBRL). This antenna is chosen because it resembles a more general type of bridge antenna and further it is relatively more complex as compared with other proposed bridge antennas (which are single-bridge-rectangular-loop and single-bridge-triangular-loop reader antennas). Good agreement for this antenna will firmly validate all of our FEKO realistic models, and hence the corresponding results obtain from these models. Procedure and the main components involved for simulation and measurement/experimentation are described below.

2.7.1 Modelling using FEKO

To electromagnetically simulate the fields on realistic antenna models we utilise FEKO which employs Method of moments as well as Finite element method [80]. This tool allows computation to be performed effectively for any arbitrary loop geometries even having complex feeding and structural arrangements. The following parameters are obtained; i) return loss of the antenna, ii) the resulting magnetic fields, and iii) the bridge signals that correspond to different positions of a tag relative to the RRA of the antenna. Detailed modelling procedure and arrangement for each computation/simulation will be explained in section 2.7.3.

2.7.1.1 Passive tag Model

We aim to demonstrate the working of the proposed Bridge loop antennas using tags that are commercially available. A tag from Texas Instrument (TI) RI-I03-114 is chosen

in this study. A tag model similar to that of the original TI tag is created in FEKO. The geometry of the tag for simulation is shown in **Figure 2-26** below.
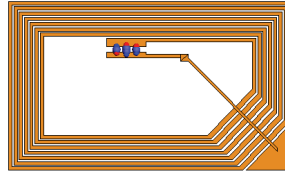
Figure 2-26: Model of TI tag employed in FEKO simulation

The typical required activation field strength for this tag is around 107 dBmA/m or 0.223A/m according to specification given by the tag's manufacturer [91]. The tag antenna is tuned so that it resonates at the HF RFID operating frequency of 13.56MHz.

2.7.2 Setup for Experimentations
2.7.2.1 Prototype of the antenna
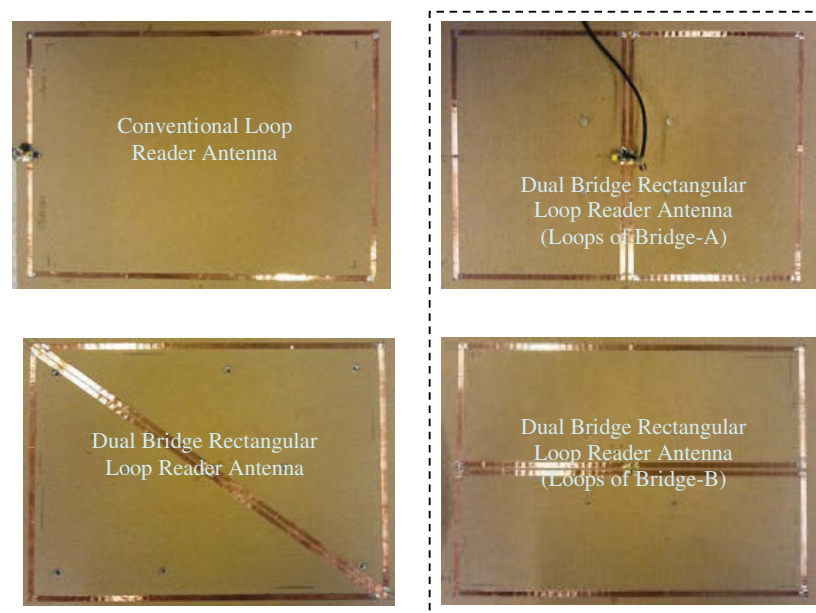
Figure 2-27: Prototype of bridge-loop reader antennas

Prototypes of some of the proposed antennas are fabricated for validation and they will be used for experimentations that will be reported in the next chapters. A picture of the prototype antennas are shown in **Figure 2-27**.

In the figure, we also include a single loop conventional reader antenna that will be used for comparison. Thin copper tapes are utilised in our prototypes to fabricate loop antenna elements. The copper tapes are attached to the surface of a thin insulating substrate material, which also functions to support the antenna elements. Feeding points, and the bridge measurement terminals are located at the centre of the antennas.

2.7.2.2 Commercial reader and tag

We employ a standard, commercially available HF RFID reader 'TRF7960' and the standard commercially available passive tags 'RI-I03-114' from Texas Instruments as indicated in **Figure 2-28** [91]. The tag contains an antenna as well as an integrated circuit (IC). The chosen reader allows recognition of various types of tags using the standard RFID protocols including (ISO/IEC 15693, ISO 14443, and ISO/IEC 18000). The reader is equipped with anti-collision algorithms to allow detection of multiple tags. The maximum output power from this reader is 200mW. We replace the standard antenna of the reader with our proposed bridge loop antenna.

(a)

(b)
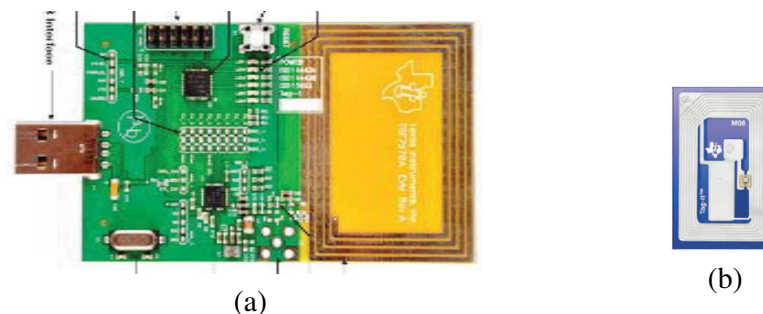
Figure 2-28: The HF RFID reader, and the Passive HF RFID tag

The specification of the tag is shown in the table below.

Table 2-3 Specifications of the tag*

	PART NUMBER
Supported standard	RI-103-114A-S1
Recommended operating frequency	ISO/IEC 15693-2, -3; ISO/IEC 18000-3
	13.56 MHz
Passive resonance frequency (at 25^0C)	13.56 MHz $\pm$ 200kHz (Includes frequency offset to compensate further integration into paper or PVC lamination)
Typical required activation field strength to read (at 25^0C)	107 dBuA/m
Typical required activation field strength to write (at 25^0C)	117 dbuA/m

* The information is obtained from[91].

2.7.3 Evalution of the performance of the bridge antennas

This section describes procedure to obtain the following bridge antenna parameters:

      i. Return loss (S11),

      ii. Magnetic fields at the tag plane (H_z), and the RRA,

      iii. Bridge signal.

The following subsections detailed out how the parameters are computed and measured. The realistic antenna models as described in the section 2.6.2 are utilised.

2.7.3.1 Return loss in dB (S11)

The FEKO is used to compute the return loss by computing the scattering parameter S11 of the proposed bridge antennas. For the experimentation, a vector network analyser (VNA) from Agilent Technologies (E5071C) is utilised. The calibration of VNA is done using the calibration standards provided by Agilent.

2.7.3.2 Magnetic fields at the tag plane (H_z A/m)

The purpose of this measurement is to obtain the profile and the level of magnetic fields of the bridge antennas. An input power of 200mW is applied which is similar to the power produced by typical HF RFID. The frequency is set to be 13.56MHz. We assume that the antenna is positioned at the centre of the x-y plane. Also, we assume that the tag plane is located parallel to the antenna plane and separated from each other by a distance of around 5-6cm. Because the tag and the antenna plane are parallel, the effective magnetic field that will be received by tags that are located in the direction normal to the plane, which in this case is the z-direction. Therefore, we will only consider this effective magnetic field component (H_z). We utilise a Digital oscilloscope (DSO-X 2004A) along with a near field probe to measure the near magnetic fields. The measurement setup and key observation points for the magnetic fields are indicated in **Figure 2-29** and **Figure 2-30** respectively.
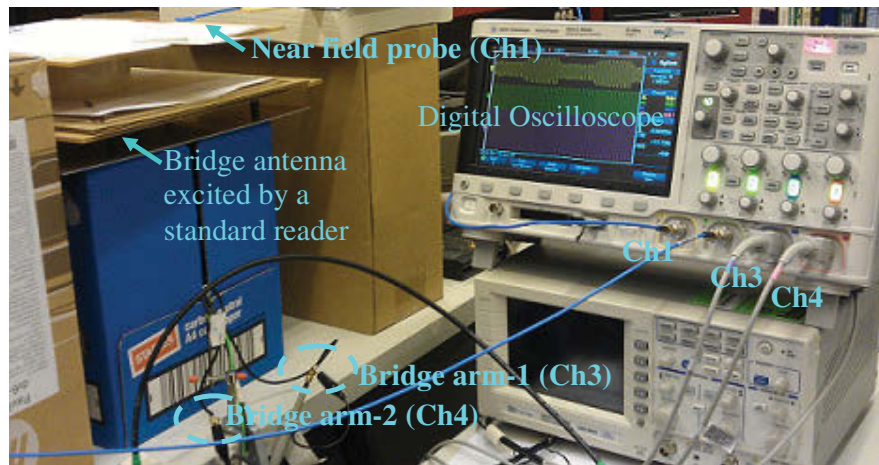
Figure 2-29 Measurement setup for measurements of magnetic fields and bridge signals
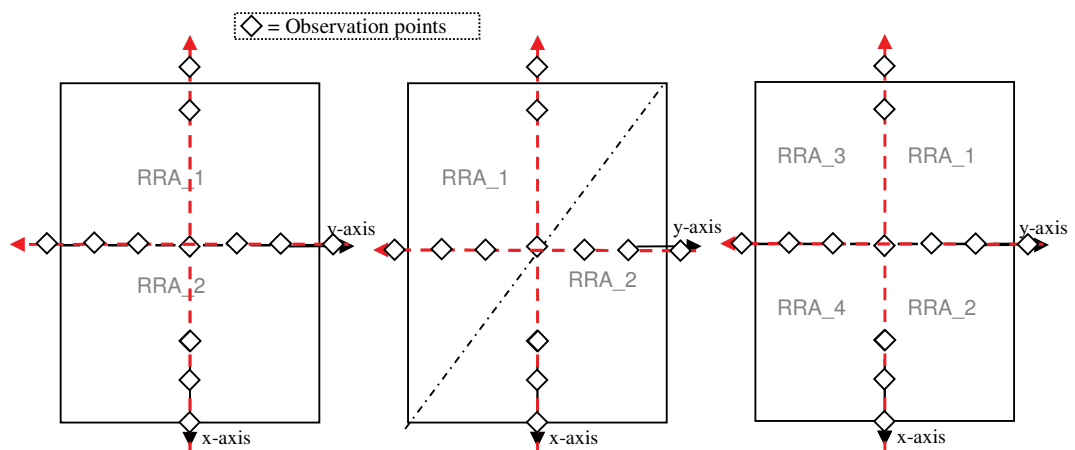
Figure 2-30 Magnetic fields along x and y axes

2.7.3.3 Computation and measurement of Bridge signals

Bridge signals are computed by first computing current induced on the antenna elements using FEKO. The bridge signals are obtained by incorporating resistive lumped circuit elements at every bridge terminal of the bridge antennas. The resistance is chosen to be much larger than the input impedance of the loop so as to minimise any unwanted effects on the operation of the antenna elements. In simulation, the bridge signal is obtained by calculating the line/segment current that passes through the resistive lumped element using FEKO, and multiplying it with the resistance of the lumped element.

As for the measurement is concerned, a Digital oscilloscope (DSO-X 2004A) is utilised to measure the voltage across the lumped circuit element that was initially soldered at the bridge terminals. Measurement setup to measure bridge signal is similar as the setup shown in **Figure 2-29**, however, the probe is replaced by a passive tag, and channel3 and channel4 are utilised to obtain bridge signal. We use the actual passive tag and its model as indicated in **Figure 2-28** (b) and **Figure 2-26** respectively for measurements and FEKO simulations. To obtain variation in bridge signal as the function of tag position, the tag has been moved to different positions for every bridge measurement. To simulate the tag movement, we integrate the Matlab and FEKO packages to automatically achieve the changes in the tag position. The path along which the tag has been moved in simulation and measurement is illustrated in **Figure 2-30**.

2.8 Results

The results on return loss (S_{11} dB), near fields (H_z A/m), and the bridge signals (V_β volt) for all the proposed antennas are presented in here. We verify the computed results, by performing a comparison with measured results obtained from dual-bridge-rectangular-loop reader antenna (DBRLA). This particular antenna is chosen as it represents a more general form of multiple bridge loop antennas, and if the results agree with this antenna, it will also validate other proposed bridge antennas, which have simpler bridge configurations.

2.8.1 Return loss (S_{11})

The results in **Figure 2-19** show the return loss (S_{11}) in dB for all the three bridge antennas. The results indicate that all the proposed antennas resonate at the HF RFID reader operating frequency (13.56MHz). The comparison between measured and the computed results from the multi-bridge-rectangular-loop antenna indicates good agreement.
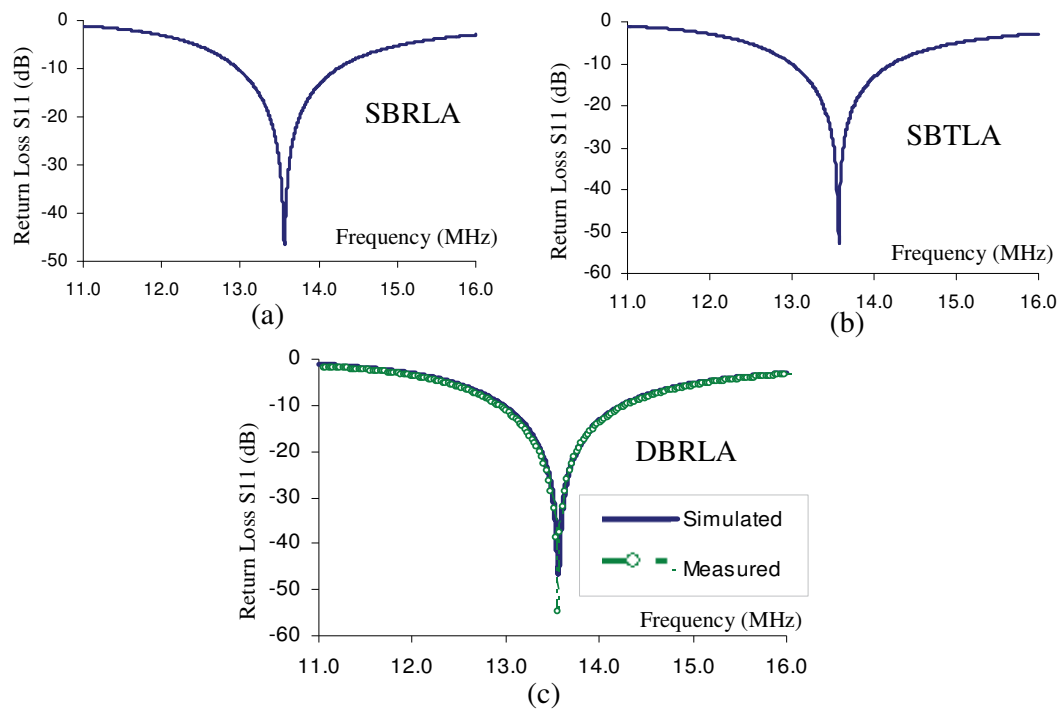
Figure 2-31: Return loss of the bridge-loop reader antennas

(a) Single-bridge-rectangular-loop, (b) Single-bridge-triangular-loop, and (c) Dual-bridge-rectangular-loop

2.8.2 Antenna performance (H-fields)

Results in **Figure 2-32**(a-c) shows the magnetic fields (H_z component) produced by the proposed bridge-loop antennas on x-y plane at z=-5cm. The levels of magnetic fields at positions projected below the antenna (i.e. at x-y plane with z=-5cm) are sufficiently large to interrogate the chosen tag ($H_z > 223mA/m$). The magnetic fields along x and y axes provide information about the size of recognition area of the reader's antenna.

In **Figure 2-32** (c-i), the comparison between computed and measured magnetic fields from the dual-bridge-rectangular-loop reader antenna shows a close agreement, which reaffirm the accuracy of our models used in FEKO.

The RRAs for all the proposed antennas obtained using realistic models in FEKO are indicated on the right side in **Figure 2-32**(a-c). For comparison, we also include the computed RRA from a conventional single loop reader antenna having the same outer dimension as that of the proposed bridge reader antennas.
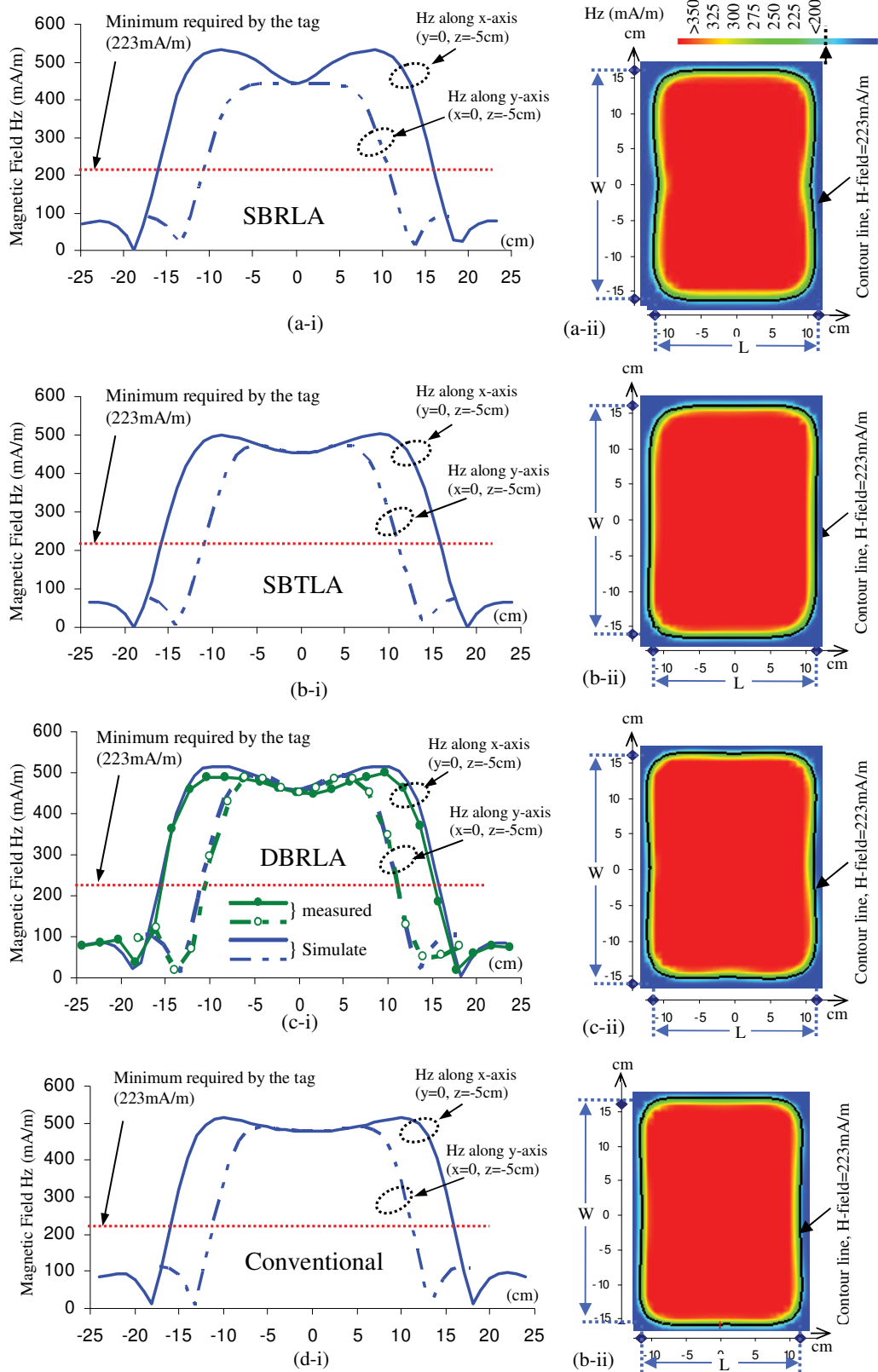
Figure 2-32: The induced H-fields and the RRAs
(a) Single bridge rectangular loop, (b) Single bridge triangular loop, and (c) Dual bridge rectangular loop, and (d) conventional loop reader antenna.

Another important parameters viz., the boundary of RRA on which the field is sufficient enough to detect a tag is highlighted with dark line on each figure. It can be seen that the RRAs of the proposed bridge antennas are comparable to that of the conventional reader antenna. It can also be observed from the figure that the shape of the RRA is approximately equal to the shape of the outer boundary of the reader antenna, which validates our earlier approximation. The shape of the RRA will be utilised in later chapters while describing the proposed localisation algorithms.

2.8.3 Antenna performance (Bridge signals)

Results in **Figure 2-33**, show the variation of the bridge signals (V_β) when a passive tag is positioned at different points on the tag plane located underneath the bridge antennas. Separation between the tag plane and the reader antenna plane is kept at 5cm.

In **Figure 2-33** (c-(i-iv)), the comparison between computed and measured bridge signals from the dual-bridge-rectangular-loop reader antenna shows a close agreement, which reaffirm the accuracy of our models used in FEKO to predict the bridge signal. Results from other bridge antennas indicate similar variations as the tag is moved at different location with respect to the RRAs of the antennas.

The polarity of the bridge signal indicates as to which loop is closer to the tag. Using the magnitude of the bridge signal can be further refined the information of the location of the tag. The shape of the bridge loop element plays an important role as it influences the behaviour of the bridge signal. Referring to **Figure 2-33** (a) and (b), the bridge signal from the rectangular shaped loop does not have much variation when the tag is moving along x-axis direction, however the bridge signal from the triangular shaped loop shows distinct variation when the tag is moving either along x or y axis. This characteristic can offer additional advantages when a loop element with triangular shape is used which will be explained in the later chapters.

The above results confirm that the proposed bridge antennas are able to produce useful bridge potential (V_β) when a typical tag is detected within its interrogation (RRA) zone.
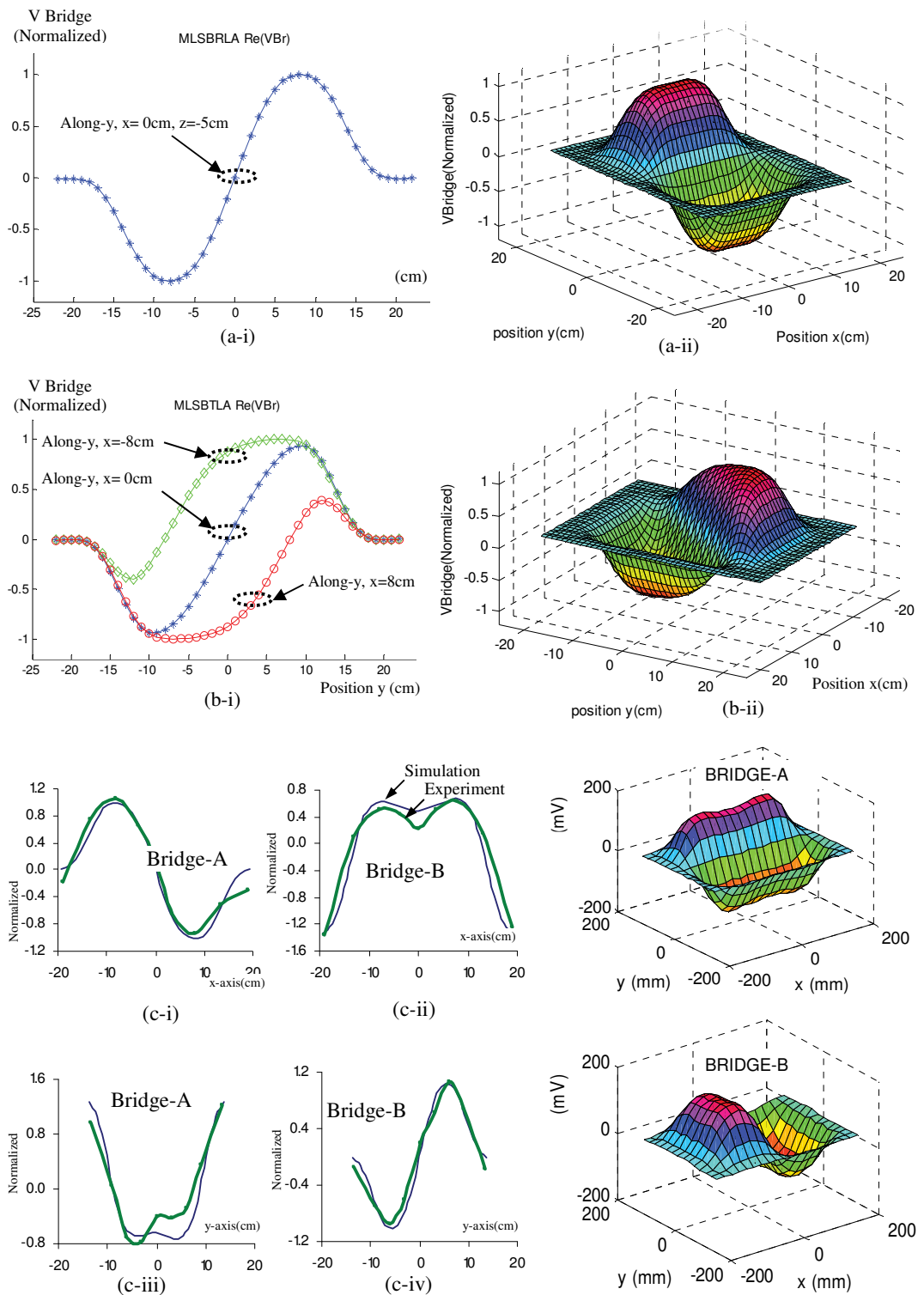
Figure 2-33: Bridge signal variation for bridge reader antennas;

(a) Single bridge rectangular loop, (b) Single bridge triangular loop, and (c) Dual bridge rectangular loop.

2.9 Summary

The concept of reader recognition area (RRA) and techniques to manipulate it are discussed in this chapter. A novel bridge loop antenna for HF RFID reader is introduced for manipulating the RRA. Different types of bridge reader antennas are described in term of their design and performance. Realistic electromagnetic simulation models of the proposed antennas are presented along with their fabricated prototypes. The proposed method will be able to bifurcate the RRA into multiple zones for localising the tag without the need of multiple readers or switches. The proposed system can offer cost-effective solution for localisation and eliminates the need for a dense grid of floor tags.

Chapter 3

Effect of Metallic Environments on the Placement of Bridge Loop Antennas

3.1 Introduction

In the previous chapter, the design and the characteristics of Bridge loop antennas under ideal scenarios were presented. However, for use in realistic environments, the RFID reader may have to be operated closer to metallic structures and objects. In such environments, due to the metallic objects, the induced magnetic field provided by the reader antenna gets distorted. This in turn can generate unintended bridge potential signal and cause errors in position estimation if bridge potential signal are used directly.

In general, proximity of metallic objects near to an antenna may degrade its performance [94-97]. For a bridge antenna, the metallic objects may also disrupt with the bridge signal (V_β) which may cause errors in position estimation. It is therefore important to characterise this effect so that methods of improvement can be identified. We consider a scenario where the bridge reader antenna is to be used to localise an autonomous wheelchair in indoor environments that have concrete floors. Therefore the bridge signals of the antenna will be interfered by metallic objects due to: i) the metallic structure of the wheelchair at the base of which the reader antenna is installed, and ii) the embedded metallic rods inside the concrete floors and in addition any other metallic object located on the floor plane, closer to the reader antenna.

In this chapter, we will first focus on the characterising the bridge signal due to the proximity effects of metallic objects. For the sake of simplicity, we consider firstly effects due to large metal plate. Appropriate approximations along with equivalent circuits are introduced to help with the analysis in minimising the effect of metallic objects. Techniques of improvement obtained form the above analysis will then be verified using FEKO simulations along with some experimentation. To simplify the discussion, we will focus our investigations on the **single-bridge-triangular-loop**

antenna. The outcomes from this analysis and would be applicable to all other HF RFID bridge reader antennas since they are based on the same concept.

Our contribution in this chapter include: i) classifying the effects of metallic objects to investigate their impact on to the performance of the bridge antenna, ii) formulate equivalent circuits to systematically characterise effects on the bridge signals, iii) propose methods to minimise the effect of metallic objects on bridge signal, and iv) validate the proposed methods through realistic simulations and experimentations with prototype of bridge reader antenna.

This chapter is organised as follows: in section 3.2, types of metallic objects and their effects to the performance of a bridge reader antenna are classified. Section 3.3 introduces equivalent circuits to characterise the bridge signals for bridge loop reader antennas. Methods to minimise the effect of metallic object are proposed in section 3.4. Analysis and experimentations using realistic antenna prototype are presented in Section 3.5 to evaluate and verify the proposed methods. Various aspects for improving and minimising the effects of metallic objects on the level of magnetic field radiated are included in section 3.6. Finally, summary of the chapter is given in section 3.7.

3.2 Classification of metallic objects and their effect

The proposed bridge antenna can be used to localise tagged objects or to localise an object carrying the antenna. The environments at which the antenna is used in general can be cluttered and surrounded by metallic objects. Only metallic objects that are relatively close to the antenna will cause interference with the operation of the antenna due to the induced magnetic field that is confined to regions closer to the antenna. From the antenna point of view, these metallic objects can be grouped into two categories:

     i) Objects relatively fixed compared to the antenna (*Fixed metallic objects*)

     ii) Objects that are present near to antenna as it moves (*Randomly present metallic objects*)

The examples of the first category include the metallic objects that are fixed to a structure to which the antenna is also attached. The second category depends on the indoor environments in which the antenna is operating. For example, a moving object may carry the antenna, and while on the move, the antenna may encounter metallic objects that may be present within the vicinity of the antenna along its travelling path.

In applications requiring the localisation of a moving object such as an autonomous wheelchair, the reader antenna is typically mounted at the base of the moving object so that the reader can detect the floor tags and then, that information is used to estimate the position. While carrying this process, the reader antenna can encounter either or both the metallic structure at the base of the moving object as well as the metallic structure that lie underneath or within the concrete floor which may be present randomly near to the reader antenna when the antenna is let to move on the floor. Both can cause disruption to the reader antenna operation.

3.2.1 Problems

It is generally known that proximity of metallic objects to any antenna affects the current flowing in the antenna, thus affecting performance of antennas. As far as the bridge antenna is concerned, the proximity to large metallic objects can potentially alter the bridge potential signal which may cause errors in localisation.

To investigate the effect of metallic objects on the bridge potential signal, we simulate two scenarios considering both the categories of metallic objects. In the simulation, the model of realistic bridge antenna and the tag as described in the previous chapter are utilised as well as the realistic geometry of the metallic object under consideration. Using the FEKO simulation tool, we estimate the resulting magnetic fields and the bride signals produced by the antenna. The simulation models for the first and second scenarios are described below.

3.2.2 Fixed metallic objects

Here, our aim is to investigate a localisation scenario where mainly to characterise the effects of the structure of the autonomous vehicle that carries reader antenna. The metallic structure of an autonomous vehicle is depicted in **Figure 3-1**. To simulate the effects of these metallic objects, we first consider the metallic structures that are located near to the reader antenna as illustrated in **Figure 3-2**. A single-bridge-triangular-loop reader antenna is positioned at the base of the moving object. The metallic structures can be considered to be fixed with respect to the position of the antenna. As depicted in the **Figure 3-2**, a metallic block is also included to consider a scenario in which the

overall metallic structure becomes unsymmetrical. Such an unsymmetrical metallic structure can potentially create an offset to the bridge signal.

The proposed reader Antenna   *The proposed reader Antenna*

Metallic structure of the wheelchair near its base where the reader antenna is installed
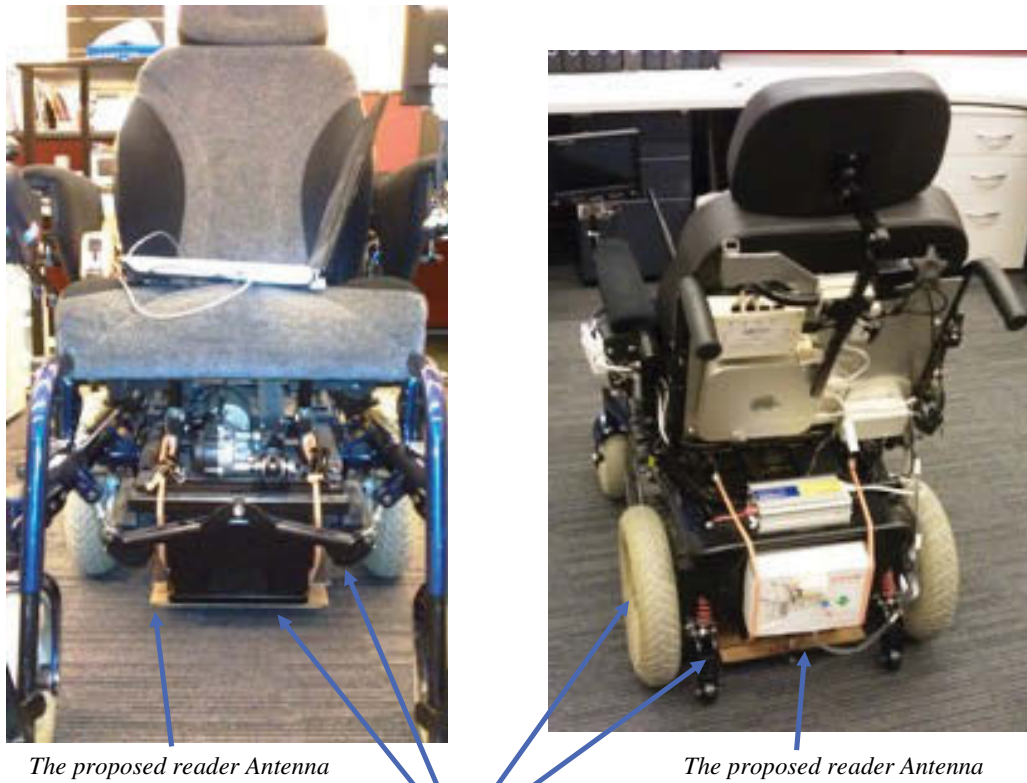
Figure 3-1: Metallic structure on the autonomous wheelchair
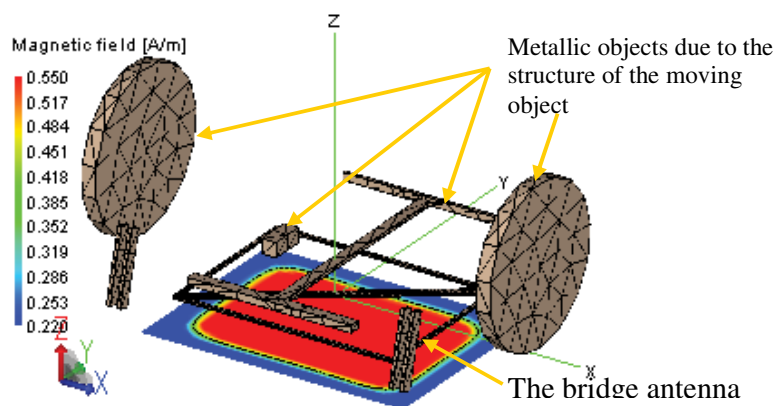
Figure 3-2: Electromagnetic (FEKO) model of fixed metallic objects near a bridge antenna

3.2.3 Randomly present metallic objects

When an autonomous moving object carrying reader moves along a concrete floor inside a multistorey building, the metallic bars that are present inside the concrete flooring can cause interference. The typical metallic structure in concrete flooring is illustrated in **Figure 3-2**.

THIS FIGURE IS EXCLUDED DUE TO COPY RIGHT

Figure 3-3: Typical metallic structures present within floor concrete [98]
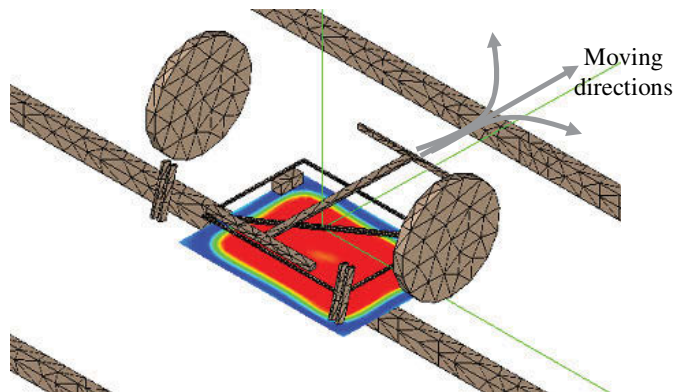
Figure 3-4: Electromagnetic model used for modelling randomly present metallic objects near a bridge antenna

To investigate the scenario due to metallic objects/structure that may present on the floor near to the reader antenna (randomly present metallic objects), the above model is modified by including metallic bars positioned underneath the floor. These bars represent the second category of metallic objects as explained earlier. The model is

shown in Figure 3-4. Other metallic objects/structures due to cabinet, partitions, etc. are not included as these objects usually placed at distances relatively far from the antenna hence their influence to the antenna can be assumed to be very small.

3.2.4 H-field and bridge signal under metallic environments

The near magnetic fields and bridge signals under the metallic environments as described above are computed using FEKO. In the model, the antenna is excited similar to the one described in the previous chapter with an input power of 200mW. The resulting magnetic fields on the tag plane (defined by x and y axes) are shown in the **Figure 3-5** (a), and the resulting bridge signals are shown in **Figure 3-5** (b).

When randomly present metallic objects are involved, the level of magnetic fields produced by the bridge reader antenna when it is not moving as shown in the **Figure 3-3**, can be considered to be the worse case scenario. In this state, we assume that metallic object is located directly underneath the antenna, making it the worse case scenario. Since their presence is random, it is fair to assume that in all the other scenarios, they may not be located directly under the antenna.

(a)   (b)
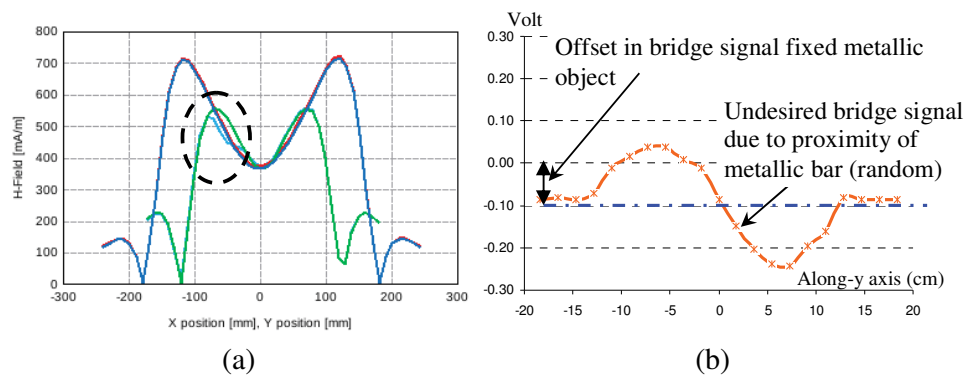
Figure 3-5: Influence of proximity of metallic object to the bridge reader antenna
(a) Magnetic fields when antenna operating near to metallic objects
(b) Bridge signal when it moves over one of the metallic bars underneath the floor (worse case scenario)

The magnitude of the induced magnetic fields is in general, reduced due to presence of both the fixed and randomly located metallic objects. The fixed metallic structures

cause constant reduction on magnetic field, for the randomly present metallic objects, the magnetic field amplitude diminishes only when the antenna passes over them. This is due to the fact that, the close proximity of metallic object to an antenna changes the antenna impedance that causes less power to be delivered thus reducing the level of magnetic fields.

As for the variation of bridge signal is concerned, the fixed metallic objects create an offset to the bridge signal, whereas a randomly present metallic object makes the bridge signal change even without the detection of any tag thus causing undesired positioning errors and confusion. The reason for this is that the operation of the bridge depends on the changes in the antenna impedance. When unsymmetrical metallic object is present in close proximity to the bridge antenna, the impedance in all the loops (which form the bridge) will be modified resulting in generation of distorted bridge signal as shown in the **Figure 3-5**(b).

The above results indicate that the presence of metallic objects in the proximity of bridge loop reader antenna reduces magnetic fields induced in the tag plane and can distort the bridge signal. Also, the reduction in the magnetic fields can reduce the ability of the reader to detect floor tags. The distortion caused to the bridge signal will result in errors to the estimation of tag's position. In the next section, we will analyse the cause of this problem and investigate methods to minimise and eliminate them.

3.3 Impedance variation of reader loop antenna using equivalent circuits

To simplify analysis and understand how a metallic object affects the magnetic fields thereby distorting the bridge signal, we will first examine the impedance characteristics of a single loop antenna, which we will denotes as the reader loop, and can be regarded as one of the loop elements in a bridge reader antenna. Factors contributing to the changes in the impedance of the reader loop can be categorised into three aspects: i) the proximity of a tag; ii) the proximity of a metallic object, and iii) proximity of both the tag and the metallic object. The change in the reader loop impedance is examined for all the three categories by considering the arrangements as illustrated in Figure 3-6.
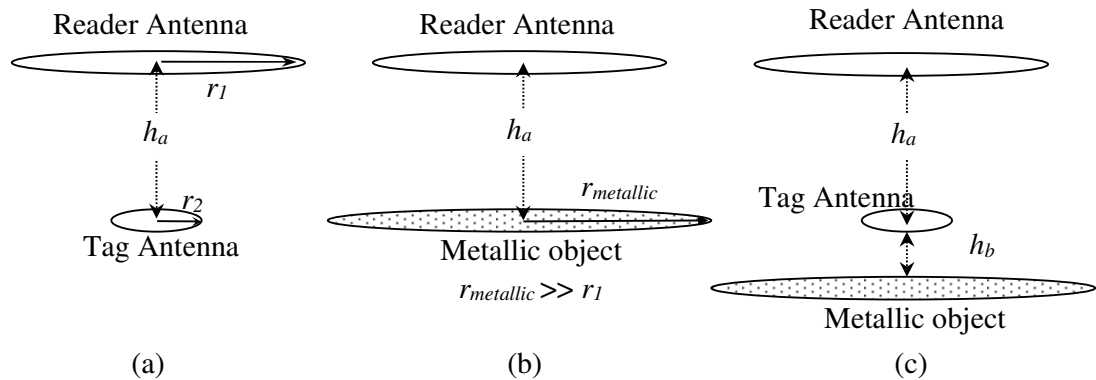
Figure 3-6: Changes to the impedance of a loop antenna

To investigate the effect, firstly the distance h_a is incrementally varied along a line that is centred and perpendicular to the plane of the reader loop. Since we are dealing with near magnetic fields, the magnetically coupled equivalent circuits can help to derive expressions for the changes in the reader loop impedance for all the three cases. This will help to identify methods to minimise the effect of metallic objects which will then lead to improvements in the performance of the bridge antenna for localisation and positioning. Note that, at this stage we limit our equivalent circuit analysis for these metallic objects that can be approximate using a large metallic plate, mainly to simplify our analysis. It will be shown in the later sections that the proposed methods of improvement that will result as an outcome of our approximated equivalent circuits can be applicable to various forms of realistic metallic objects that are either not necessarily large or not be located on the plane parallel to the reader antenna.

3.3.1 Equivalent circuit

Magnetically coupled equivalent circuit is typically employed to investigate the operational performance of loop antennas [50, 99]. We extend the technique with appropriate modifications to investigate the changes in the reader loop impedance for the three scenarios shown in Figure 3-6.

Also, to simplify the problem, the following assumptions are made so as to ensure that the equivalent circuits closely represent the scenarios considered here. Firstly, the diameter of tag's antenna, which is also another loop antenna, is much smaller than that of the reader loop antenna. Secondly, the surface area of the metallic object (a large metallic plate is considered here) is assumed to be much larger than that of the area of

the reader loop antenna. Thirdly, the planes containing the reader loop, tag loop, and the metallic plate are all parallel to each other and their centres are aligned as illustrated in Figure 3-6. Since we assume large metallic plate, we can utilise the method of images to simplify the analysis. All the three equivalent circuits and the resulting expressions for the variation in the reader loop impedance are described in the following sub sections.

3.3.1.1 Proximity of a tag to a reader antenna

Here we will look at the influence of reader-tag proximity to the impedance of the reader loop. Let us examine the equivalent circuit representing the elements associated with the reader and a tag loop antennas as shown in **Figure 3-7**. The terms R_1, R_2, L_1, and L_2 represent resistance and inductance of the reader and tag antennas respectively. Other circuit elements with subscript 'p' and 's' represent components for impedance matching networks. The subscripts '1' and '2' denote elements associated with the reader and tag respectively. The reader is excited by a source V_0 that has source impedance R_0. The load at the tag antenna R_L represents the impedance of the tag's IC.
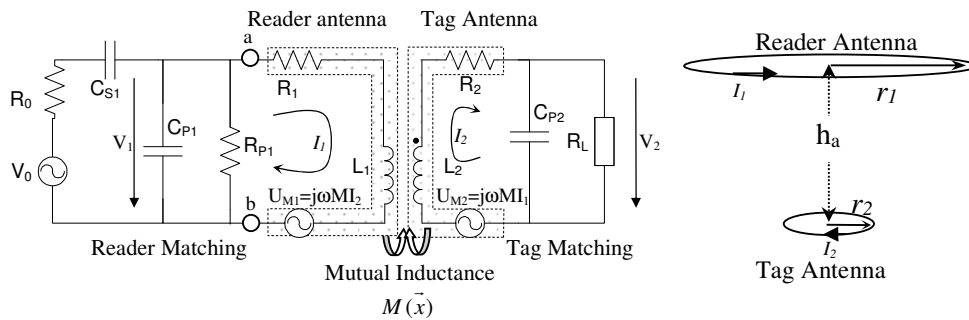
Figure 3-7: Equivalent circuit for reader-tag mutual inductance

Referring to **Figure 3-7**, the flow of current I_1 in the reader antenna creates a varying magnetic field near to the reader loop. Placing the tag closer to the reader loop will energise the tag circuitry through the induction of current I_2 in the tag's loop antenna. This current I_2 will produce magnetic fields that oppose the initial fields by means of magnetic mutual inductance due to Lenz's law [100].

An imaginary impedance '$j\omega M$' with the current I_2 can be introduced within the reader antenna equivalent circuit to represent potential 'U_{M1}' due to mutual inductance effect [51, 99]. Similarly, in the equivalent circuit of the tag antenna, the potential due to coupling is represented as U_{M2}.

Since the potential U_{M1} is the function of I_2, it implies that U_{M1} is the function of circuit parameters of the tag antenna. To clarify this, we extract some of the useful expressions from the above equivalent circuit. At points 'a' and 'b' we can write the following equation:

$$V_1 = V_{R1} + V_{L1} - U_{M1} = I_1 R_1 + I_1 j\omega L_1 - I_2 j\omega M \tag{3.1}$$

The term I_2 can be obtained from the tag antenna circuit through the following equation:

$$U_{M2} = V_{L2} + V_{R2} + V_2 = I_2 j\omega L_2 + I_2 R_2 + I_2 \left(\frac{\frac{1}{j\omega C_{P2}} R_L}{\frac{1}{j\omega C_{P2}} + R_L} \right) = I_2 j\omega L_2 + I_2 R_2 + I_2 \left(\frac{R_L}{1 + j\omega C_{P2} R_L} \right)$$

Rearrange for I_2:

$$I_2 = \frac{U_{M2}}{j\omega L_2 + R_2 + \left(\dfrac{R_L}{1 + j\omega C_{P2} R_L} \right)} = \frac{j\omega M I_1}{j\omega L_2 + R_2 + \left(\dfrac{R_L}{1 + j\omega C_{P2} R_L} \right)} \tag{3.2}$$

Substituting I_2 into (3.1) yields

$$V_1 = I_1 R_1 + I_1 j\omega L_1 - \frac{j\omega M I_1}{j\omega L_2 + R_2 + \left(\dfrac{R_L}{1 + j\omega C_{P2} R_L} \right)} j\omega M$$

$$V_1 = I_1 R_1 + I_1 j\omega L_1 + I_1 \frac{\omega^2 M^2}{j\omega L_2 + R_2 + \left(\dfrac{R_L}{1 + j\omega C_{P2} R_L} \right)} \tag{3.3}$$

Divide both the sides of (3.3) by I_1 gives the impedance of the reader loop:

$$\frac{V_1}{I_1} = R_1 + j\omega L_1 + \frac{\omega^2 M^2}{j\omega L_2 + R_2 + \left(\dfrac{R_L}{1 + j\omega C_{P2} R_L} \right)} \tag{3.4}$$

The first and the second terms in (3.4) are the initial reader loop resistance and reactance respectively. The last term in (3.4) is the impedance due to inductive interaction between the reader loop and the tag loop. The denominator of the last term clearly indicates the elements of tag impedance, which include the original tag's loop impedance, the matching impedance, and the load impedance of tag's IC chip. This last term will be denoted as *transformed tag impedance* Z'$_{\text{Tag}}$, given by

$$Z'_{Tag} = \frac{\omega^2 M^2}{j\omega L_2 + R_2 + \left(\dfrac{R_L}{1 + j\omega C_{P2} R_L}\right)} .$$ (3.5)

Now we need to obtain Z'_{Tag} as a function of reader tag separation h_a. The only parameter which influences the reader-tag separation in the above equation is the mutual inductance M. Consider the reader and tag loops having radius r_1 and r_2 respectively with $r_2 \leq r_1$. The planes of the loops are assumed to be always parallel and their separation is h. The centres of both the loops are also assumed to be aligned. Under this configuration, the mutual inductance 'M' between the two loops is related to the loop geometry and the separation between the two loops, which is given by [51]:

$$M = \frac{\mu_0 r_1^2 r_2^2 \pi}{2\left(r_1^2 + h_a^2\right)^{3/2}}$$ (3.6)

Substituting (3.6) into (3.5) gives:

$$Z'_{Tag} = \frac{(\mu_0 \omega\, N_1 N_2 r_1^2 r_2^2 \pi)^2}{\left(j\omega L_2 + R_2 + \left(\dfrac{R_L}{1 + j\omega C_{P2} R_L}\right)\right) 4\left(r_1^2 + h_a^2\right)}$$ (3.7)

Using the parameters listed in **Table 3-1**, the relationship between tag proximity and the change in the transformed tag impedance Z'_{Tag} that seen in the reader loop antenna is plotted in **Figure 3-8**.

Table 3-1: Parameters used to evaluate proximity of tag

Parameters	Values
r_1	$0.32*0.23/\pi$ meter
r_2	$r_1/4$ meter
N_1	1
N_2	1
f	13.56MHz
u_0	$4\pi*10^{-7}$ H
R_L	300 Ohm
L_2	$(N_1 u_0 \pi\, r_2)/2$ Henry
R_2	0.5 Ohm
C_{P2}	$[(2\pi f)^2 L_2]^{-1}$ Farad
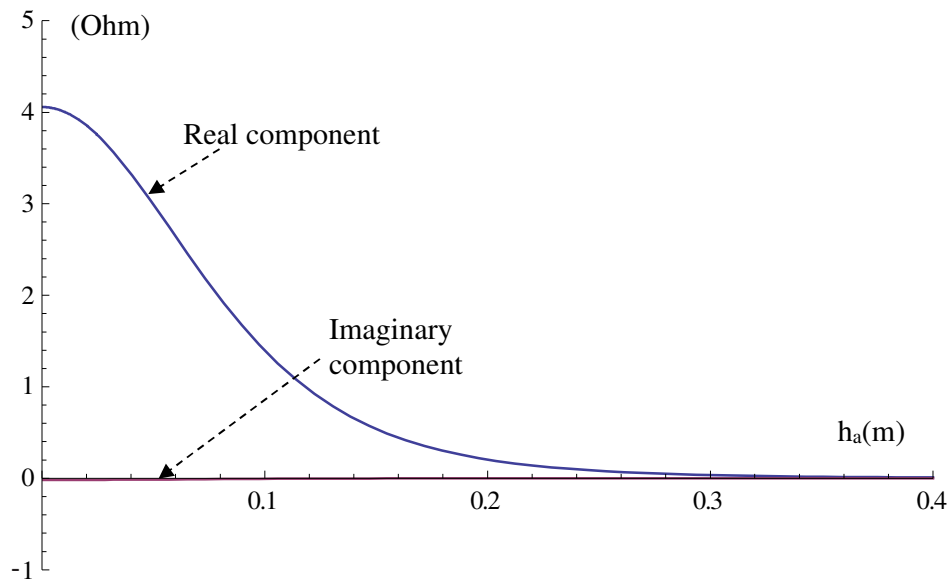
Figure 3-8: Change in the transformed tag impedance (Z'_{Tag}) seen at the reader loop.

Results in **Figure 3-8** indicate that the real component changes significantly compared to the imaginary component. Now let us examine the change in the loop impedance when placed in close proximity to a large metallic plate.

3.3.1.2 Proximity of a metallic object to a loop reader antenna
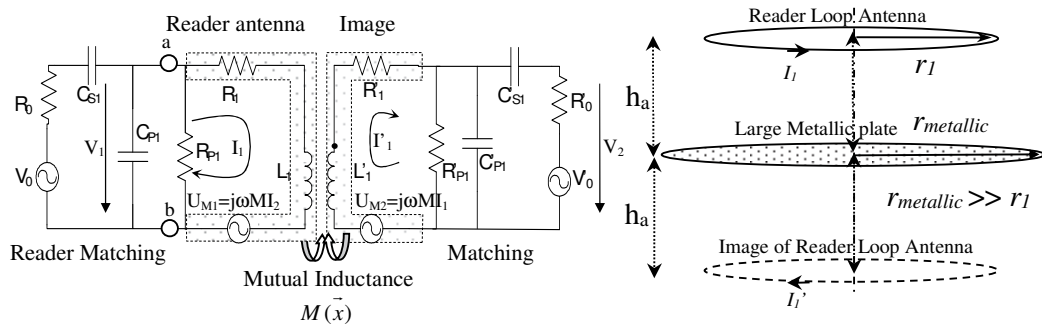
Figure 3-9: Equivalent circuit for reader-image mutual inductance

To investigate the influence of metallic object on the input impedance of the loop antenna, we consider the scenario as illustrated in Figure 3-9. The metallic object is considered to have dimensions larger than the loop reader antenna. Under this scenario, method of images can be applied [101]. Considering the image of the current in the loop with respect to the metallic plate, a modified equivalent circuit can be developed to analyse the effects mutual inductance as shown in Figure 3-9.

The above circuit is quite similar to the previous one except the tag is replaced by image of reader loop antenna. From image theory we know that the magnitude of image current $|I_1'|$ is equal to the magnitude of the current in the reader loop $|I_1|$. Applying the same procedure as in the previous analysis but with consideration that the currents in both the loops having the same magnitude i.e. $|I_1|=|I_2|$, we can obtain the input impedance in the reader's loop due to the presence of large metallic plate using

$$Z_{R'}' = j\omega M \tag{3.8}$$

This impedance is denoted as transformed impedance $Z'_{Reader'}$. The mutual inductance M in the above equation can be expressed by

$$M = \frac{\mu_0 r_1^4 \pi}{2\left(r_1^2 + h_a^2\right)^{3/2}} . \tag{3.9}$$

Applying this mutual inductance to (3.8), we obtain $Z'_{Reader'}$ as a function of separation between the metallic object and the reader antenna.

$$Z'_{Reader'} = j\omega \frac{\mu_0 r_1^4 \pi}{2\left(r_1^2 + h_a^2\right)^{3/2}} \tag{3.10}$$

Using (3.10) and applying the value of variables and constant from **Table 3-1**, the impedance change in the loop reader antenna is plotted in Figure 3-10.
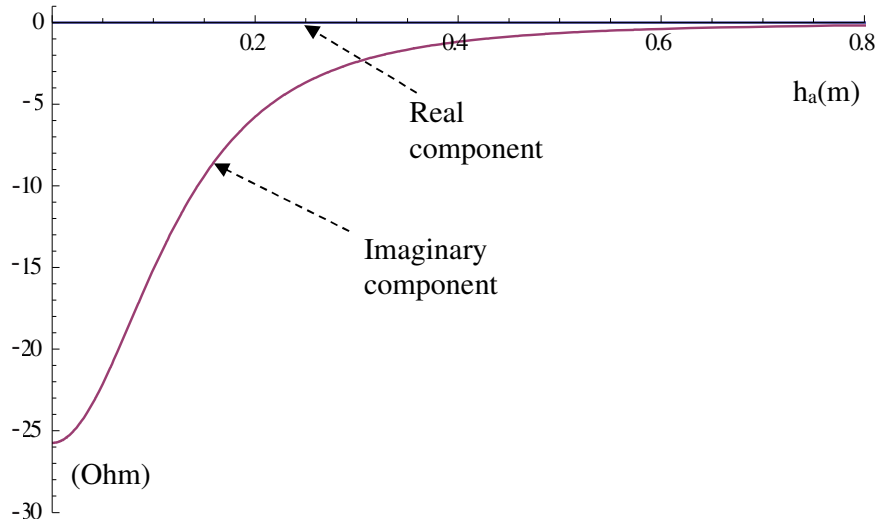
Figure 3-10: The input impedance in the reader's loop due to the presence of large metallic plate or transformed impedance **Z'Reader'.**

Results indicate that the presence of metallic object alters the imaginary component. The results in Figure 3-9 and Figure 3-10 signify that it is possible to differentiate

whether the change in loop impedance is caused due to a metallic plate or a tag by simply examining the changes that occur in the reader loop impedance. Any increase or decrease in real component indicates that a tag is present. On the other hand, if imaginary component shows a decreasing or increasing trend, it indicates the presence of a metallic plate. The changes in the loop impedance can then be obtained from voltage and current across the loop. Now let us consider the third case where both the tag and metallic plate are present together in the close proximity of the reader loop antenna.

3.3.1.3 Reader antenna placed in proximity of a tag and a metallic plate
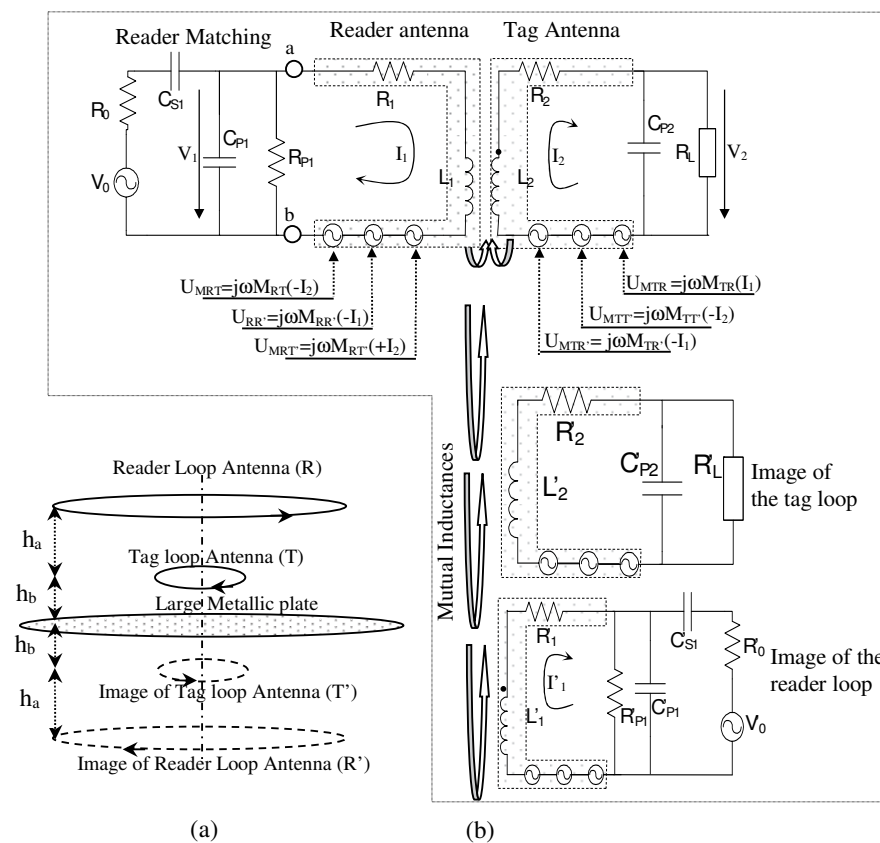
Figure 3-11: Equivalent circuit for the effect of mutual inductance when both the tag and the metallic plate present near the reader loop antenna.

Here, we consider a case when both the tag and a metallic plate are present in close proximity to the reader loop antenna. Our aim is to investigate the changes that may occur in impedance of the reader loop antenna when the separation of the tag and the distance from the metallic object to the reader loop antenna is varied. To simplify this problem, again, we apply the assumptions mentioned earlier. We apply the method of

images to both the reader loop antenna and the tag loop antenna, and use the simplified formulas for self and mutual inductances. The images of both the antennas are illustrated in the **Figure 3-11** (a).

The problem is then transformed into analysing four loop antennas using equivalent circuits. The equivalent circuit for finding the changes in the impedance of the reader loop antenna (denoted as Z'$_{TT'R'}$) due to mutual inductances caused by these loops is illustrated as in **Figure 3-11** (b). Due to the effect of mutual inductances, a set of potentials are induced in the reader loop which are indicated by U$_{MRT'}$, U$_{MRR'}$, and U$_{MRT}$. Utilising the same procedure as in previous section (equation (3.1) to (3.5)), the impedance change in the reader loop can be determined by dividing the potential due to the mutual inductance with the current I_1. Here, we apply the same approach along with the superposition principle to include all the effects of mutual inductances influenced by the reader loop. Applying the above steps, we have

$$Z'_{TT'R'} = \frac{U_{M_{RT}} + U_{M_{RT'}} + U_{M_{RR'}}}{I_1},$$ (3.11a)

$$Z'_{TT'R'} = \frac{j\omega M_{RT}(-I_2) + j\omega M_{RT'}(I_2) + j\omega M_{RR'}(-I_1)}{I_1}.$$ (3.11b)

The term I_2 in (3.11b) can be obtained by examining the equivalent circuit of the tag loop antenna in the **Figure 3-11**. From the tag's loop equivalent circuit, I_2 can be expressed as:

$$I_2 = \frac{U_{M_{TR}} + U_{M_{TT'}} + U_{M_{TR'}}}{j\omega L_2 + R_2 + \left(\dfrac{R_L}{1 + j\omega C_{P2} R_L}\right)} = \frac{j\omega M_{TR}(I_1) + j\omega M_{TT'}(-I_2) + j\omega M_{TR'}(I_1)}{j\omega L_2 + R_2 + \left(\dfrac{R_L}{1 + j\omega C_{P2} R_L}\right)}$$

Solving for I_2:

$$I_2 = \frac{j\omega(M_{TR} + M_{TR'})(I_1)}{j\omega M_{TT'} + \left(j\omega L_2 + R_2 + \left(\dfrac{R_L}{1 + j\omega C_{P2} R_L}\right)\right)}$$ (3.12)

Substituting I_2 into 3.11 we get:

$$Z'_{TT'R'} = \frac{-\omega^2 (M_{TR} + M_{TR'})(M_{RT'} + M_{RT})}{j\omega M_{TT'} + \left(j\omega L_2 + R_2 + \left(\dfrac{R_L}{1 + j\omega C_{P2} R_L}\right)\right)} - j\omega M_{RR'}$$ (3.13)

Mutual inductance M_{ij} can be calculated using:

$$M_{ij} = \begin{cases} \dfrac{\mu_0 r_i^2 r_j^2 \pi}{2\left(r_i^2 + h_{ij}^2\right)^{3/2}} & \text{for i} \geq \text{j}, \\[3ex] \dfrac{\mu_0 r_i^2 r_j^2 \pi}{2\left(r_j^2 + h_{ij}^2\right)^{3/2}} & \text{for i<j}, \end{cases} \qquad i,j = \{T,R,T',R'\}. \qquad (3.14)$$

In (3.14), the distances $h_{ij} = \{h_{TR}, h_{TR'}, h_{RT'}, h_{RT}, h_{TT'}, h_{RR'}\}$ can be obtained by examining the separations involving reader and the tag antennas along with their images illustrated in **Figure 3-11** (a). For convenience, we tabulated these distances in **Table 3-2** below.

Table 3-2: The distance h_{ij} and its relation with the parameters h_a and h_b

h_{ij}	Distance in term of h_a and h_b
h_{TR}	h_a
$h_{TR'}$	h_a
$h_{RT'}$	$h_a + 2h_b$
h_{RT}	h_a
$h_{TT'}$	$2h_b$
$h_{RR'}$	$2(h_a + h_b)$

Using (3.13) with the parameters from **Table 3-1**, the changes in impedance of the reader loop antenna are computed and plotted in **Figure 3-12** and **Figure 3-13** by fixing h_b=5cm and h_b=10cm respectively, while varying h_a from 0 to 40cm.

Figure 3-12 and **Figure 3-13** indicate that both the real and imaginary parts of the reader loop impedance get modified for different h_a. Significant changes seem to occur on the imaginary part compared to the real part. The reason for this is when a tag is placed very close to a metallic plate, the magnetic fields of the tag get severely perturbed by the metallic plate. This problem can be minimised by placing the tag at some distance away from the metallic plane/object as indicated in the second plot. In other words, the changes in the real part that is caused due to the tag can be improved by increasing the distance h_b between tag plane and the metallic plate. The change in the imaginary part is negative while it is positive for the real part. We will demonstrate the significance of these results for predicting the performance of the bridge antenna in the next section.
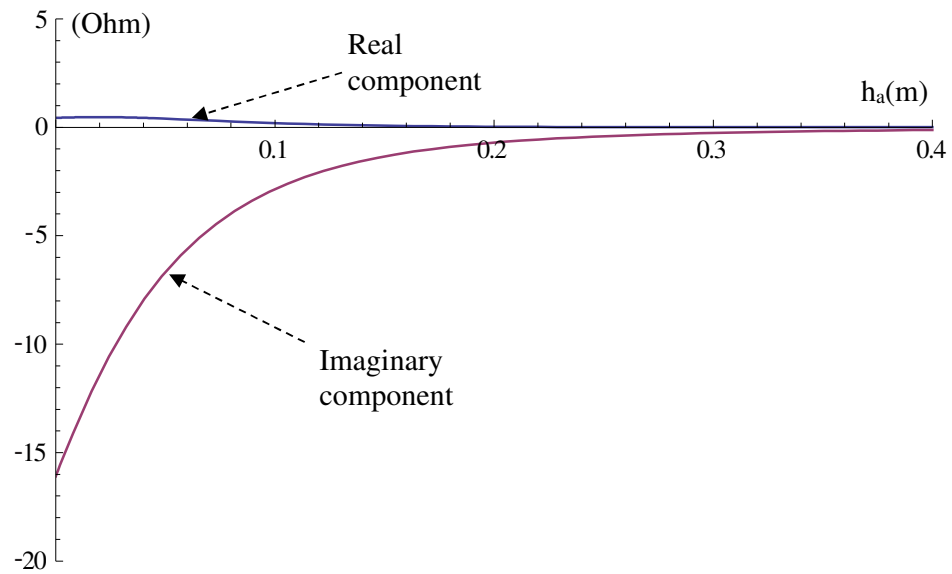
Figure 3-12: Change in the impedance of the reader loop antenna for the separation h_b=5cm
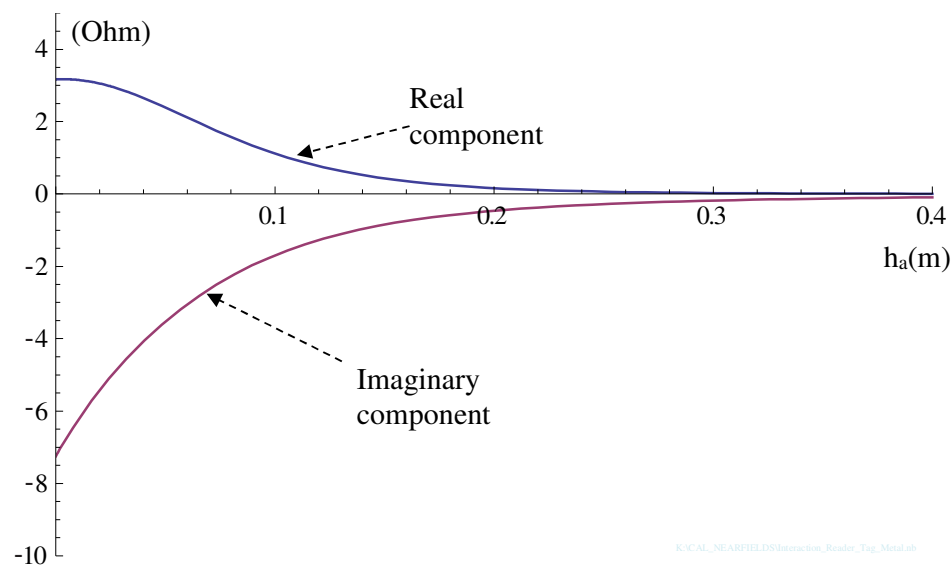
Figure 3-13: Change in the impedance of the reader loop antenna for the separation h_b=10cm

3.3.2 Techniques to improve bridge antenna performance

The bridge loop antenna contains many loop elements and any changes in a single reader loop will contribute to changes in the overall bride loop antenna. It is important to highlight the possible methods to improve the performance of the bride loop antenna based on the results from equivalent circuit presented so far.

3.3.2.1 Interference due to magnetic fields

The results presented in previous section show that the imaginary part of the reader loop impedance decreases when the reader loop gets closer to a metallic plate. This means the inductance of the reader loop reduces with the proximity of the metallic plate and thus reducing the induced magnetic fields.

In addition, the change in the reader loop impedance also detunes the impedance match of the reader loop. As a result, the maximum current flowing in the reader loop will be decreased.

To ensure that both the reader and tag antennas provide sufficient magnetic fields for successful detection, metallic objects must not be placed too close to the antennas. This can be ensured by installing the reader and the tag antennas at a sufficient distance from the nearby metallic structures.

The reader impedance mismatch due to presence of fixed metallic structure in its proximity can be improved by properly changing the matching elements. This makes the antenna to revert back to resonance at the operating frequency, thus maximising the current to the antenna from the reader.

3.3.2.2 Interference with Bridge signal ($V_β$)

The separation between the metallic object and the reader as well as tag antennas are considered to be sufficient enough to allow adequate level of magnetic fields for interrogation. The loop elements of the bridge antennas are assumed to be identical and each loop behaves similarly to the reader loop antenna presented in the last section.

In general, when a metallic object is not symmetrically located with respect to the central line of the bridge antenna, a bridge potential will be produced. This is because the metallic object alters impedance of the bridge loops unequally; hence causes imbalance in the bridge, which then produces the bridge potential ($V_β$).

The alteration of the bridge potential depends on the position of the metallic objects with respect to central line of the antenna. Metallic objects that are fixed and located asymmetrically with respect to the antenna cause a constant offset in the bridge potential. Mainly the metallic structure of the moving object to which the reader antenna

is attached to, can be considered under this scenario. The effect of this metallic structure can be indirectly eliminated by a shielding plate to shield the metallic structure from the antenna. The effect of shielding plate will be discussed in detail in the later sections. Since the shielding plate is symmetrically positioned with respect to the antenna, the perturbation of magnetic fields gets cancelled thus no voltage offset is generated at bridge terminals.

The other types of metallic objects that can alter the bridge potential are those that are randomly present in the path followed by the antenna. The magnitude of bridge signal can be high when the interfere due to the randomly located metallic objects get too close to the antenna. This interference therefore contributes to the false signal resulting in error for the location estimation of tags. Thus, the severely altered bridge signal cannot be directly used to identify the position of tags. They have to be corrected to minimise effect of interference that cause the unnecessary alterations. Further analysis and possible methods of improvement are discussed in the next section.

3.4 Methods to minimize the effect of metallic objects

The previous section presents an analysis on the changes in impedance of a single loop reader antenna due to tags and metallic structure placed in its close proximity. We showed that proximity of metallic objects dominantly alters the imaginary part of reader loop impedance while the proximity of tags alters its real part. This characteristic makes it possible to discriminate between a tag and a metallic object. However, the changes in impedance that occur within the loop elements of a bridge antenna cannot be easily measurable directly. Therefore other form of signals that have similar characteristic need to be identified.

To investigate this, we consider our analysis on a single bridge antenna, which is schematically shown in **Figure 3-14**. The measurable signals at the bridge are potential $V_{\beta 1}$ and $V_{\beta 2}$ as denoted in **Figure 3-14** (b). We therefore need to manipulate these signals so that they can provide a clue to the position of the detected tag irrespective of the proximity of any metallic objects. In other words, we aim to get an expression out of $V_{\beta 1}$ and $V_{\beta 2}$ so that it is a function of the position of the detected tag regardless the effects due to the proximity of metallic objects.
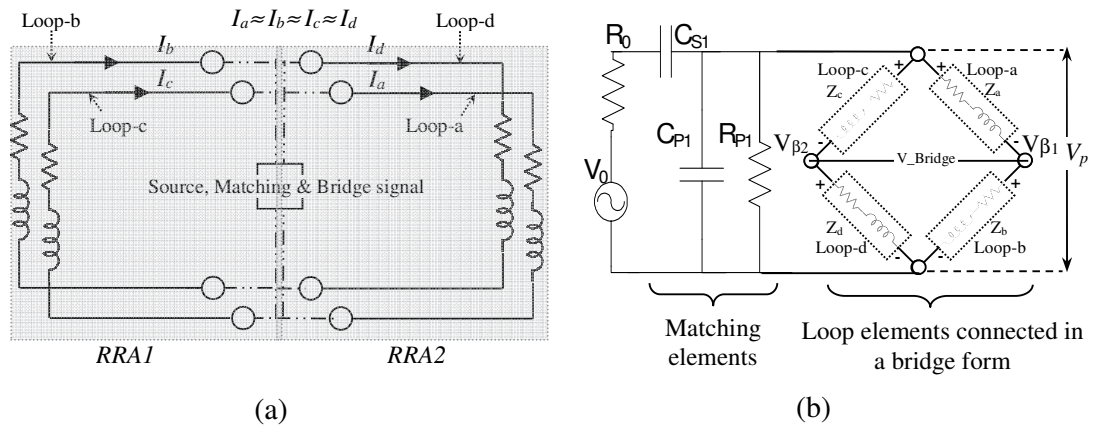
Figure 3-14: Loop elements of a bridge antenna, and its equivalent circuit with matching elements

To achieve this aim, we firstly obtain the expression of $V_{\beta 1}$ and $V_{\beta 2}$ as a function of separation of tags and metallic objects from the bridge antenna. We will use the bridge equations as well as the equations of equivalent circuits derived previously. To simplify analysis, we regard each loop of the bridge antenna in **Figure 3-14** is similar to the reader loop antenna used in the equivalent circuits in section 3.3, and the proximity of tag and/or metallic object is within reader recognition area (RRA1) of the bridge antenna. The tag is assumed to be a small single loop antenna as used previously. Therefore, proximity of tags and/or metallic objects is assumed to occur only on the loop-b and loop-c of **Figure 3-14**. The effect on impedances of both loop-b and loop-c due to proximity of tag and/or metallic object are also assumed to be similar to the single reader loop presented in section 3.3. The assumptions and separation parameters considered in the section 3.3 are also applied to these loops. The changes on impedances of these two loops cause $V_{\beta 1}$ and $V_{\beta 2}$ to vary. The three scenarios are considered: 1) proximity of a tag; 2) proximity of metallic object (in the form of large plate); and 3) proximity of both the tag and the metallic object. The changes in loop impedance under the above mentioned three scenarios are obtained using (3.7), (3.10) and (3.13) respectively as

$$\Delta Z_m = \Delta R_m + j\Delta X_{L,m}, \qquad (3.15)$$

where, $m = \{Tag, Metal, Tag\,\&\,Metal\}$, which denotes the three scenarios.

Applying the changes/effects corresponding to the above three scenarios to the corresponding loops in the bridge, we can obtain the bride signals associated with the three scenarios. The bridge equations described in chapter-2 viz., equations (2.10a) and (2.10b) are used to get expressions for $V_{\beta 1}$ and $V_{\beta 2}$ as

$$V_{\beta 1,m} = \frac{Z}{2Z \pm \Delta Z_m} V_p = \frac{Z}{2Z \pm (\Delta R_m + j\Delta X_{L,m})} V_p, \qquad (3.16)$$

and

$$V_{\beta 2,m} = \frac{Z \pm \Delta Z_m}{2Z \pm \Delta Z_m} V_p = \frac{Z \pm (\Delta R_m + j\Delta X_{L,m})}{2Z \pm (\Delta R_m + j\Delta X_{L,m})} V_p. \qquad (3.17)$$

The V_p is the voltage across the R_p, the C_p and the bridge source terminals as indicated in **Figure 3-14** (b). By examining $V_{\beta 1}$ and the $V_{\beta 2}$ we can obtain an appropriate expression that is a function of the position of the detected tag with respect to the bridge antenna irrespective of its proximity to any metallic object.

Note that in the above expressions, we consider proximity with respect to RRA1. This is sufficient because RRA1 and RAA2 are symmetrical, and hence the effects on the bridge potential due to proximity of tag/or metallic object between these two are just a reverse version of one another. Another important assumption is that, we use large metallic plate to simplify our analysis, in this case we assume that loops of RRA2 are isolated and do not interact with the metal plate because we only interested to examine the effect of proximity of metal/tag on loops of RRA1. We also assume each loop of RRA1 behaves as the single loop reader antenna presented earlier. To ensure the applicability of our analysis, we will re-validate our findings using results from simulation and experimentation considering more realistic scenarios, which will be presented in the later sections. In the following subsections, we will examine $V_{\beta 1}$ and the $V_{\beta 2}$ of the bridge antenna as to obtain the useful expressions to minimise or eliminate the effect proximity of metallic object.

3.4.1 $V_{\beta 1}$-$V_{\beta 2}$ under constant V_p

We firstly look at the potential difference $V_{\beta 1}$-$V_{\beta 2}$ for a fixed value of V_p considering the three scenarios mentioned earlier. These potentials are plotted as in **Figure 3-15**, which indicate that the imaginary part does not change with the close proximity of metallic object but change occurs only with the proximity tag. This feature therefore can be utilised to identify the presence of a tag and its position while at the same time

eliminating the effect of close by metallic objects. The imaginary part of the potentials, i.e. Im($V_{\beta1}$-$V_{\beta2}$) for all the three cases are re-plotted separately in **Figure 3-16** for comparison.
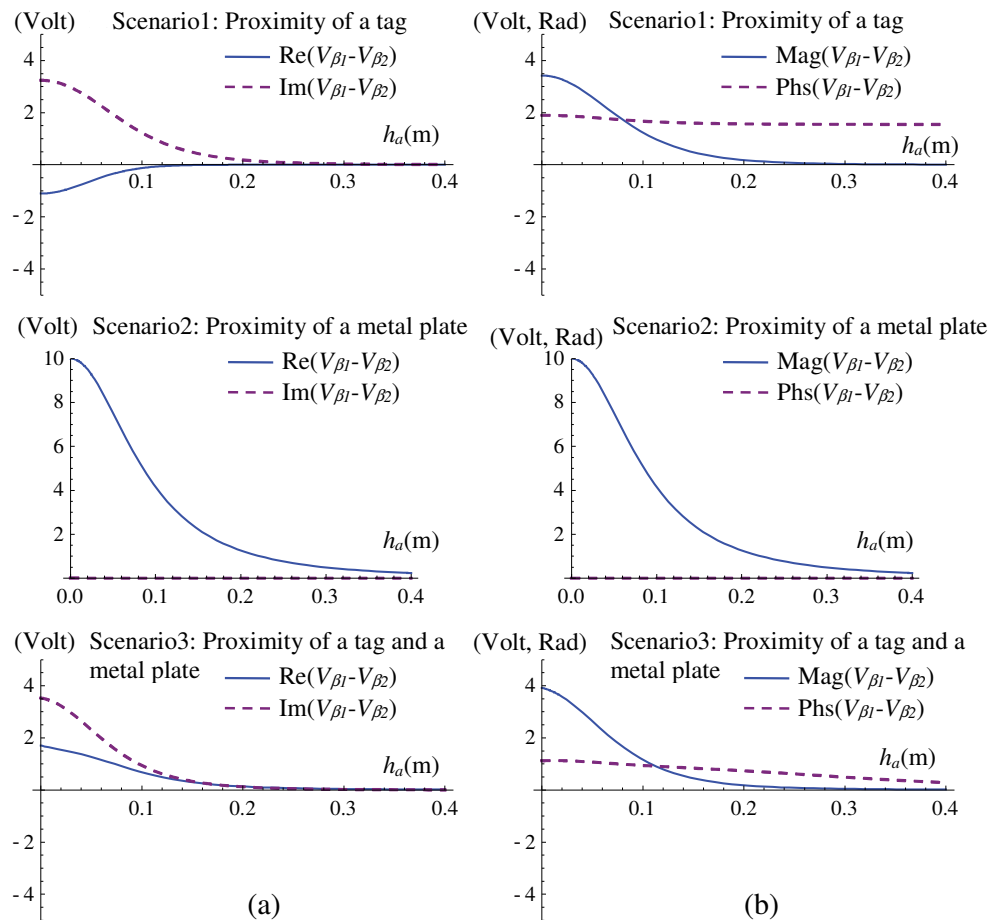
Figure 3-15: $V_{\beta1}$-$V_{\beta2}$ for the three scenarios, V_p is set constant equal to V_{reader}
a) real and imaginary components, and b) magnitude and phase values.

As can be seen in **Figure 3-16**, whenever a tag is present, in close proximity to the reader's antenna, the imaginary component Im($V_{\beta1}$-$V_{\beta2}$) of the bridge potential increases, and there are almost no change in this signal due to close proximity of the metallic object. Referring to the plot, the slight difference between the two lines that correspond to scenario1 and scenario3 is because, when both metallic object and the tag are in close proximity, the metallic object influences the performance of the tag's antenna, which reduces the performance of the tag. This can be minimised by ensuring that tags are not placed too close to metallic objects.
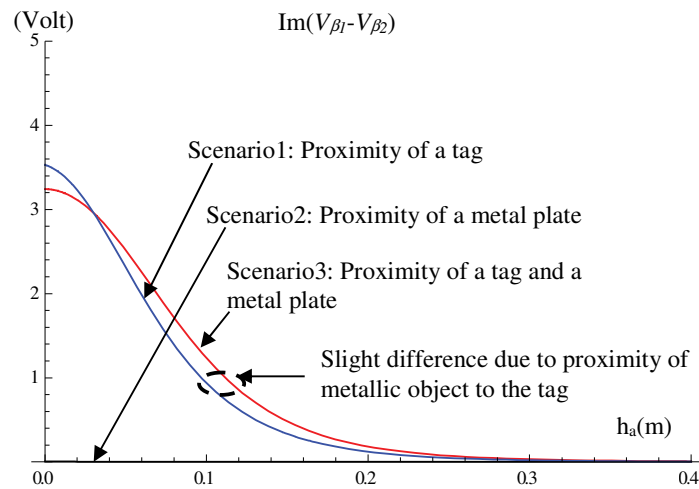
Figure 3-16: Comparison of the imaginary component for all the three cases

These results however require constant V_p which is not the case for a simple bridge antenna. The V_p varies with the impedance of the antenna, and also it depends on the excitation from the RFID reader. To ensure constant V_p, additional circuit is required to regulate the value of V_p, but this is not desirable and impractical because it involves additional components and they must be located close to the bridge terminals of the antenna. Alterative way is to incorporate simple measurement to monitor V_p, and use this V_p to normalise $V_{\beta 1}$ and $V_{\beta 2}$, which will be discussed in the next section.

3.4.2 $V_{\beta 1}$-$V_{\beta 2}$ when V_p is not constant

The potential across the bridge source Vp (see **Figure 3-14** (b)) gets fluctuated due to several factors such as, the changes in the impedance of the bridge, effect of tag-reader interaction etc. Due to this, the potential difference between the left and the right arms of the bridge antenna ($V_{\beta 1}$-$V_{\beta 2}$) does not offer consistent indication about the changes in the impedance of the bridge loops, which makes the previous method not directly applicable under this scenario. The results for ($V_{\beta 1}$-$V_{\beta 2}$) when V_p is not constant are plotted in **Figure 3-17**.
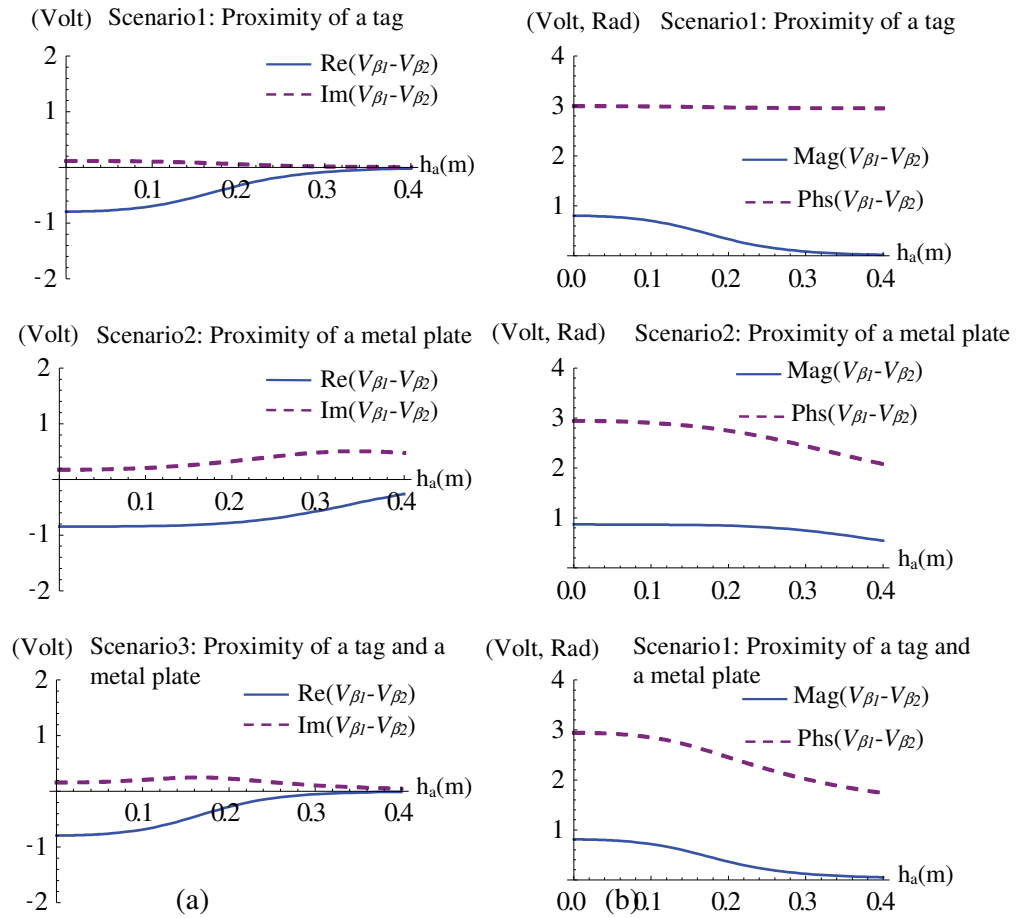
Figure 3-17: $V_{\beta 1}$-$V_{\beta 2}$ for the three cases, when V_p is not fixed
(a) real and imaginary, and (b) magnitude and phase values.

The above results indicate that the imaginary part of the bridge signal $Im(V_{\beta 1}-V_{\beta 2})$ is no longer behave as desired. Hence, it cannot be directly utilised to minimise the effect of proximity of metallic object.

The above problem can be solved if the value of V_p is known. From (3.16) and (3.17) we can rewrite the expressions for $V_{\beta 1}$ and $V_{\beta 2}$ as

$$V_{\beta 1} = \frac{Z}{2Z \pm \Delta Z}V_p = \frac{Z}{2Z \pm (\Delta R + j\Delta X_L)}V_p = H_{\beta 1}V_p$$

$$V_{\beta 2} = \frac{Z \pm \Delta Z}{2Z \pm \Delta Z}V_p = \frac{Z \pm (\Delta R + j\Delta X_L)}{2Z \pm (\Delta R + j\Delta X_L)}V_p = H_{\beta 2}V_p$$

and

$$V_{\beta 1} - V_{\beta 2} = H_{\beta 1}V_p - H_{\beta 2}V_p = (H_{\beta 1} - H_{\beta 2})V_p. \qquad (3.18)$$

An expression independent from V_p can be obtained by simply divide (3.18) with V_p.

$$(V_{\beta 1} - V_{\beta 2}) / V_p = H_{\beta 1} - H_{\beta 2} \qquad\qquad (3.19)$$

The term $(H_{\beta 1} - H_{\beta 2})$ varies with the change of the impedances of the bridge loops and the change pattern can be comparable to the results given in the previous section whose V_p was set to a constant value.

In the previous section, we have observed that the imaginary component of $(V_{\beta 1} - V_{\beta 2})$ has useful information to provide information about the proximity of a tag regardless the effect of proximity of metallic object to the reader antenna. The similar results are obtained when the above expression (3.19) is applied for the three scenarios viz., scenario1: proximity of a tag; scenario2: proximity of metal plate; and scenario3: proximity of a tag and a metal plate. The results are plotted in **Figure 3-18**.
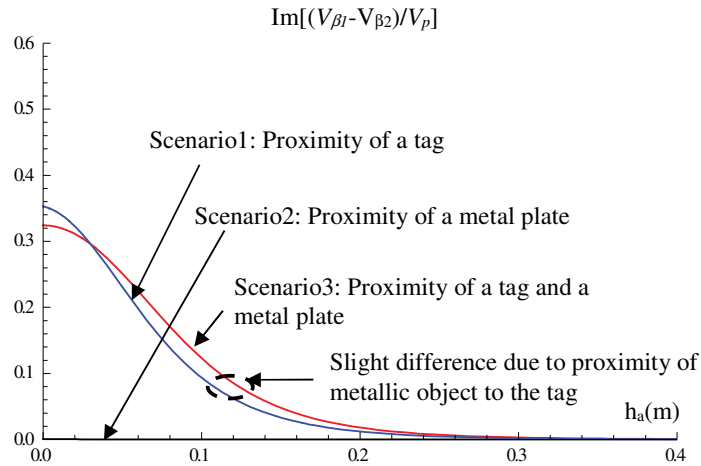
Figure 3-18: Imaginary components independent from V_p, for the three scenarios

The results are now similar to the results obtained in the previous section (see **Figure 3-16**) i.e. when the V_p was kept constant. The results presented in **Figure 3-18** are the scaled version of the results in **Figure 3-16**. The technique presented here eliminates the need of additional components at the antenna to keep constant V_p and therefore much practical. However, we need to measure V_P. In the next sections, we will investigate other alternative techniques.

3.4.3 Use of ratio $V_{\beta 1}/V_{\beta 2}$

Another alternative method is to use the ratio between $V_{\beta 1}$ and $V_{\beta 2}$. Using (3.16) and (3.17) for $V_{\beta 1}$ and $V_{\beta 2}$ respectively, the complex components (real and imaginary) and polar components (magnitude and phase) of the ratio $(V_{\beta 1}/V_{\beta 2})$ are plotted in **Figure 3-19**.
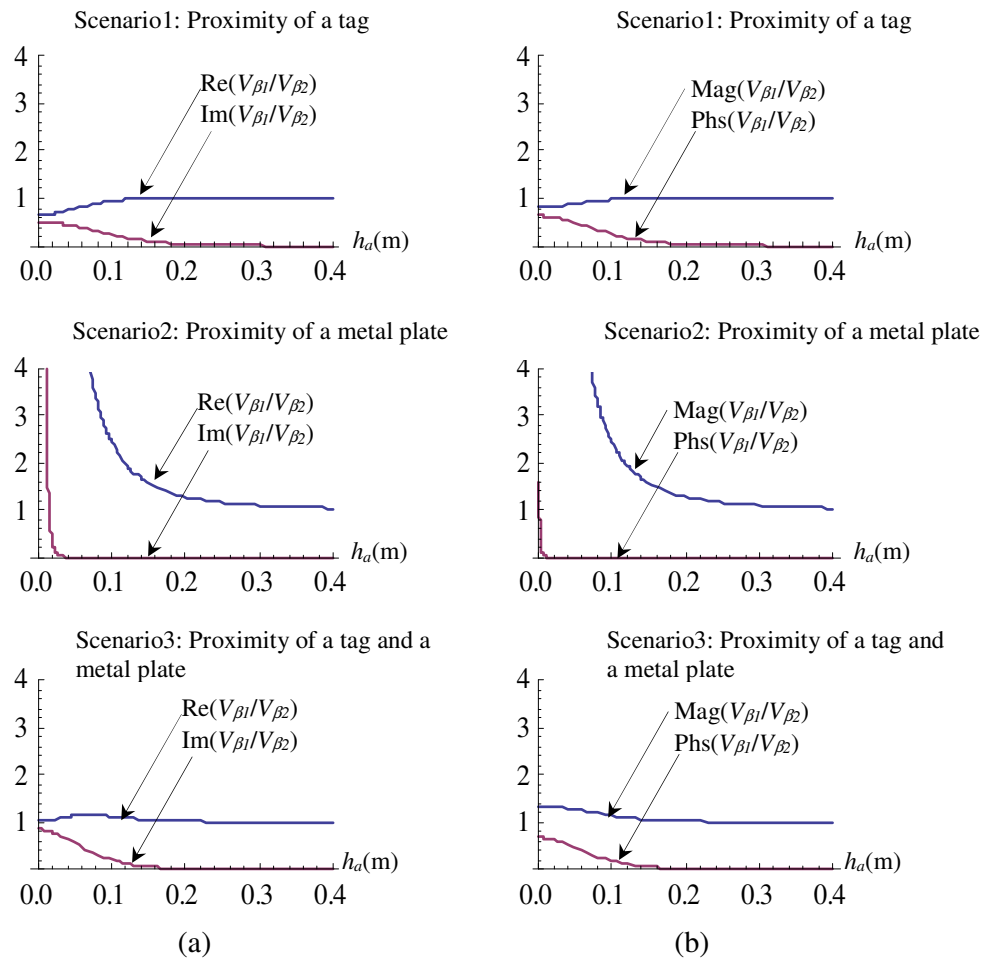
Figure 3-19: The ratio of $V_{\beta 1}$ to $V_{\beta 2}$, for the three cases
(a) real and imaginary components, and (b) magnitude and phase.

The trends from the plot in **Figure 3-19** indicate that, the imaginary part 'Im($V_{\beta 1}/V_{\beta 2}$)' and the phase 'Phs($V_{\beta 1}/V_{\beta 2}$)' of the ratio ($V_{\beta 1}/V_{\beta 2}$) are almost independent to the proximity of metallic plate. Hence, they can be useful to minimise and/or eliminate the effect of proximity of metallic object. These useable signals are combined for all the three cases and they are replotted side-by-side in **Figure 3-20** for better comparisons.
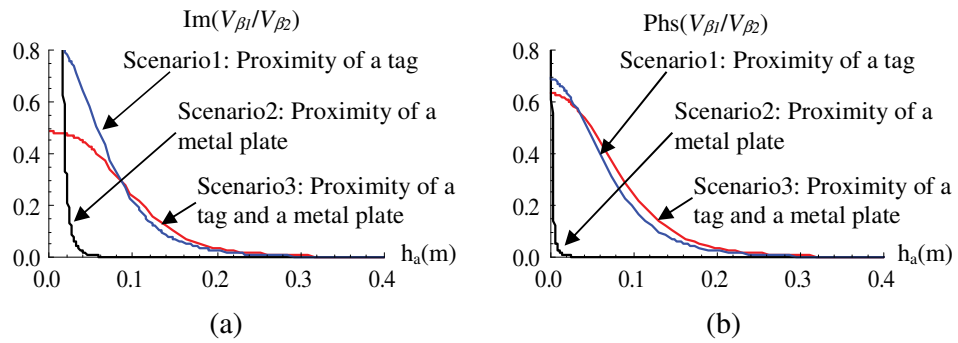
Figure 3-20: Changed in signals derived from the ratio if $V_{\beta 1}/V_{\beta 2}$ for the three scenarios:
(a) the imaginary component of the ratio 'Im($V_{\beta 1}/V_{\beta 2}$)', (b) the phase of the ratio
'Phs($V_{\beta 1}/V_{\beta 2}$)'.

The results in **Figure 3-20** are quite comparable to the one obtained in the previous two sections plotted in **Figure 3-16** and **Figure 3-18**. The main advantage of this technique is that no extra measurement V_p is required. However, we must be careful that when metallic objects are located too close to the reader antenna, this method can also be affected by the interference.

Between these the two proposed approaches in this section, viz., (i) use of imaginary component "Im($V_{\beta 1}/V_{\beta 2}$)", and (ii) use of phase "Phs($V_{\beta 1}/V_{\beta 2}$)"), the second approach appears to provide much better performance as evident from the plots shown in **Figure 3-20**. This second method is less sensitive to the distance of the metallic objects from the reader as against to the first one.

To measure, the phase of the ratio ($V_{\beta 1}/V_{\beta 2}$), we need not to measure individual magnitudes and phases of $V_{\beta 1}$ and $V_{\beta 2}$. Since, the resulting phase is the phase difference between the two signals, this technique is therefore greatly simplify our measurement. This phase different measurements can be achieved using phase detectors that are commercially available.

From **Figure 3-20**(b), we can observe that the difference between signal due to third scenario (i.e. due to proximity both the tag and metallic object) and that of the first scenario (i.e. due to proximity of tags only without metallic object) is very small. Again, we would like to restate that, this slight difference is mainly due to the interference at the tag cause by the metallic object. The metallic object distorts the magnetic field which change the signal received by the tag. Also, the metallic object reduces the

magnetic fields induced from the tag. This problem can be minimised by ensuring that the tags are placed away from any obvious metallic objects. If a tag has to be placed closer to a metallic object (provided it can still readable by the reader), a correction factor associated with the tag can be incorporated into the database, so that the signal can be corrected. The efficacy of the proposed technique of using phase of the gain (i.e. $Phs(V_{\beta1}/V_{\beta2})$) will be investigated using realistic models and experimentations which will be discussed in the next section.

3.5 Validation of the proposed technique

In the previous section, bridge antenna potentials were analysed considering a simple loop with simplified assumptions so that the effect of metallic object on the bridge potential can be established. However, use of realistic antenna and realistic metallic object are necessary to establish the usefulness of the proposed techniques. The metallic object may not always be in the form of large metal plate, so that the use of method of images may not be accurate. It is therefore very useful to analyse using realistic numerical electromagnetic models on the methods proposed.

In this section, we use FEKO simulation using an extension of the bridge antenna explained in chapter-2 by incorporating a shielding plate to the bridge reader antenna. The clearance distance between the shielding plate and the antenna is chosen to be 3cm. The selection of this clearance distance is based on the analysis in section 3.5 that will be described later. Magnetic fields and the resulting bridge potential signals produced from this model are computed using FEKO. Before performing extensive analysis on the realistic model it is very important to firstly validate this antenna model.

3.5.1 Shielded single bridge triangular loop reader antenna

The antenna used in validating the proposed technique is the shielded single-bridge-triangular-loop, whose realistic numerical model and the fabricated prototype depicted in **Figure 3-21**. Detained geometry of this antenna without shielding is indicated in section 2.6.2.2 of chapter-2.

We firstly validate our analysis by comparing results (magnetic fields and bridge signals) obtained from FEKO computations using realistic models of the bridge reader antenna with the measured results using a prototype.

(a)   (b)
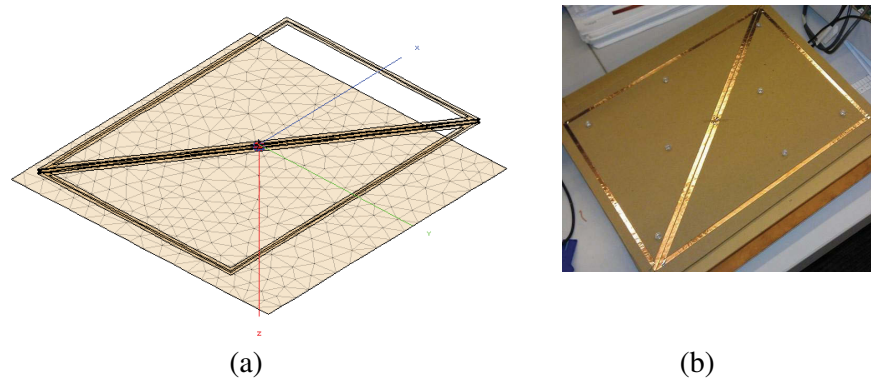
Figure 3-21: The single-bridge-triangular-loop reader antenna
(a) the realistic reader antenna model, and (b) the prototype.

Measured and computed results for magnetic fields along x and y axes on the tag plane at z=-6cm are indicated in **Figure 3-22**(a). The results on bridge potential are obtained when a tag is positioned at different positions relative to the reader recognition area (RRA) of the triangular loop antenna. The procedure is similar to the one provided in the chapter-2. Results on the bridge potential obtained from measurement and FEKO simulations are plotted together in **Figure 3-22**(b).

(a)

(b)
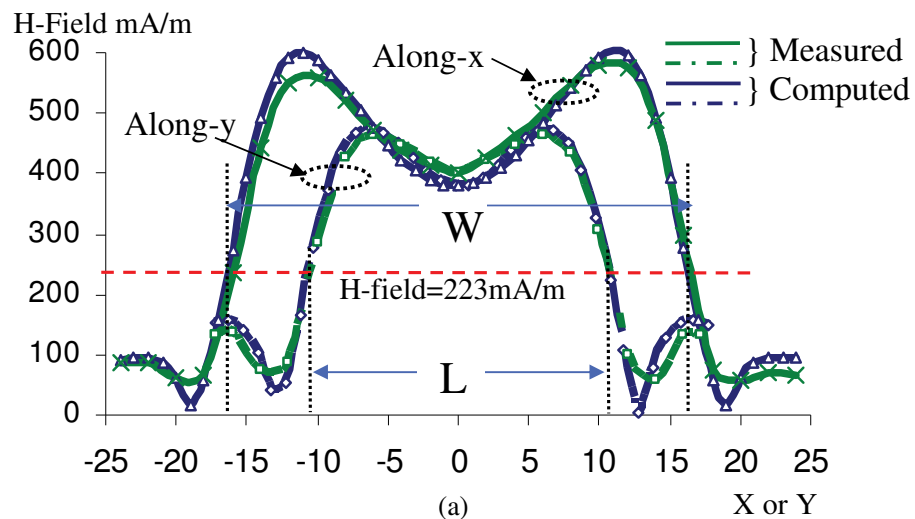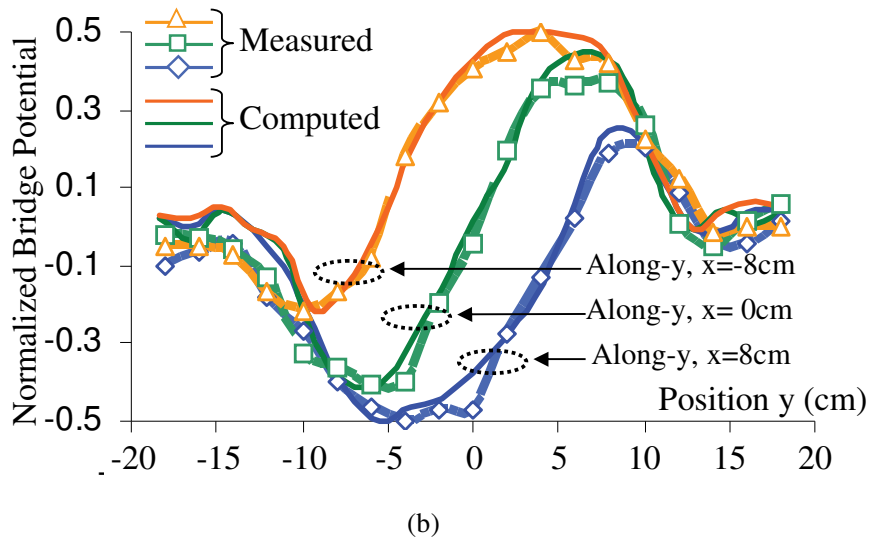
Figure 3-22: Validation of realistic model of shielded single bridge triangular loop reader antenna (TLB).

(a) Magnetic fields, and (b) Bridge signal.

The above results on the magnetic fields and the bridge signal show a very good agreement between the FEKO simulation results using the realistic model and measurements from the prototype. These confirm the accuracy of the antenna model and the FEKO computations. The use of realistic antenna model with FEKO is very useful to effectively investigate the antenna performance especially when it involves with determination of magnetic fields on a plane near to an obstacle which can be difficult to measure. We will use the above shielded bridge antenna realistic model and its prototype to evaluate the proposed techniques for minimising the effect of proximity of metallic objects that will be described below.

3.5.2 Validation for improved bridge signal

In the section of 3.4.3 we have identified that, the use of phase of the gain between signals at arm-1 and arm-2 of a bridge antenna "Phs($V_{\beta 1}/V_{\beta 2}$) or simply $\theta_{V1/V2}$" is able to minimise the effect of proximity of metallic object. Here, we aim to validate the proposed technique using realistic models with FEKO simulations and measurements on prototype. The following three scenarios are considered: i) Only tag is present, ii) Only metallic object is present, and iii) both the tag and the metallic object are present. The type of bridge antenna use is Single Bridge-Triangular Loop equipped with

shielding, the one we readily described in section 3.5.1. The tag used is this validation is similar to the one described in section 2.7. As for the metallic object, we use metallic bar having dimension of (330 mm x 30 mm x 2.5 mm). The antenna is positioned so that its centre is located at origin in a Cartesian coordinates as illustrated in **Figure 2-23** . Both the tag and the metallic bar are positioned in its own planes that are parallel to the plane of the antenna. The centre of tag and the metallic bar are aligned so that they are fixed at x=0 as illustrated in **Figure 2-23**. The vertical separation distance for the tag plane and the metallic plane to the plane of the antenna are denoted by 'h_a' and 'h_m' respectively. In each scenario the tag and/or metallic object is positioned below the antenna at points along y-axis, x=0, so that the tag and/or metal crosses the plane below the antenna as indicated in the Figure 3-23. This to represent the changes in positions of tag and/or metallic object with respect to the antenna so that there will be changes in the bridge signal.
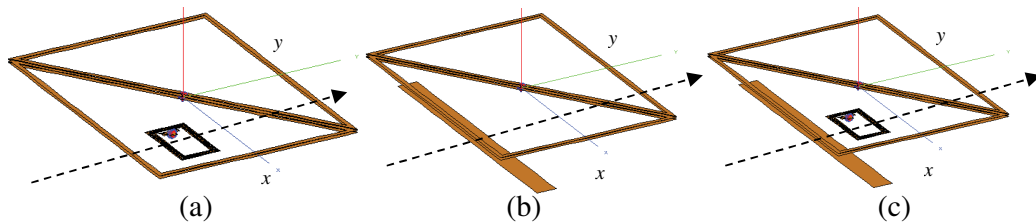
Figure 3-23: Single Bridge-Triangular loop antenna under three scenarios*
(a) Only tag presented, (b) Only when metal object is present, and (c) Both tag and metallic object are present
* The shielding element is not shown as to help with illustration.

    FEKO simulation, and experimental measurements on the prototype antenna considering the above three scenarios are performed by fixing the separation distance 'h_a' and 'h_m'. The changes in the bridge antenna are recorded correspond to the location of the tag and/or metallic bar. We repeat the FEKO simulation and experimental measurement for different set of $h_m = \{10\text{cm}, 8\text{cm}, 3\text{cm}\}$. The '$h_a$' is fixed at '5cm' to represent the typical operating distance. For comparison, we plot the bridge signals, before and after applying the proposed technique. Results for the simulation and experiment are plotted in Figure 3-24 and Figure 3-25 respectively.
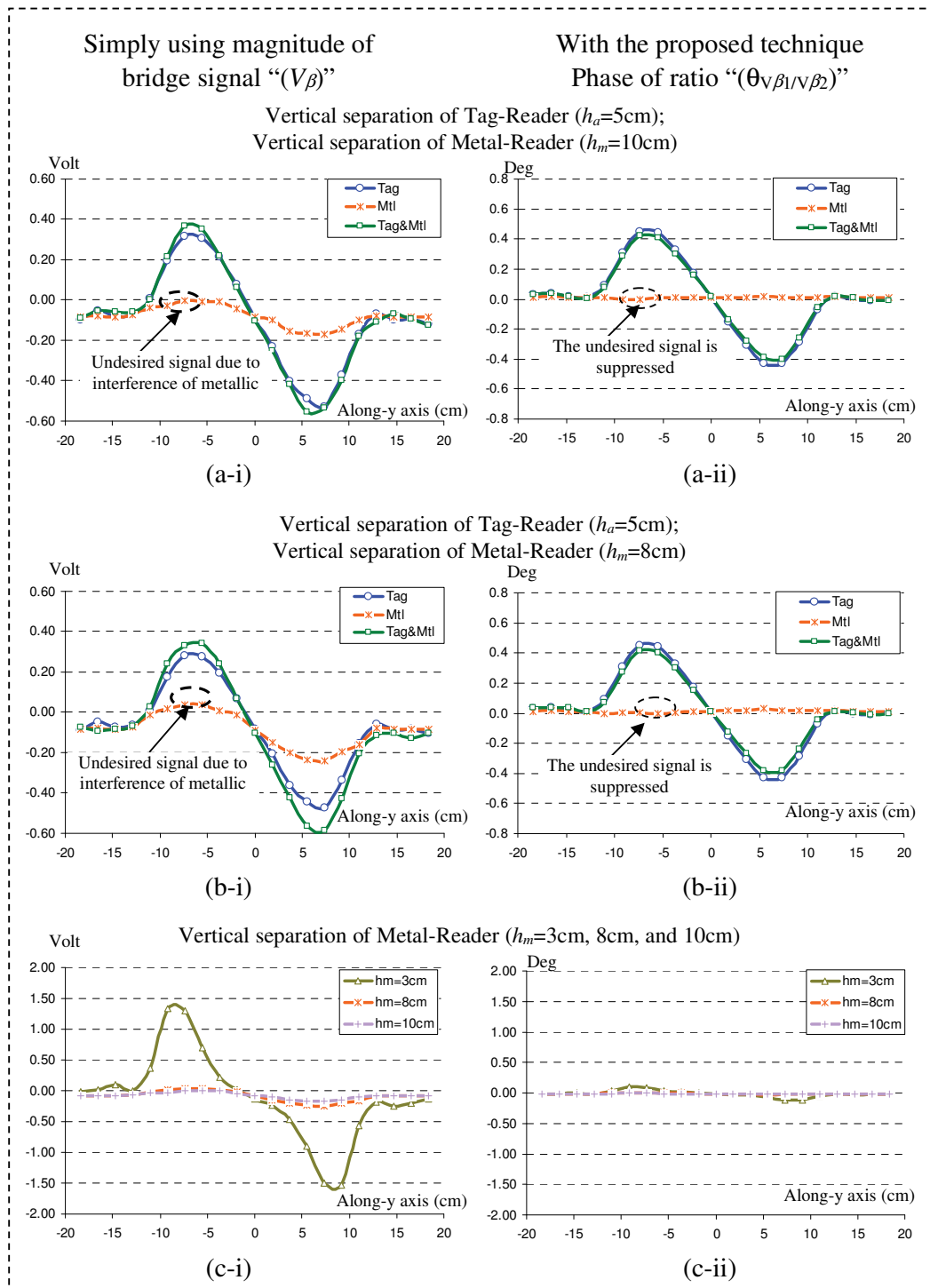
Figure 3-24: FEKO results, Comparison between signals before and after applying the proposed technique
(a) the vertical separation between the Metallic object and the Reader is fixed at h_m=10cm, (b) the separation h_m=8cm, (c) Comparison for extreme case when h_m is varied down to 3cm.
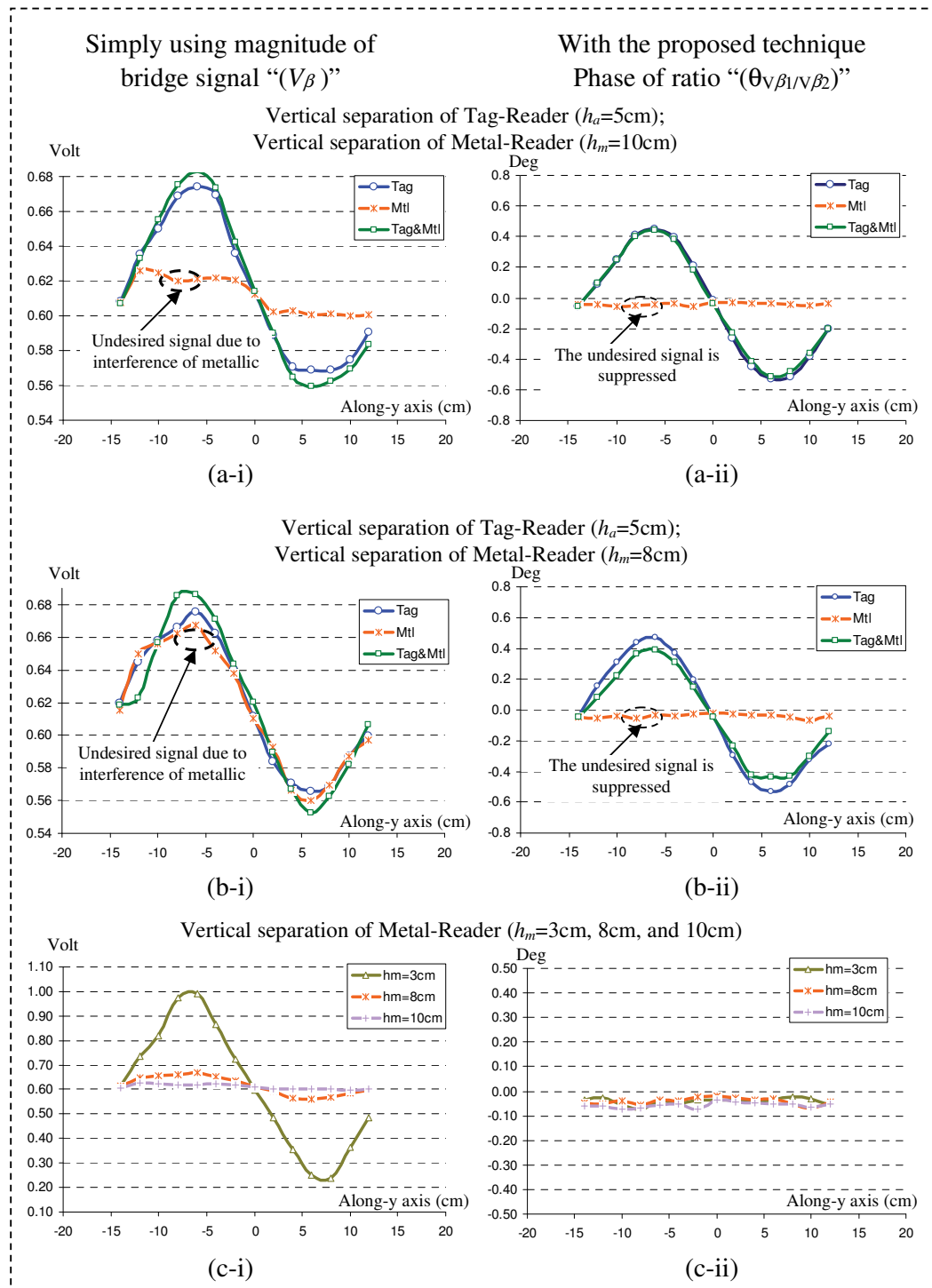
Figure 3-25: Experimental results, comparison between signals before and after applying the proposed technique

(a) the vertical separation between the Metallic object and the Reader is fixed at h_m=10cm, (b) the separation h_m=8cm, (c) Comparison for extreme case when h_m is varied down to 3cm.

Results from both the experiment and simulation indicate that the use of 'Phase of ratio ($\theta_{V1/V2}$)' be able minimise the effect of close proximity of metallic object. When using magnitude of the bridge signal ($V_{1\beta}$ - $V_{2\beta}$) the close proximity of metallic object modifies this signal, even there is no tag near to the antenna. The closer the metallic object to the antenna, the higher the interference it caused to the bridge signal, i.e. when 'h_m' is reduced the interference become much severe as can be seen in (a-i), (b-i), and (c-i) of Figure 3-24 and Figure 3-25. This interference is undesirable as we need the signal to only change with the position of the tag. The use of 'Phase of ratio ($\theta_{V\beta1/V\beta2}$)' however, overcomes this problem, whereby the proximity of metallic object almost does not cause changes in this signal as evidence in (a-ii), (b-ii), and (c-ii) of Figure 3-24 and Figure 3-25. This signal changes only with the position of the tag regardless whether the metallic object is present or not.

Results indicate the proposed method capable to eliminate the effect of metallic objects, and hence the obtained bridge signal can be reliably provide the signal variations as the function of position of the detected tag with respect to the canter of the proposed bridle loop antenna.

3.6 Method to improve magnetic fields reliability and to limit interference from the antenna

3.6.1 Problems

In the previous section, it was mentioned that the change in the reader loop impedance reduces the magnitude of magnetic fields. This happens due to two factors: i) magnetic field perturbation with metallic object, and ii) Shift in antenna resonance frequency. The first factor can be minimised by ensuring the antenna is not operates close to large flat metallic objects. The shift in resonance frequency can be overcome by retuning the antenna matching elements so that the antenna resonates at the operating frequency.

Another important aspect is to limit magnetic field from the reader antenna so as to ensure minimal interaction with other electronic devices that may be present in the environment. For example, in applications involving localisation of a wheelchair, it is necessary to reduce the level of magnetic fields at the top side of the wheelchair so that any electronic devices on the wheelchair or used by the user will not be interfered.

3.6.2 Shielding

One of the effective ways to reduce interference is through the use of metallic shielding plate [85]. Also, use of shielding plate will make the antenna's resonance becomes more stable because any present of metallic object on the shielded side will almost not affecting the resonance of the antenna because magnetic fields interaction will stop at the shielding plate. It also reduces inducing any voltage offset in the bridge signal which typically occurs when unshielded bridge antenna is attached to any metallic structure. The clearance distance between the antenna and the shielding metal plate, need to be chosen carefully as to ensure the proper operation of the antenna.

3.6.3 Clearance distance of shielding plate

The clearance distance between shielding plate and the reader antenna can be determined by examining the level of magnetic fields on the tag plane by varying the clearance distance as done in **Fig. 3-26**. The magnetic fields are computed using FEKO. In the computational model, a metal shielding plate is also considered whose dimensions are same as that of the bridge antenna.
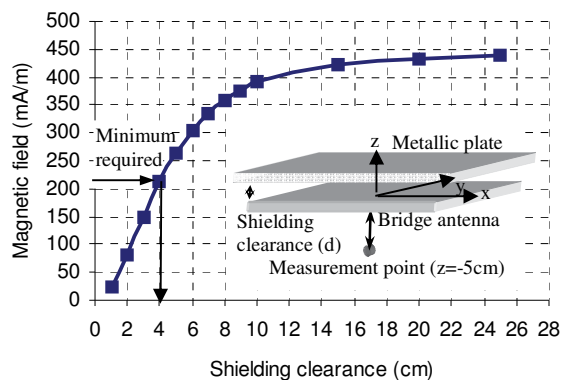
Fig. 3-26. Effect of shielding clearance on the magnetic field of the antenna with the input of 100mW from the reader

A smaller clearance distance results lower in magnetic field at the tag plane as indicated in the plot in **Fig. 3-26**. The maximum clearance distance can be determined by considering the level of magnetic field induced on the tag which is still above the nominal level required by the chosen tag as per tag's manufacturer data. For example, considering the nominal magnetic field required by the floor tags is 223mA/m, and from the plot **Fig. 3-26**, the minimum clearance distance is 4cm. It must be remembered, a smaller distance can be still possible but it requires that the antenna must be fed with

higher input power from reader as to increase the level of magnetic field on tag plane, or alternatively, by adjusting the quality factor of the antenna. The use of higher quality factor must consider the bandwidth constrain required for modulation which has been discussed in section 2.6.4 of chapter-2.
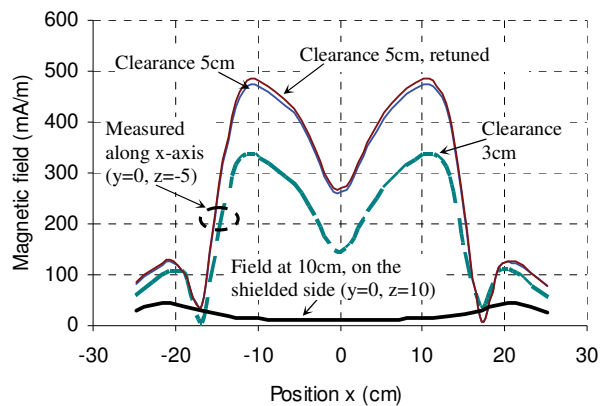
Fig. 3-27. Magnetic Field due to metal shielding on the propose bridge-loop with input power of 100mW from the reader.

Incorporation of shielding plate detunes the antenna matching, but retuning its impedance match will help to slightly increase the level of magnetic field produced by the antenna as indicated in **Fig. 3-27**. Simulation results indicate that the resulting magnetic field lie within an acceptable range to energise floor tags. Also, very minimal magnetic field appears on the other side of shielded side as can be seen in the plot, which is desirable.

3.7 Summary

In this chapter, we have described the effect of proximity of metallic object. Equivalent circuits for various scenarios are introduced to investigate methods to overcome the effect of metallic object to the bridge signals. Techniques to improve the performance of the proposed antenna have been described along with experimental and simulation results that validate the proposed techniques.

Chapter 4

Improving HF RFID Based Positioning System

4.1 Introduction

The previous chapters established that the bridge antenna could provide a bridge signal that varies with the position of a detected tag. In this chapter, we utilise this and demonstrate the usefulness of bridge antennas for HF RFID based positioning system to localise a moving object in indoor environments under sparse floor tag. HF RFID can be used for positioning and localisation of either tags or readers. However, localisations using HF RFID with conventional methods have limitations [11, 12]. To alleviate these limitations, many approaches are reported in literature which can be grouped into three categories: i) change the floor tag arrangement [11]; ii) reduce the size of reader recognition area and employ multiple readers for larger recognition area [102, 103]; and iii) use of additional sensors [23]. Here we propose a method that seeks to manipulate the reader antenna to gain extra information. The proposed method is advantageous over the existing techniques because it does not require multiple readers or switches, and it works with any commercially existing HF RFID reader system. In addition, it offers improved position and orientation estimation even under sparsely located floor-tag thus helping to improve the flexibility of the infrastructure.

In this chapter, we propose an efficient HF RFID based positioning system to localise any autonomous vehicle in indoor environments having floor tags. Algorithms to estimate the position and orientation of the moving object are introduced and evaluated using experimental prototype. The prototype bridge antenna as described in chapter-3 will be utilised. The techniques proposed in chapter-3 to minimise the effects of interference due to metallic objects will also be incorporated in this chapter.

Initially, we will evaluate the algorithm using MATLAB based simulations to show as to how the proposed algorithms perform under various inter floor tag separations.

The algorithms are then evaluated by experimental campaigns to localise an autonomous wheelchair. The results are then compared with the data from the recently published literature.

Our contributions in this chapter include: i) A novel HF RFID based positioning system using bridge antennas, ii) New algorithms that can provide improved estimation of position and orientation, and iii) methods that lead to reduced density of floor tags required per unit area which contributes to the flexibility and cost effectiveness of floor tag infrastructure.

This chapter is organised as follows: the section 4.2 introduces HF RFID based positioning system, which incorporates the previously discussed bridge antennas. The main sub systems involved in this system are also described in this section. The characterisation of RRA to improve positioning is introduced in section 4.3. In section 4.4, the novel algorithms for position and orientation estimations are described. Section 4.5 presents results of the simulations on the effect of tag-grid sparcity. To fully evaluate the propose algorithms we perform experimentations that are described in section 4.6. The results and discussion are given in section 4.7. Finally, conclusions for this chapter are given in section 4.8.

4.2 Proposed HF RFID Reader Based Positioning System
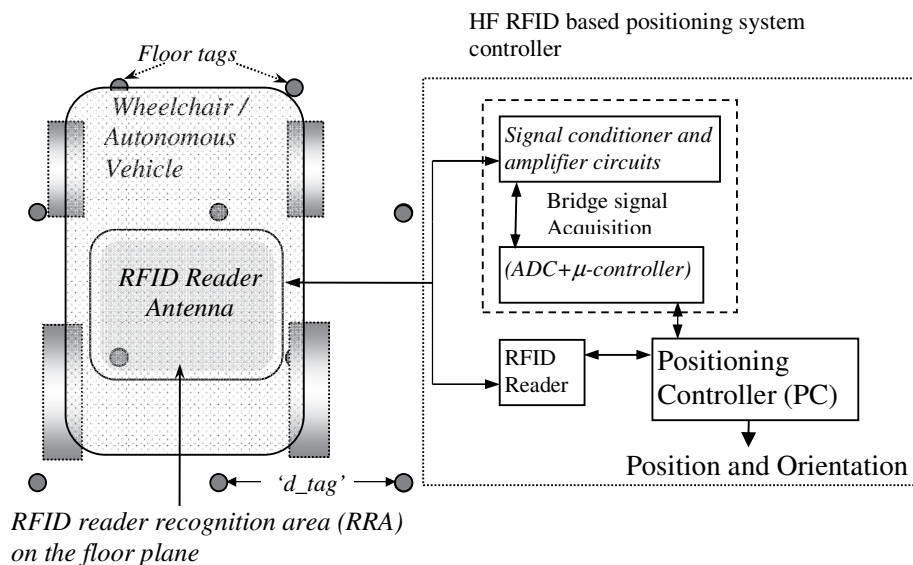
Figure 4-1: HF RFID based positioning system on a moving vehicle.

The propose HF RFID reader based positioning system for positioning of a moving vehicle is illustrated in **Figure 4-1**. In this thesis, we consider positioning an autonomous wheelchair. The main components of the system include: i) a reader antenna installed at the base of the moving object; ii) passive tags deployed on the floor as floor-tag; iii) a data acquisition unit; iv) a commercially available HF RFID reader, and vi) a Positioning Controller (PC).

The moving object that carries the reader system moves on a floor covered by a grid of passive tags. The reader antenna that is fixed to the base of the object is parallel to the floor plane on which tags are positioned. The tags are detected by the reader whenever any of them lie within the reader recognition area (RRA) of the reader antenna. When the bridge reader antenna is used, its RRA is divided into multiple zones, and whenever a tag is present within any of the zones a change in impedance (ΔX) will be created that will cause an electric 'bridge' potential to be developed across the bridge terminals. Techniques of minimising the effect of proximity of metallic objects as discussed in chapter can be applied to obtain a more reliable bridge signal. In this study, we use an autonomous wheelchair to test our RFID based positioning system. The next subsections describe the main components for our HF RFID based positioning system.

4.2.1 Reader antennas

We will be using a bridge antenna that is described in earlier chapter. In addition, we will also employ a conventional commercially available HF RFID antenna for the sake of comparison. Both the antennas are chosen to have similar outer dimensions of W_{ant} = 32 cm x L_{ant} = 23 cm, and they both fed with same amount of input power from RFID reader. Thus, the resulting RRAs for all the antennas are similar so as to ensure fair comparisons. The bridge antennas to be used here similar as the one presented in the chapter-2 and 3.

The bridge antenna is equipped with metallic shielding made of a copper plate having width and length of about 20% extra than the antenna counterparts. A gap equal to 3cm is kept between the shielding plate and the antenna. The dimensions and the shielding gap are chosen so that the antenna fits on to the base of the wheelchair. The incorporation of shielding plate is to ensure the bridge signal does not get offset and the

resonance frequency unchanged when it is installed at the bottom side of the moving wheelchair. The shielding also reduces interference to the electronic devices available on the moving wheelchair.

4.2.1.1 Criteria for selecting the shape of the bridge reader antennas

It was indicated in chapter-2 that the bridge signal from a bridge reader antenna changes as a function of tag's positions within the reader recognition area (RRA) of the reader antenna. Here we investigate as to how the shape of the loop element influences the estimation of position and orientation, so that an appropriately shaped loop element can be selected for localisation of a moving object.

Referring to chapter-2, let us consider the three bridge antennas viz., i) Single-bridge-rectangular-loop (SBRLA), ii) single-bridge-rectangular-loop (SBTLA), and iii) Dual-bridge-rectangular-loop-antenna (DBRLA) their loop elements and their corresponding RRA from top view are illustrated in **Figure 4-2** (a-c). Each antenna is assumed to be fitted at the base of a moving object with its longest dimension 'W' is aligned with y-axis as indicated in **Figure 4-2** (d).

Recall that, in chapter-2 we have established that the shape of loop elements determines the shapes of the smaller RRA zones and the bridge signal will also be influenced by the shape of the loop. We will use this information to deduce the resulting bridge signals when a bridge antenna moves over a detected tag when the tag located at y=0, +W/4 and –W/4 with respect to y-axis of the antennas.

Assuming that the object is moving along x-axis with a constant speed and tags are sparsely arranged on the floor so that at any time instant the antenna detects only one tag. The complete cycles of bridge signals associated with positions of the detected tag when the reader antenna passes over it as the vehicle moves are illustrated in the **Figure 4-2**.

We first compare the bridge signals of the first two antennas: singe bridge rectangular loop antenna (SBRLA) and the single bridge triangular loop antenna (SBTLA). The bridge signals for both the antennas can allow identification along x-axis direction because the bridge signal variation corresponds to locations of tag when its position vary on x-axis. However, for identification along-y axis, only the bridge signals from the second antenna SBTLA provide signal variations with the location of

the tag along y-axis, the bridge signals from the first antenna SBRLA do not vary with the locations of tag along y-axis. Therefore, for the case considered above, the first bridge antenna is limited to only provide localisation in one direction but the second antenna offers localisation for both directions.
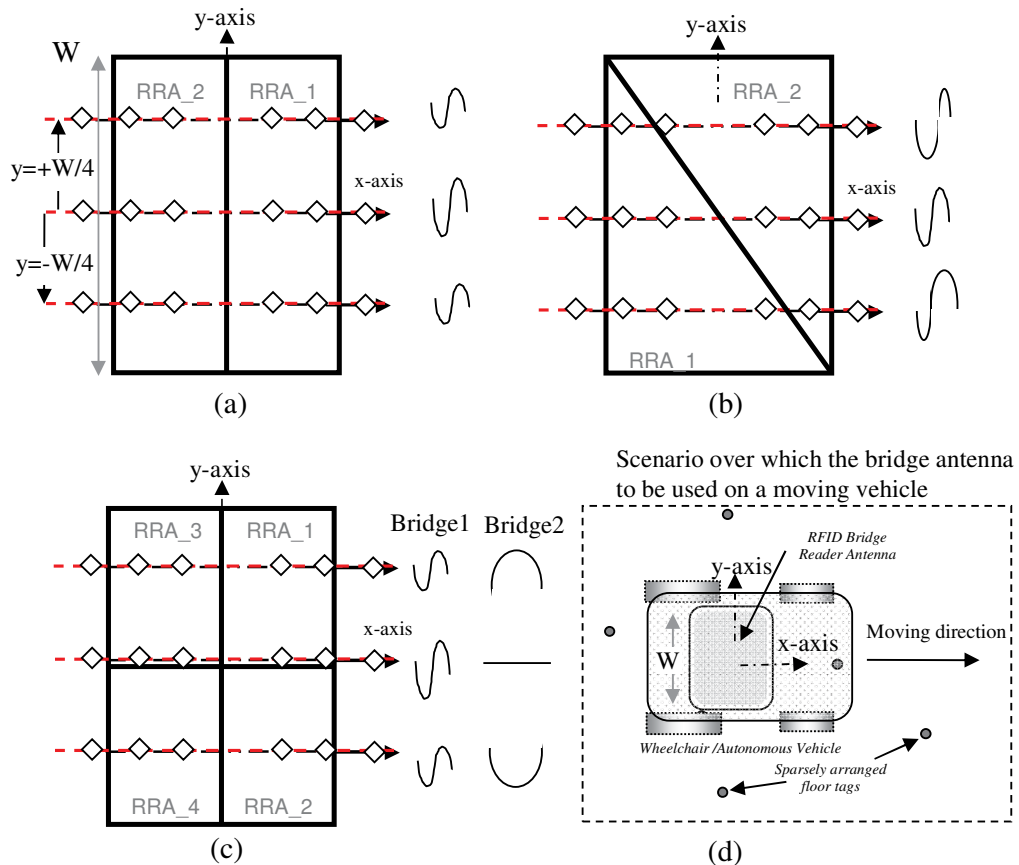
Figure 4-2: Changes of bridge signal when a bridge reader antenna passes above a floor-tag. (a) Single-bridge-rectangular-loop (SBRLA), (b) single-bridge-rectangular-loop (SBTLA), and (c) Dual-bridge-rectangular-loop-antenna (DBRLA), (d) The position of a bridge loop antenna on a moving vehicle

The limitation of the first antenna can be overcome by extending the number of bridges. The double bridge rectangular loop antenna (DBRLA) is an extension of the single bridge, because the loop elements of both the bridges are similar however, they are arranged orthogonally. Thus, it can help localise simultaneously on both the x and y axes.

To simplify the discussion, we initially limit our investigation to a single bridge triangular loop antenna with an aim to obtain positioning accuracy obtainable with the

simplest of the bridge antennas. For this reason in this chapter, we consider to use the single-bridge-triangular-loop antenna. Henceforth in this chapter, we refer to SBTLA as TLB (Triangular Loop Bridge) for the sake of brevity.

The prototype of the TLB used in this chapter is similar to the one evaluated in chapter-3 (see **Figure 3-21** b). The TLB reader antenna is installed at the base of an autonomous wheelchair as depicted in **Figure 4-3**.

Figure 4-3: Triangular loop bridge reader antenna installed at the base of moving vehicle

4.2.2 Data acquisition unit

Data acquisition unit consists of a signal conditioner, and an 8-bit microcontroller that are commercially available. This unit is packed into a rigid box so that it can be carried by the moving object as depicted in **Figure 4-4**. The unit is used to acquire the bridge signal and feed it to the "*Positioning Controller*" (PC) unit as illustrated in **Figure 4-1**.
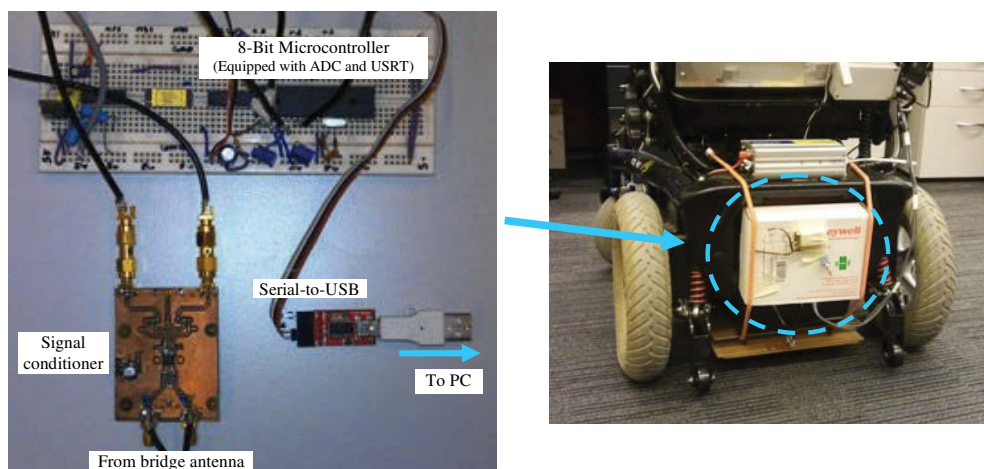
Figure 4-4: A photograph of signal conditioning unit

4.2.3 HF RFID Reader and Passive tag

We employ a standard, commercially available HF RFID reader 'TRF7960' and passive tags 'RI-I03-114' from Texas Instruments [91, 104]. The reader allows recognition of various types of tag protocols, and it is equipped with anti-collision algorithms to allow detection of multi tags. The photographs of the reader and the tag are shown in **Figure 2-28** (a) and (b) of chapter-2.

4.2.4 Positioning Controller (PC)

The positioning controller represents a processing unit capable of receiving data from RFID reader and data acquisition units. The positioning algorithm to be explained later in section 4-4 of this chapter will be executed within this PC. The outputs of the PC unit are the position and orientation of the object.

4.3 Characterization of RRA for positioning

4.3.1 Reader Recognition Area (RRA)

Reader Recognition Area (RRA) is one of the key factors contributing to positioning accuracy in HF RFID based system [12, 23, 72]. It is defined as an area on a tag plane over which the magnetic field from the reader antenna is sufficiently strong so as to interrogate nearby tag(s) that are located on the same plane.

Depending on tag's sensitivity and the distance 'h_{ant}' between the plane of the reader antenna and the plane of the tags (floor in our case), the size of the RRA may vary. In certain cases involving sensitive tags, when the tag's plane is closer to the antenna's plane (i.e. $h_{ant} < 3$ cm), multiple RRA zones may be formed, typically beyond the projected antenna boundary on to the floor (please refer to chapter-2 figure 2-6). Here we consider that the plane of the reader antenna to be always parallel to the plane of the tags i.e., reader antenna is kept parallel to the floor even when the object is moving so that the centres of the RRA and the antenna are always aligned.

As far as the shape and location of the RRA is concerned, we approximate that for a reasonable clearance distance between the floor and reader antenna (i.e., 3 cm < H_{ant} < 8 cm). The RRA is generally located on the floor parallel and directly below to the reader antenna and has a shape approximately rectangular resembling the physical shape of the outer antenna boundary.

This approximation is reasonable since significant amount of near magnetic field produced by the HF RFID reader antenna falls within this area therefore, most of the tags can be interrogated successfully if they are present within this region.

The RRA of the reader antenna can be estimated by considering the H-field over regions on the plane of the tags, (which is same as the floor in our case) that has the field strength exceeding the minimum threshold required to interrogate the tags. The threshold value can vary for different tags and the data is usually provided by the tag manufacturers. Here, we employ tags made by Texas Instruments (RI-I03-114) which require a minimum of 223mA/m as per the data provided by the manufacturer. The reader antenna is fixed to the base of the moving object and a shielding plate is inserted so as to minimise unwanted interference as well as to ensure that the field on the tag plane is not modified by the metallic structure of the moving object.

The size and the shape of RRA would play an important role in the proposed positioning algorithms. The RRA dimensions (W and L) for a given reader antenna is derived from the minimum magnetic field required to interrogate a particular tag which are specified by the tag manufacturers as explained earlier. In our proposed positioning system, these predetermined parameters are stored within the system memory of the positioning controller so that the positioning algorithm will automatically choose the appropriate RRA dimensions as per the type of detected tag.

4.3.2 RRA of TLB versus conventional loop reader antenna

It would be useful to verify and compare the performances of the proposed TLB antenna with any conventional (commercially available) loop reader HF RFID antenna by examining the induced magnetic field 'H' on the tag's plane. A full wave electromagnetic simulation tool FEKO [80] was used to accurately estimate the induced H fields for both the antennas that have similar dimensions (L_{ant} x W_{ant}). Input power of 200 mW is used for both the antennas. The antennas are positioned on x-y plane at z = 0 cm. H fields in 'z' direction at tag plane z = -6 cm are then computed. The H-field also represents the RRA of the antennas as shown in **Figure 4-5** (a-b). It can be seen that the RRA of the proposed TLB antenna is comparable to that of the chosen conventional reader antenna. It can also be seen from the figure that the shape of the RRA is approximately equal to the shape of the reader antenna in both the cases which validates

our approximation. The boundary on which the field is sufficient for a tag to be detected is highlighted with dark line on each figure.
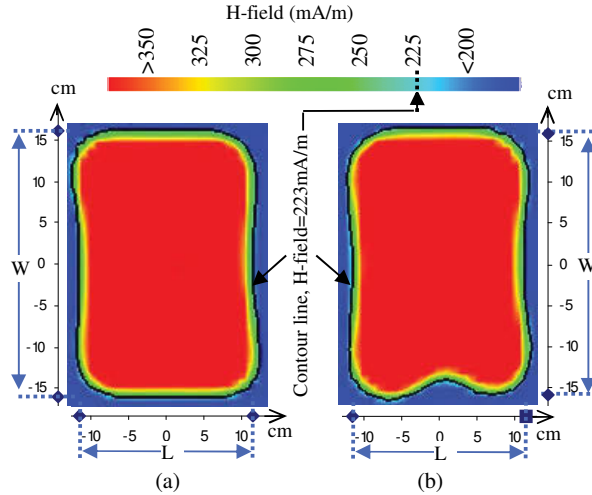
Figure 4-5: Comparison of RRA between commercial reader antenna and the proposed TLB reader antenna.

4.3.3 Positioning Error
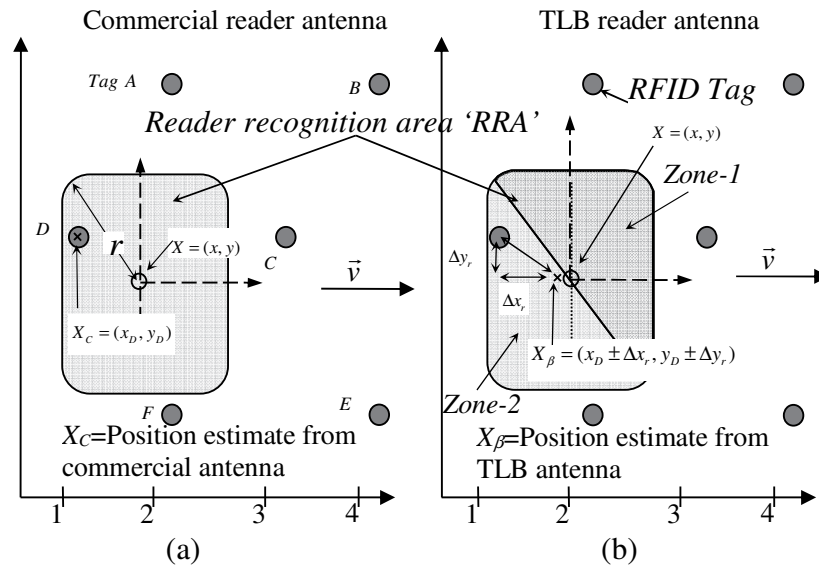
Figure 4-6: Positioning error between conventional reader antenna and the proposed TLB reader antenna.

Position estimation with i) using a commercially available conventional loop reader antenna and ii) using the proposed TLB reader antenna is shown schematically in **Figure 4-6** (a-b). Note the subscripts 'c' and 'β' represent conventional and TLB antennas

respectively. We assume that both the antennas have the same maximum uncertainty represented by a circle of radius 'r'. We also assume that the floor tags are sparsely arranged on a grid so that at any time instant only one tag is detected by the reader. Let us define r_β as the radial distance between X_β and the detected tag position as shown in **Figure 4-6** (b). The positioning errors can be represented by:

$$e_C = \left| X - X_C \right| \leq r,$$

(4.1)

and

$$e_\beta = \left| X - X_\beta \right| \leq r - r_\beta.$$

(4.2)

Where, X and $X_{\{C \; or \; \beta\}}$ are the actual object position and the estimated object position respectively.

As can be seen, any HF RFID based positioning system employing a conventional loop reader antenna rely only on the position of the detected tag for which the error can vary from zero up to a maximum uncertainty equal to the radius 'r' of its RRA. However, when the proposed TLB reader antenna is used with any existing HF RFID readers, additional information is available in the form of bridge potential (BP). The BP allows a correction to be applied so that the positioning error can be reduced to lie anywhere between zero and ($r - r_\beta$). Thus, the use of the proposed TLB reader antenna improves the positioning accuracy. Methods to obtain r_β are presented in section 4.4.

4.3.4 Increase in tag sparcity without reducing accuracy

The floor tags are usually arranged in a dense rectangular grid with close separation distance so that the reader can read tags at closely spaced intervals. To achieve a sparse grid of floor tags, the tag separation on the grid must be increased while at the same time ensuring that at any instant at least the reader detects one tag, so that no reduction in the positioning accuracy can occur.

To achieve this, the RRA of the reader antenna can be made larger by increasing the antenna's physical size [84]. We illustrate two scenarios for system using smaller RRA and using larger RRA in **Figure 4-7** (a-b). Given the same area of localisation with dimensions of (W_{Floor} x L_{Floor}), a relatively denser floor tag is required for small RRA. On the other hand, the use of larger RRA allows a sparser floor tag.

With reader antennas having larger RRA, tags can be detected at larger distances and hence the floor tag grid separation can be made equal to the maximum dimension '$W_{antenna}$' of the reader antenna.

(a)

(b)
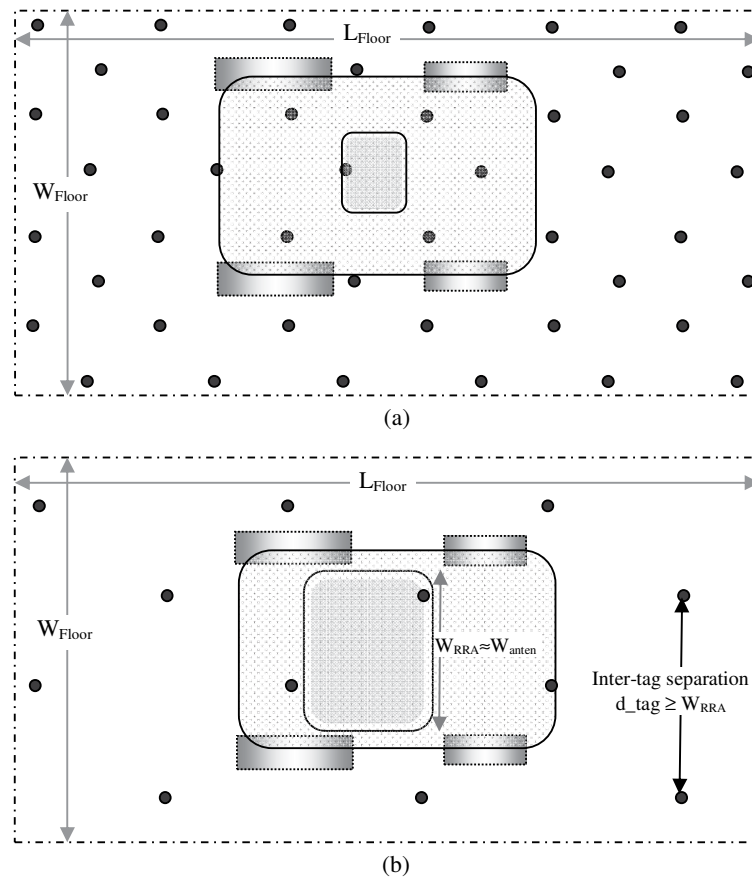
Figure 4-7: Utilisation of larger reader recognition area (RRA) for a sparser inter-tag separation

One of limitations of HF RFID is its inability to detect tags placed very close to metallic objects (typically <1 cm). This can potentially make the reader to miss the tags, which affects the corresponding bridge signal measurement. Sometimes, this is minimised by properly installing tags at some distance away from obvious metallic objects in a given user environment. To overcome this problem, the technique proposed in this chapter incorporates the object position information available from the wheel encoders in addition to the RFID tag readings. Thus, these two independent measurements can be effectively utilised to compensate and overcome limitations of each other. This can help to increase the tag separation on the floor to sparser floor tag grid.

Sparse tag grid can be achieved by considering the arrangement of the floor tags to allow at least one tag be detected for travel over short distances (1 to 2 meters). To ensure this, tags can be placed along the expected travel path of the object under consideration. This can be useful in scenarios when the object under consideration moves (i) either along a narrow path way or indoor corridors; or ii) along a predefined path (in factory floors or warehouses, etc.). In between any two consecutive tags, when no direct reading is made, the position can be estimated from the readily available wheel encoder data with a reference taken from previously estimated position of detected tags stored in the RFID database. The use of information from RFID database minimises any unwanted errors associated with the wheel encoder data. Thus, the number of tags to be deployed on the floor can be minimised further resulting in a simplified deployment without sacrificing the positioning accuracy.

4.4 Positioning with the Proposed Bridge Reader Antenna

Our proposed positioning algorithm uses geometric approach to match boundaries of RRA with the *time flags of key events* that occur during the detection of tags as depicted in **Figure 4-8**. When employing the proposed TLB antenna for sparse floor tag-grid infrastructure, the positioning can be categorised into two modes viz., Mode-1 and Mode-2.

This categorisation takes into consideration the available information of the current detected tag at the positioning controller. In Mode-1, position estimation is performed using only the bridge signal that will be coupled with tag position information already recorded in the RFID database. Under Mode-2, all the information that is available under MODE-1 is included and in addition, the information from object dynamics will also utilised for estimating the position. It is not difficult to guess that the use of Mode-2 is always desirable as it can obtain improved accuracy of estimation. However, Mode-1 can be useful for a very basic system when no dynamic motion information is available.

4.4.1 Key Parameters for positioning of moving reader employing the TLB antenna
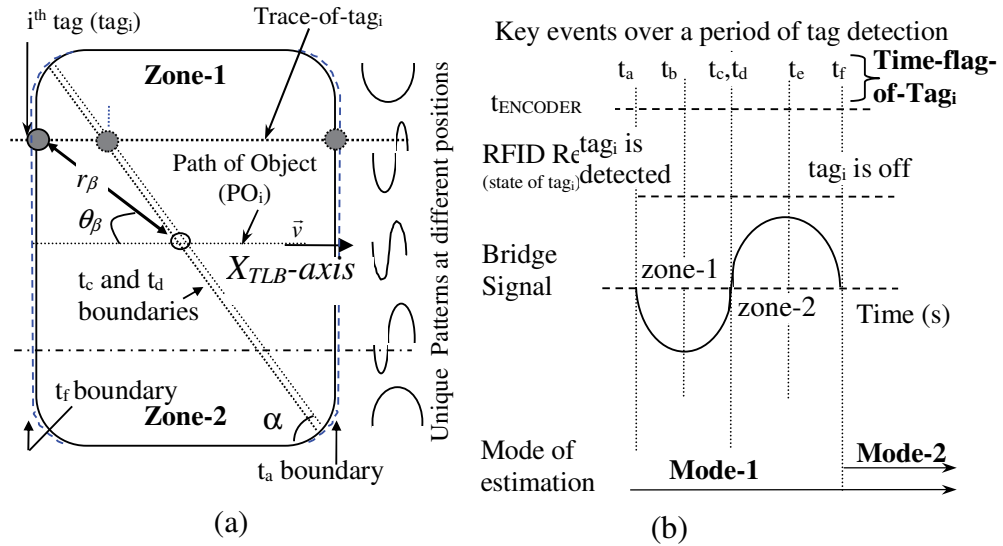
Figure 4-8: Key parameters for positioning with the TLB reader antenna
(a) the TLB antenna and its RRA (b) Illustration over the time period of ith tag detection.

The temporal events that occur while the reader antenna moves along the tag plane are important in positioning. Let us first define the following key parameters that will be used in our proposed algorithm: i) **Time-Flag-of-Tag$_i$** ii) **Trace-of-Tag$_i$** iii) **Path of the Object$_i$** and iv) **Points of Intersection** and v) **TLB Correction Factor**. **Figure 4-8** and **Figure 4-9** are used to illustrate how these parameters are related with RRA and key time events when an object that is carrying the reader moves over a tag, say ' i[th] tag '.

The projected RRA on the floor (tag) plane is assumed to be parallel to the antenna, with the centre point of the RRA aligned with the centre of the antenna. We refer to this centre point as the position of the moving object.

The measurements are recorded continuously and the data is buffered into the PC memory. Thus, all the data are assumed to be readily available as inputs to the proposed positioning algorithm. The algorithm requires that these data be sampled at closer time intervals depending on speed of the object. The minimum time interval is determined by delays in sensor measurement typically being less than 3msec.

All the measured data are correlated in time. Hence, a set of data from different measurements for a specific event can be acquired when time flag of the event is known.

i) ***Time-Flag-of-Tag$_i$*** (***t_a, t_b, t_c, t_d,*** **and** ***t_f***)**:** Each time flag represents a key event when the reader antenna moves over a particular tag placed on the floor. This also corresponds to the movement associated with the boundaries of the RRA of the reader antenna with respect to the tag and the resulting bridge signal variation associated with the position of the tag with respect to RRA. The parameter t_a is the time instant when the current tag gets detected (i.e. just after the RRA of the reader antenna moves over the tag), and t_f is the time when reader antenna moves off the tag. The t_c and t_d indicate the times that correspond to transition of the tag between the boundaries of Zone-1 and Zone-2 of the RRA. The t_b and t_e are the flags that occur at the mid points of the boundaries of zone1 and zone 2 respectively. The relation of these time flags with the changes of bridge signal is illustrated in **Figure 4-8** (b). These time flags are obtained using information from RFID reader database and changes of the bridge potential when a particular tag, say i^{th} tag (tag_i), is detected.

ii) ***Trace-of-Tag$_i$***: It indicates the changes occurring in location of the detected tag with respect to the trajectory of the moving RRA within that time frame t_a to t_f. It is important as it indicates the orientation of RRA with respect to the position of the detected tag_i.

iii) **Path of the Object** (*PO_i*): It is a curve connecting series of points tracing the position of the object as it moves during the time frame t_a to t_f with respect to tag_i. The PO_i is obtained from the information derived from the wheel encoder within the specified time frame. It is related to the '*Trace-of-Tag$_i$*' and useful for the estimation of the position of the object relative to the coordinates of the detected 'tag_i'.

iii) **Points of Intersections (P$_a$, P$_{c,d}$, and P$_f$).** These are the points on the *path of the object* (*PO_i*) corresponding to the time flags of *tag_i* as illustrated in **Figure 4-9**. These points must fall on the boundary of the RRA# which is a scaled image of the original RRA as illustrated in **Figure 4-9**.

iv) ***TLB correction factors*** (*r_β* and *θ_β*): These parameters are used to obtain relative position of the object with respect to detected i^{th} tag as shown in **Figure 4-9**. The r_β is

the radial distance as defined previously in (4.2). The θ_β is the angle between radial line drawn in the direction of r_β and the middle line along X_{TLB}-axis which crosses the centre of the antenna as illustrated in **Figure 4-8** (a) and **Figure 4-9**.

4.4.2 Position estimation with Mode-1

Mode-1 is suitable for any basic system for which the wheel encoder data is not available. In such a case, the system uses only bridge signal and the coordinates of the detected tag already stored in the reader database to calculate the position of the object. The bridge signal will be continuously monitored and whenever a tag is detected by the reader, it compares the bridge signal at that time instant to a reference (see **Figure 4-8**). The magnitude and polarity of the bridge signal helps to decide whether the tag is located closer to zone-1 or zone-2 of the bifurcated RRA. Once a proximal zone of RRA is identified, the centroid of that zone is taken as the estimated object position. This simple approach leads to improvement of the estimation of the position when operating under sparse tag-grid as compared to some existing methods [11, 71]. For this mode, the orientation of the object can be approximated following the method discussed in [12] which utilises only the previous and current tag positions.

4.4.3 Position estimation with Mode-2

Our focus is on Mode-2, which obtains higher accuracy. In this mode, in addition to the information from RFID measurements (recorded information from reader database and acquired bridge signal from TLB antenna), the wheel encoder data is also utilised to estimate the position.

In particular, the key aspect of Mode 2 is the determination of the TLB correction factors (r_β and θ_β) so that the object's relative position with respect to a detected i^{th} tag can be estimated. The true location of the object is obtained by adding the object's relative position to the coordinates of the ith tag that is available with the RFID database. Below, we describe the step-by-step process involved in the estimation of the position with Mode-2

i) Extraction of key parameters from sensors:

When a TLB reader antenna moves over a tag, changes in its bridge potential allow the system to recognise different time flags viz., (t_a, t_b, t_c, t_d, and t_f). Using t_a and t_f time flags as markers, the system obtains path of the object (PO_i) from the encoder data.

Similarly, referring to **Figure 4-9**, the intersection points (P_a, $P_{c,d}$, and P_f) can be obtained from the encoder data at times t_a, (t_c+t_d)/2, and t_f . These intersection points lead to formation of straight lines l_{ac}, l_{df}, l_{af} as can be seen from the same figure.

The path of the object PO_i that is obtained from the encoder data can either be straight line or a curve, depending on how the object that carries the reader moves. However, to improve generality, we consider the path to be a curved line. It must be noted that, any accumulated drift or offset in the encoder data will not affect our algorithm because, we only utilise path shape within short distance associated with the time frame t_a-t_f.

ii) Determination of RRA and RRA$^{\#}$:

The results in section 4.3.2, (see **Figure 4-5**), demonstrate that the overall RRA of a HF RFID reader antenna is closely related to the physical shape of outer dimensions of the reader antenna. We therefore, approximate the RRA of the TLB reader antenna to be of rectangular shape with the dimensions W and L that are chosen from the predetermined parameters stored in the system memory mentioned previously in section 4.3.1.

Further, we know that the overall RRA has two distinct zones in triangular shape, which we denote as zone-1 and zone-2 as shown in **Figure 4-9**. These triangular shaped zones allow localisation of the detected tag in both directions vertically and horizontally with respect to the centre of its overall RRA as previously discussed in section 4.2.1.1. This is the main reason for the selection of this antenna. An imaginary straight line is drawn at the middle of the overall RRA to bifurcate it into zones 1 and 2 as shown in the same figure so that a junction is formed between these two zones. The overall RRA and its boundaries are shown in **Figure 4-9**.
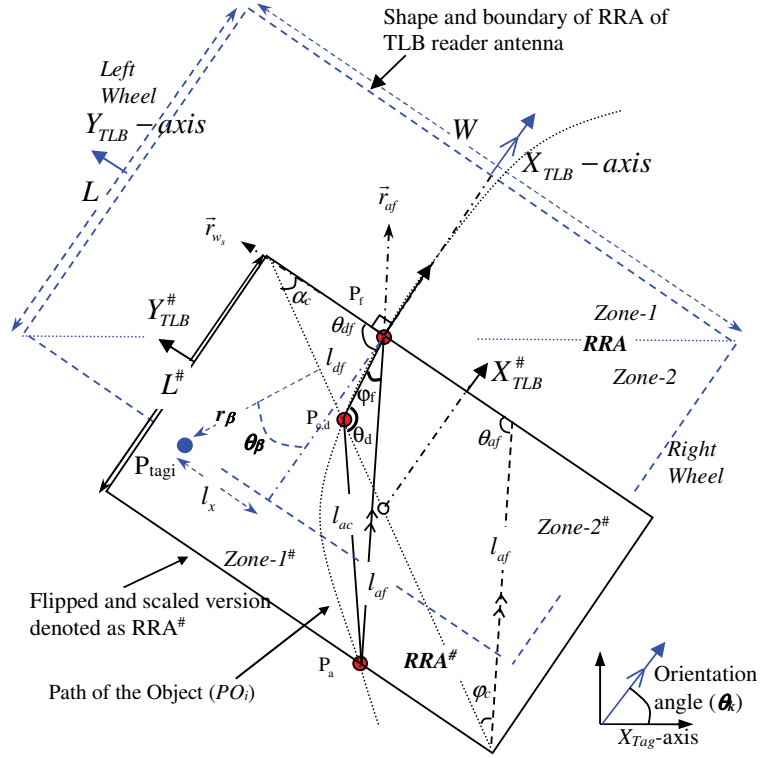
Figure 4-9: Flipped and scaled RRA, Path of the Object, and Intersection Points.

The RRA# is obtained by flipping and scaling the RRA using a scaling factor ρ to create a new scaled version of the RRA (on the same plane as that of the original RRA) as depicted in **Figure 4-9**. We utilise the boundaries of RRA# and the intersection points (P_a, $P_{c,d}$ and P_f) that lie on the path of the object (PO_i) to obtain the TLB correction factors r_β and θ_β.

The scaling factor ρ is determined as follows: referring to **Figure 4-9**, at the point P_f, the PO_i can be considered to be tangential to the X_{TLB}-axis and perpendicular to the RRA# boundary at which P_f lies. Using these features and considering that the RRA# plane is parallel to X-Y plane; a unit vector $\hat{r}_{w_s}$ can be obtained. In a similar manner, another unit vector $\hat{r}_{fa}$ along l_{af} can also be obtained. This helps to calculate θ_{af}, and the scale factor ρ is determined using the following expressions:

$$\theta_{af} = \cos^{-1}(\hat{r}_{w_s} \cdot \hat{r}_{fa}),$$ (4.3)

and $\quad \rho = L/(l_{af} \sin(\theta_{af}))$. (4.4)

*iii) **Finding TLB correction factors by fitting the intersection points to the RRA#:***

The aim here is to obtain the bridge correction factor (r_β and θ_β) by fitting the points of intersection (P_a, $P_{c,d}$ and P_f) to the boundaries of RRA#. We will employ a geometric approach in order to solve this problem. Referring to **Figure 4-9**, the bridge correction parameters can be determined by

$$r_\beta = \sqrt{l_x^2 + (L/2)^2},$$ (4.5)

$$\theta_\beta = \tan^{-1}(l_x/(L/2)).$$ (4.6)

Where;

$$l_x = (l_{df}\sin(\theta_d)/\sin(\alpha_c))\rho - \frac{W}{2},$$

$$\theta_d = \pi - (\varphi_c + \varphi_f),\ \alpha_c = \tan^{-1}(L/W),$$

$$\varphi_c = \begin{cases} \alpha_c - \theta_{af} & ,\ \text{for}\ \ \theta_{df} \ge \theta_{af} \\ \pi - (\alpha_c + \theta_{af}) & ,\ \text{for}\ \ \theta_{df} < \theta_{af} \end{cases},$$

$$\varphi_f = \cos^{-1}\left(\frac{l_{af}^2 + l_{df}^2 - l_{ac}^2}{(2l_{af}l_{df})}\right),\ \theta_{df} = \cos^{-1}(\hat{r}_{w_s} \cdot \hat{r}_{fd}).$$

*iv) **Find the position of the object:***

Having calculated the bridge potential correction factors, we will now obtain relative position of the object with respect to the detected tag as

$$P_{Rel\_Tag_i} = \begin{bmatrix} r_\beta\cos(\theta_k + \theta_\beta) \\ r_\beta\sin(\theta_k + \theta_\beta) \end{bmatrix}_{Tag_i}.$$ (4.7)

The term θ_k is heading of the object relative to X_{Tag}-axis. Finally, the object position $P_{TLB}(t)$ at time 't_f' is estimated using both the relative position of the object $P_{Rel\_Tag_i}$ and the coordinates of the detected tag P_{Tag_i} as

$$P_{TLB}(t) = \begin{bmatrix} x_{Tag_i} + r_\beta\cos(\theta_k + \theta_\beta) \\ y_{Tag_i} + r_\beta\sin(\theta_k + \theta_\beta) \end{bmatrix}.$$ (4.8)

Now, we need to obtain θ_k which is discussed in the section below.

4.4.4 Estimation of the object orientation

The object orientation θ_k is defined as the angle between X_{TLB}-axis at current position of the object and X_{Tag}-axis as shown in **Figure 4-10**. The object orientation can be estimated using current and previous estimated positions as described in [11-13]. Considering the scenario in **Figure 4-10**, the object orientation using the method in [11-13] is regarded as the angle between slope of the line connecting the current and previous detected tags to X_{Tag}-axis, and this angle is estimated using:

$$\theta_{AB} = \text{atan2}((y_{tag_B} - y_{tag_A}),(x_{tag_A} - x_{tag_B})). \qquad (4.9)$$

In (4.9), the actual detected tag positions are retrieved from the RFID reader database. The above method although it is simple, it however, suffers from position uncertainty caused by the RRA which leads to errors in the estimated object orientation. Since the proposed TLB antenna can reduce the uncertainty caused by RRA, it is worthwhile investigating whether it can also help to improve the estimation of orientation.
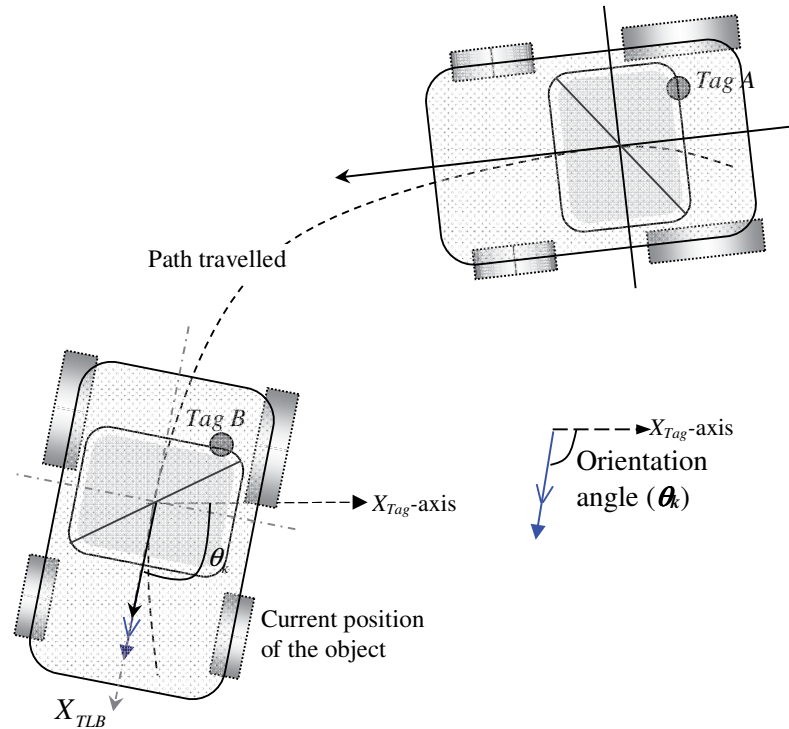
Figure 4-10: Object orientation at current position

The orientation estimation can be obtained by utilising the information from the TLB reader antenna and the path travelled between previous and current detected tags.

This algorithm does not rely on exact path as it only requires information on relative positions of the object within the path.

First, the locations of the object at relative to the path travelled corresponding to two consecutive tags (say Tag A and Tag B) is obtained using the Mode-2 positioning algorithm. Consider the scenario illustrated in **Figure 4-10** is redrawn as in **Figure 4-11** to highlight the RRA at two locations and the tags, so that we can focus on the important parameters.
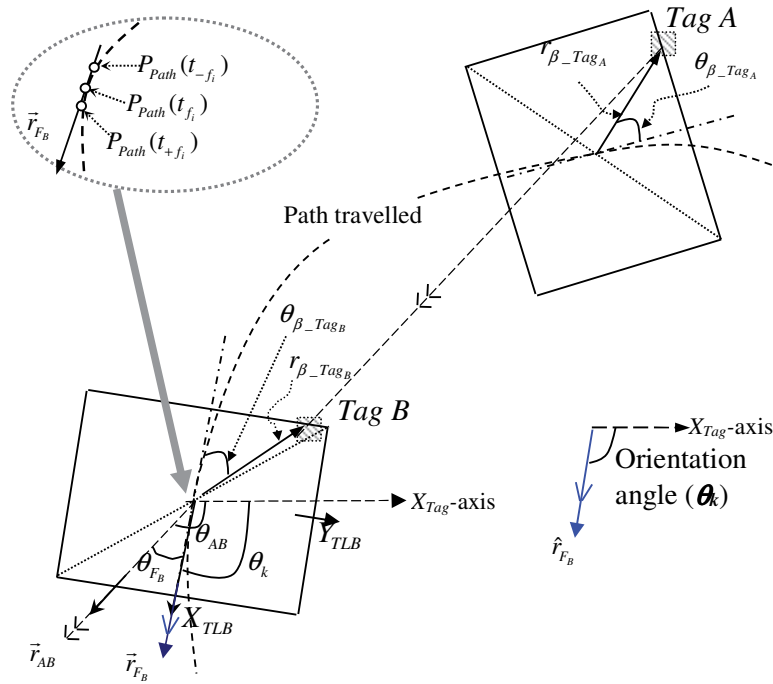
Figure 4-11: Estimation of orientation angle using tag positions along the travelled path using TLB reader antenna

We can estimate current orientation of the object using

$$\theta_k = \theta_{AB} + \theta_{F_B} . \tag{4.10}$$

The θ_{AB} is is calculated using (4.9)

The θ_{F_B} in (4.10) is the angle between the current object heading vector $\vec{r}_{F_B}$ and another vector $\vec{r}_{AB}$ linking previous and current estimated tag positions. The θ_{F_B} is obtained using

$$\theta_{F_B} = \pm \cos^{-1}(\hat{r}_{AB} \cdot \hat{r}_{F_B}) . \tag{4.11}$$

The $\hat{r}_{AB}$ and $\hat{r}_{F_B}$ are the unit vectors of $\vec{r}_{AB}$ and $\vec{r}_{F_B}$ respectively. These vectors are obtained from

$$\vec{r}_{AB} = P_{Tag_B\_Path}(t_{f_B}) - P_{Tag_A\_Path}(t_{f_A}), \quad (4.12)$$

and

$$\vec{r}_{F_B} = P_{Path}(t_{+f_B}) - P_{Path}(t_{-f_B}). \quad (4.13)$$

where;

$$P_{Tag_i\_Path} = P_{Path}(t_{f_i}) + \begin{bmatrix} r_{\beta_i} \cos(\theta_{k\_Path_i} + \theta_{\beta_i}) \\ r_{\beta_i} \sin(\theta_{k\_Path_i} + \theta_{\beta_i}) \end{bmatrix},$$

$$\theta_{k\_Path_i} = \text{atan2}\big((y_{Path_i}(t_f) - y_{Path_{i-1}}(t_f),$$

$$x_{Path_i}(t_f) - x_{Path_{i-1}}(t_f)\big),$$

and, $i \in \{A, B, ..\}.$

The P$_{Tagi\_Path}(t_i)$ in (4.12) represents coordinates of tag$_i$ at time t_i, and in (4.13), the P$_{Path}(t_i)$ indicates coordinates of any point on the path as illustrated in **Figure 4-11**. These coordinates (P$_{Tagi\_Path}(t_i)$ and P$_{Path}(t_i)$) are relative to a reference point that can be chosen anywhere near the path. The reference, therefore, can be independent. In other words, the actual coordinates for (P$_{Tagi\_Path}(t_i)$ and P$_{Path}(t_i)$) are not necessarily known. Hence, the accumulated errors that might occur in the encoder data prior to estimation of the previous tag, do not affect the accuracy of the algorithm used for orientation estimation.

4.4.5 The overall positioning algorithm

The overall sequence of our proposed positioning algorithm is illustrated in the flow chart presented in **Figure 4-12**. The proposed algorithm allows any moving object to be localised for both dense and sparse arrangement of tags on a grid. The algorithm is mainly optimised for sparse tag-grid floor infrastructure as it helps to achieve cost effectiveness of installation and makes the deployment flexible enough to suit any application environments or infrastructure scenarios.

In the event that no tag gets detected, the system derives position using wheel encoder data (object dynamic) with its reference taken from the most recent RFID measurement. This approach reduces potential errors that may be caused by any

accumulated offset or drift in the encoder data. In addition, it also ensures continuity in positioning.

This overall positioning algorithm is utilised in both simulations and experimentation. Results obtained from the simulation are discussed in sections V-F and results from the experimentation are presented in VII. Both the results demonstrate the efficacy of our proposed approach.
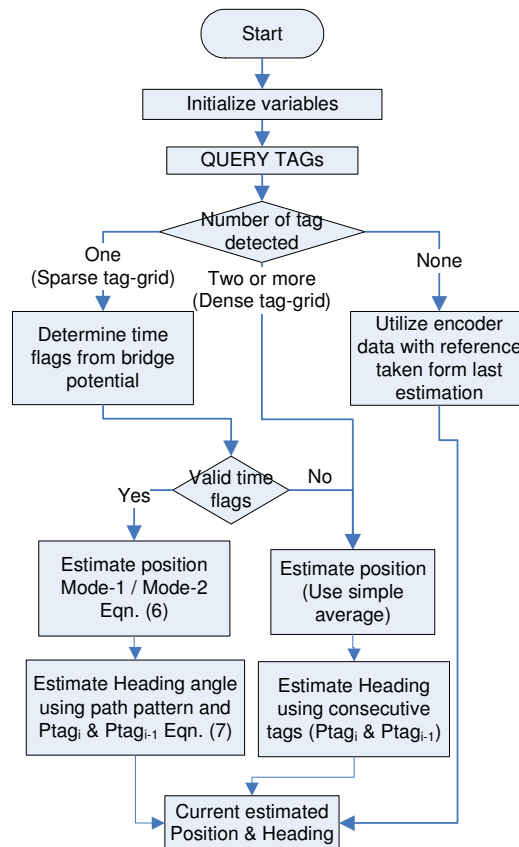
Figure 4-12: Flow diagram of RFID based positioning using triangular bridge-loop antenna.

4.5 Error comparison for different tag-grid sparcity

To indicate the improvement in positioning when using the proposed triangular bridge-loop (TLB) reader antenna, we make a comparison of positioning performance between a system that uses a conventional loop antenna (denoted as **Sys-A**), and another system that uses the proposed TLB reader antenna (denoted as **Sys-B-M1** when using Mode-1, and **Sys-B-M2** when using Mode-2). We assume orientation of the object at any instance to be known for all the cases.

The floor tag-grid is arranged in triangular pattern as illustrated in **Figure 4-13**. This arrangement is suitable to reduce the number of floor tags [11]. Tag-grid is considered sparse when only one tag can be detected at any instant. It is the case when the parameter h_{tag} as shown in **Figure 4-13** becomes larger than the width 'W' of the RRA of the antenna. When the tag grid is dense (i.e. when two or more tags being detected), the system averages the coordinates of all the detected tags to estimate the current position.
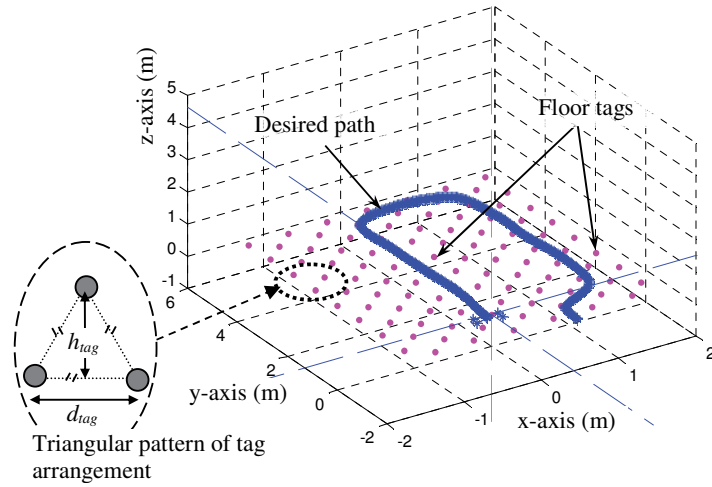
Figure 4-13: Tag floor and the desired path

Under sparse tag arrangement i.e., when only a single tag gets detected, the systems employing Mode-1 (Sys-B-M1) and Mode-2 (Sys-B-M2) use algorithms that are described in sections V-B and V-C respectively. To make a proper comparison, we simulate the movement of an autonomous object that is equipped with HF RFID reader to follow a defined path as shown in **Figure 4-13**. Estimations are repeated for different tag-grid sparsity by increasing the inter tag separations 'd_{tag}'. Average position errors over tag separations are computed using

$$\text{Average Position Error} = \frac{1}{T}\sum_{t}^{T} e(t) \qquad (4.14)$$

where 't' is the instance of position estimation, and 'T' is the total number of position estimations required for the object to traverse the chosen path completely. The term $e(t)$ is a position error between an actual position X and an estimated position $\hat{X}$ computed as: $e(t) = \sqrt{(x - \hat{x})^2 + (y - \hat{y})^2}$.
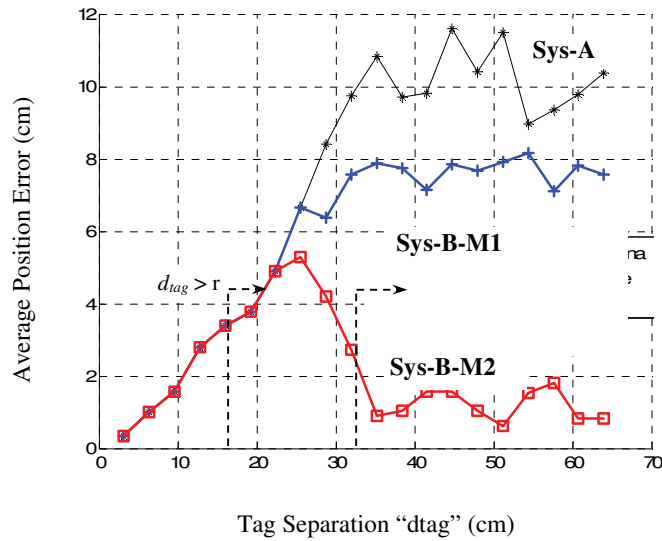
Figure 4-14: Comparison of positioning error using conventional reader antenna versus proposed triangular bridge-loop antenna

The average positioning error is plotted in **Figure 4-14** which clearly demonstrate that the system using TLB reader antenna outperforms those using the conventional loop reader antenna especially under sparse tag-grid separation.

For conventional HF RFID reader antennas that do not employ bridge signals, when the tag separation d_{tag} becomes larger than the dimension of the RRA, the number of detectable tags by the reader is reduced leading to increased positioning errors. For this case, the errors become much higher when just one tag is detected which starts to occur when tag separation $d_{tag}>r$, as shown in **Figure 4-14** (r is the maximum uncertainty of the antenna, please refer to refer to **Figure 4-6** (a)). For our case this happens at around d_{tag} = 19cm. Further increasing the tag grid separation i.e., making the tag-grid sparser, will further degrade the accuracy of positioning when conventional reader antennas are used because only single tag gets detected. However, our proposed system performs well for situation where only single tag is detected. The proposed TLB antenna (Sys-B) is optimised to perform when single tag detection occur. The errors obtained by Sys-B-M1 are lower than those of the conventional system (Sys-A) for larger separation when the detection of a single tag starts to dominate. The performance of system using bridge antenna under Mode-1 (Sys-B-M1) becomes stable with its error slightly below 8cm after reaching d_{tag} of 36 cm.

As for the system using bridge antenna under Mode-2 (Sys-B-M2), starting at a tag separation of around 23 cm, its average position errors begin to reduce gradually. This happens due to the utilisation of bridge potential signal. At a tag separation of 36 cm that is when h_{tag}>W, the errors tend to become stable below 2cm. The main reason is that, beyond this sparse tag separation, there is only one tag that can be detected by the reader.

The dimensions of reader antenna play a significant role as they determine the required tag infrastructure, and the level of accuracy. The dimensions of the antenna must not be chosen to be too small to avoid null tag detection throughout the localisation process. The reduction in reader antenna dimensions will also reduce the chances of reading a tag. For a smaller sized reader antenna, the tag–grid spacing must also be not too sparse as it increases the error due to reduced chance tag detection.

The above results confirm the efficacy of our proposed method employing the TLB antenna for sparse floor tag-grid infrastructure. It is worth mentioning here that the bridge signal from the proposed antenna can also be utilised for dense tag infrastructure. However, as the focus of this chapter is on sparse tag grid infrastructure, it is not presented here.

To further validate our claims of the efficacy of the proposed TLB antenna and positioning algorithms, we performed series of experiments using an autonomous wheelchair by employing sparse tag-grid on the floor and the results are presented in the next section.

4.6 Experiments

We validate our proposed approach by performing series of experimentations on localising an autonomous wheelchair in a multi-story building. The location used for experimentations was in UTS building 1, level 20. The floor is made of concrete and covered with a thin wooden layer.
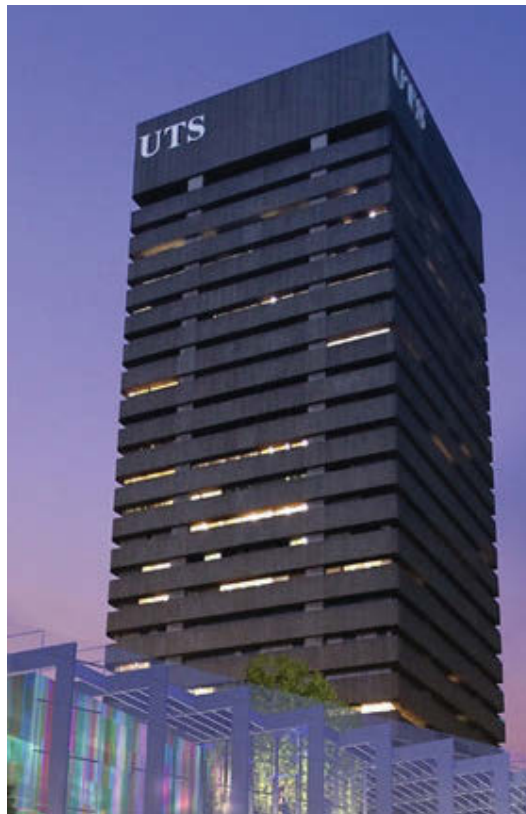
Figure 4-15: UTS multi storey building at which the experiments were conducted

Results are used for two comparisons. Firstly, we compare the results obtained using the proposed TLB reader antenna with those obtained from a conventional loop reader antenna. Secondly, we compare our approach with the recently published results given in [23] and [13].

The experimental setup used in our experimentations is shown in Figure 4-16. Passive tags are sparsely arranged on the floor with a tag separation of about 1.3 meters. The reader antenna is mounted at the base of the moving autonomous wheelchair. For a fair comparison, the TLB antenna is chosen to have the same outer dimensions (230mm

x 320mm) as that of the conventional loop reader antenna. This is to ensure that both the antennas to have comparable-sized RRAs.

The wheelchair is moved on the floor concrete floor to follow a prescribed path as depicted in **Figure 4-16** (a). The speed of the object is set to be consistent around 16.6 cm/sec so as to ensure that the tags be successfully read by the reader. A faster reader can be used if faster speed is desired without any modification to the proposed algorithm. Measurements from HF RFID reader database, the bridge potential and the wheel encoder data are acquired and fed as inputs to our localisation algorithm. The overall positioning algorithm described in section 4.4.5 is employed. In particular, the wheelchair position and orientation are estimated using the (4.8) and (4.10) respectively when the system employs the proposed TLB reader antenna.

(a)

The Proposed Bridge antenna
(Installed at the wheelchair base)

(b)
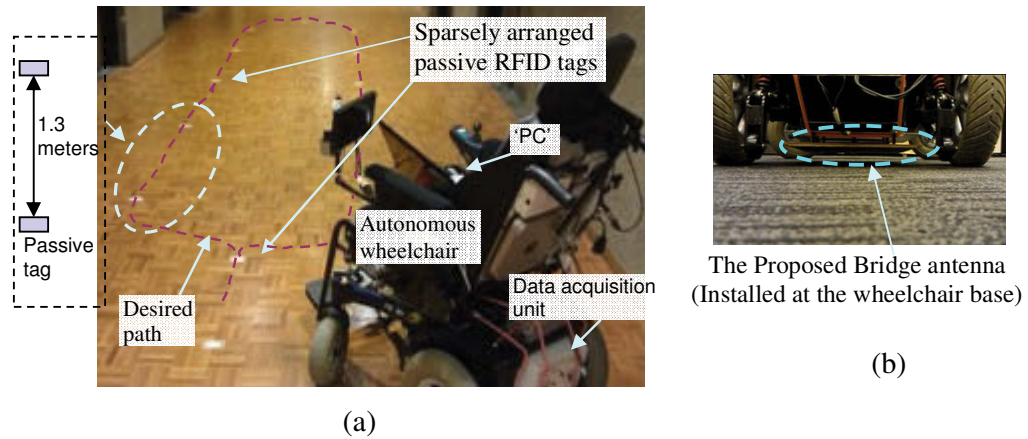
Figure 4-16: HF RFID reader based positioning for an autonomous wheelchair

When the system uses conventional loop antenna, the commonly used position estimation algorithm given in [11] will be employed to estimate the position, and to estimate orientation, the equation indicated in (4.9) is used [12]. The positioning error and the average positioning error are calculated using discussion given in section 4.5. The orientation error θ_{error} is calculated as:

$$\theta_{error} = |\theta - \hat{\theta}|, \tag{4.15}$$

where θ and $\hat{\theta}$ are the actual and the estimated heading angles respectively. The average of heading angle is calculated using:

$$\text{Average Orientation Error} = \frac{1}{T}\sum_{t}^{T}\theta_{error}(t). \tag{4.16}$$

where the terms *t* and *T* are same as previously defined in section 4.5. The experimental results and discussions are presented in the next section.

4.7 Results

Error comparisons for position and orientation estimations are plotted in **Figure 4-17** and **Figure 4-18**. Results in **Figure 4-17** indicate that, the proposed method that incorporates the TLB antenna and the positioning algorithm offers smaller errors over the period of the localisation as compared to the use of conventional reader antenna and traditional positioning methods. On the average, the proposed method obtains average positioning error of 4.05cm as opposed to an average positioning error of 12.41cm for a system that employs a conventional reader antenna.

There are slight differences that can be observed between our simulation and the experimental results which are attributable mainly to the simple rectangular shaped RRA boundary chosen in our algorithm. This choice was made to make the algorithm simple while closely reflecting the reality. However, the actual RRA boundary cannot exactly be rectangular shaped. Further, the actual RRA could get modified by the variation of tag sensitivity and due to the presence of metallic structures that may be present underneath the concrete floor close to the tag; these factors could have influenced the overall accuracy of measured data. In spite of these, the deviation between simulation and measured results is quite small.

4.7.1 Performance comparison: Proposed reader antenna versus conventional loop reader antenna

Our proposed algorithm for orientation estimation also offers relatively smaller errors when compared to the conventional approach [12]. The proposed method can perform relatively well even at critical points i.e. when the object to be localised makes a turn as indicated in **Figure 4-18**. On an average, our orientation algorithm gives an error of 4.51degrees as compared with the 14.80 degree error obtained by the available method of orientation estimation. A Comparison of average errors is tabulated in **Table 4-1**.
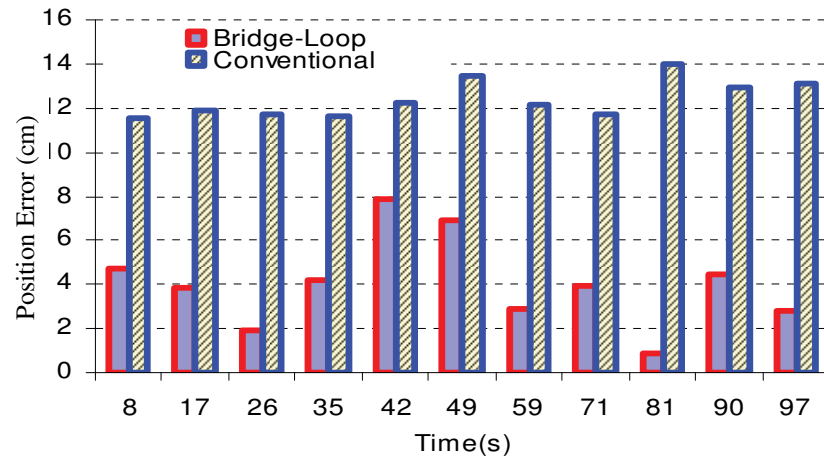
Figure 4-17: Comparison of positioning error: Positioning with the proposed TLB reader antenna versus conventional reader antennas.
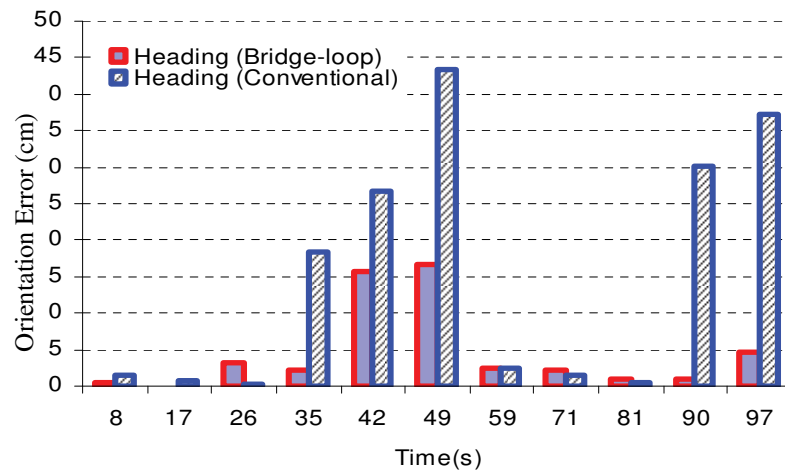
Figure 4-18: Comparison of orientation estimation errors: Proposed method versus conventional method.

Table 4-1: Comparison of average errors

Estimation methods	Average values	
	Position Error (cm)	Orientation Error (Degree)
Conventional [12]	12.41	14.80
Proposed method with bridge-loop antenna	4.05	4.51

4.7.2 Comparison with the recent methods published in literature

Here we compare the performance of our proposed system with the recently published results given in [23] and [13]. For effective comparison, we use antenna radius parameter of the proposed systems to indicate improvement over the *maximum error*. The *maximum error* is obtained from the radius of recognition area. Also, for fairer comparison, we have considered cases that use only sparse tag arrangement where, on an average only one tag is detected by the reader. Error improvement is calculated using:

$$Improvement = \left(\frac{MaximumError - AverageError}{MaximumError} \right) \times 100\% \qquad (4.17)$$

The comparison is tabulated in **Table 4-2**.

Table 4-2: Comparison of RFID based positioning methods

Positioning Methods	Tag separation (d_{tag} cm)	Radius of recognition area (R_{RA} cm)	Average error (r_{error} cm)	Improvement (%)
Sunhong's [13]	34	17.0	$x_{error} = 6.2$ $y_{error} = 5.4$ $*r_{error} = 8.22$	52
Choi et al [105] repeated in [23] at sparser tag separation, (RFID system + Encoder)	50	30.0	$r_{error} = 10.52$	65
Proposed method in this chapter using single bridge triangular loop reader antenna (TLB)	**130**	19.7	$r_{error} = 4.05$	**79**

* Derived from x_{error} and y_{error}

The method published in [13] reports an improvement of 52% whereas the method given in [105] which is also repeated in [23] with sparser floor tag-grid (d_{tag} = 30cm) reports an improvement of 65%. Our results consistently demonstrate that our proposed method outperforms the both the published approaches by offering improvement of

around 79%. In addition, our method employs much higher sparsity in tag separation of about 130 cm compared with 50 cm and 34 cm as quoted in the literature [23],[13].

4.8 Summary

We have presented a method to improve HF RFID based positioning under sparse floor tag-grid infrastructure using the proposed bridge reader antenna. The antenna provides bridge potential as a function of tag's location with respect to reader recognition area. We have also proposed a positioning algorithm which advantageously employs the bridge potential to estimate position and orientation of a moving object. The proposed system allows sparser floor tag infrastructure leading to lower cost and flexible tag deployment that can adapt to any application or infrastructure scenarios. Simulations and experimental results and the comparison with existing techniques show improvement in positioning accuracy even for large tag separations that make the tag-grid highly sparse. Our studies also indicate that for HF RFID based positioning, larger recognition area may not necessarily cause higher uncertainties. The novel bridge-loop concept can also be extended for many other RFID applications.

Chapter 5

Use of Tag Load Modulation to Enhance the Positioning

5.1 Introduction

In the previous chapter, the use of bridge antenna is demonstrated for localisation of a moving object using sparse floor-tag infrastructure. At any instance of time, the reader just requires one tag to accurately localise the moving object. The technique provides simple and elegant way of localisation requiring less number of tags while still maintaining good positioning accuracy, thus achieving localisation using sparser floor tag infrastructure. However, the algorithm presented in the previous chapter can be further improved for situations when two or more tags are detected.

The proposed bridge antenna can also be employed to offer additional advantages for applications or scenarios when there are two or more tags present within the antenna's RRA. For example, if the inter tag separation on a floor tag grid is not large, thus more than one tag can be detected by the reader. Under such scenarios, a system equipped with proposed bridge loop antenna can provide further improvements due to its ability to provide extra information in term of variations in the resulting bridge signals caused by multiple tags. One major improvement, which it can offer, is the estimation of instantaneous orientation of the moving object, which can be directly obtained solely on RFID measurements (along with the bridge signal) at a single location. This information can be useful when a moving object has to be localised in areas where many obstacles may be present or when it is traversing a narrow path. Thus, an added advantage can be helpful unlike the conventional techniques which normally require measurements from at least two locations [11-13, 103] or require additional sensors to obtain position [23].

In some other application scenarios, such as in smart spaces, smart cabinets or sorting tagged items, it is desirable to use the antenna to localise the locations of tags

under the presence of two or more tags. Unlike the conventional antenna, the bridge antenna allows the location of each tag with respect to the antenna. Here we propose a technique utilising the bridge antenna to locate individual tag in the presence of many other tags.

Contributions in this chapter includes; i) characterisation of the bridge potentials due to the effect of load modulation at the tags, ii) proposing a technique to manipulate the effect of tags' load modulation to obtain orientation of the antenna when two or more tags are present, iii) validation of the techniques through simulations and experiments.

This chapter is organised as follows: the section 5.2 describes the characterisation of bridge signals under the presence of multiple tags using tag's load modulation. Method to obtain bridge signal associated with each of the detected tag is described in section 5.3. Evaluation on realistic model is performed in section 5.4. In section 5.5, technique to practically acquire bridge signal is proposed. 5.6, followed by algorithm to determine the location and the orientation using state of tag load modulation, which presented in section 5.6. Experimentation to validate the proposed technique of splitting the bridge signal is given in section 5.7. Finally, we summarise this chapter in section 5.8.

5.2 Characterisation of bridge signals under the presence of multiple tags using tag's load modulation

When two or more tags are present within the RRA of a bridge loop antenna, further improvement can be made because additional information is available. However, an additional step is required to differentiate and identify to which tag is causing the change in the bridge potential signal, in order to recognise their locations. Fortunately, the standard RFID protocols allow a reader to communicate with a single tag even when there are other tags detected, but a proper analysis on the behaviour of the bride signal during tag's load modulation is necessary. We propose to utilise the aspect of tag's load modulation in our analysis in this chapter to identify methods to localise multiple tags. This is important as to enhance our HF RFID based positioning algorithm.

5.2.1 Tag's load modulation

Under a standard HF RFID protocol, a tag communicates with a reader by changing its load impedance, typically known as load modulation (see **Figure 5-1** (a)). There are two major types of load modulation typically used: i) Ohmic load modulation, and ii) Capacitive load modulation. The resulting signal due to the load modulation will be first experienced by the reader's antenna which is then relayed to the reader.
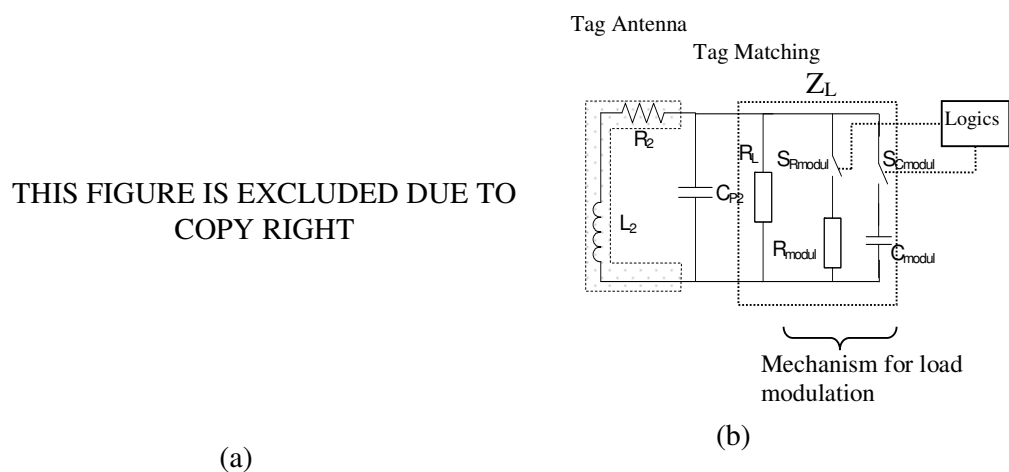
Figure 5-1: Load modulation at the tag

(a) Formation of load modulated signal [51], (b) a simplified circuit for load modulation

Under ohmic load modulation, R_{modul} is alternately switched so that it becomes parallel to the load resistance 'R_L' as illustrated in the schematic in **Figure 5-1** (b). This causes change in the overall impedance at the tag antenna thus altering the tag's transformed impedance which in turn affects the impedance of the reader antenna. Similar effects can also occur for capacitive load modulation, where switching a capacitor C_{modul} is involved which then alters impedance of the reader antenna. The difference between the two is that, the capacitive load modulation involves phase alteration.

These properties can be utilised to improve localisation by employing the proposed bridge loop reader antenna. To understand how the bridge signals (V_1 and V_2) are varied due to the change in tags' load impedance. We will first examine the change in impedance for a single loop reader antenna.

5.2.2 Effect of tag's load impedance on the impedance of a single loop reader antenna

Consider the equivalent circuit shown in **Figure 5-2** with R_{modul} and C_{modul} parallel to the R_L on the tag's antenna. The change in the reader's antenna loop can be obtained using similar expression as in (3.7) of chapter-3 but with slight modification so that the load resistance 'R_L' is parallel to R_{modul} or C_{modul}.
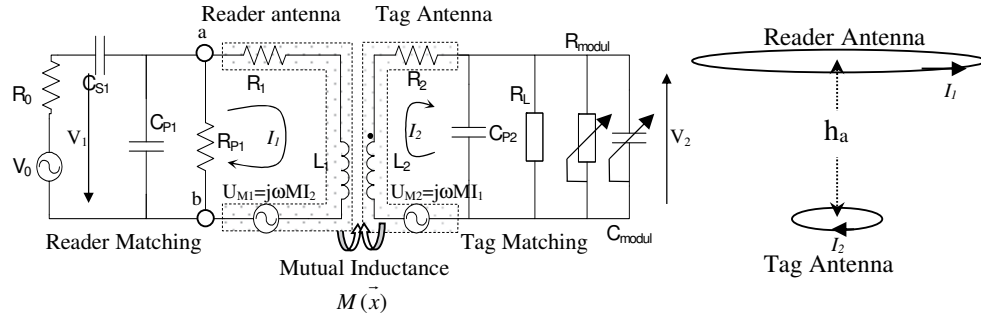
Figure 5-2: Equivalent circuit to obtain impedance change in a single reader loop antenna when the tag's load is varied.

$$\Delta Z_{reader} = Z'_{Tag} = \frac{(\mu_0 \omega N_1 N_2 r_1^2 r_2^2 \pi)^2}{\left(j\omega L_2 + R_2 + \left(\dfrac{R_L \| (R_{modul} \text{ or } C_{modul})}{1 + j\omega C_{P2} R_L \| (R_{modul} \text{ or } C_{modul})} \right) \right) 4\left(r_1^2 + h_a^2 \right)} \qquad (5.1)$$

We also investigate for the scenario when both the tag and a large metallic object are present near the single loop reader antenna illustrated in **Figure 5-3** below. Vertical separation between reader and tag antennas is denoted by 'h_a', while the separation between tag antenna and the metallic plate is denoted by 'h_b'.
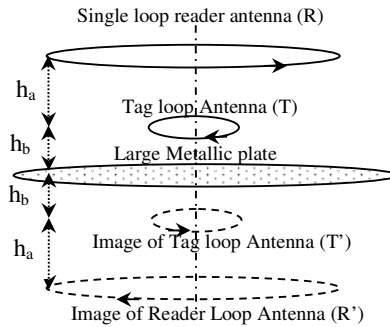
Figure 5-3: Scenario when both the tag and a metallic object are present near the single loop reader antenna

For this case, the resulting transformed impedance is obtained by modifying (3.13) of chapter-3 to include the parallel components R_{modul} and C_{modul}. The resulting expression is given by

$$\Delta Z_{reader} = Z'_{TT'R'}$$

$$= \frac{-\omega^2 (M_{TR} + M_{TR'})(M_{RT'} + M_{RT})}{j\omega M_{TT'} + \left(j\omega L_2 + R_2 + \left(\dfrac{R_L \parallel (R_{modul} \text{ or } C_{modul})}{1 + j\omega C_{P2} R_L \parallel (R_{modul} \text{ or } C_{modul})} \right) \right)} - j\omega M_{RR'} \qquad (5.2)$$

Mutual inductance M_{ij} is calculated using:

$$M_{ij} = \begin{cases} \dfrac{\mu_0 r_i^2 r_j^2 \pi}{2\left(r_i^2 + h_{ij}^2\right)^{3/2}} & \text{for i} \geq \text{j,} \\[4mm] \dfrac{\mu_0 r_i^2 r_j^2 \pi}{2\left(r_j^2 + h_{ij}^2\right)^{3/2}} & \text{for i<j,} \end{cases} \qquad i,j = \{T, R, T', R'\}. \qquad (5.3)$$

The term h_{ij} is related to the separation of reader-tag antennas 'h_a' and h_b as previously indicated in **Table 3-2** of chapter-3.

Recall that the above equations are known as transformed impedance, which indicate the change in impedance at the reader loop antenna. It depends on the parameters at the tag and also the distance h_a. Since we are only interested to know the effect of the reader loop impedance when the R_{modul} or C_{modul} are varied, we let other parameters to remain constant. We use the parameter values indicated in the Table 3-1. All the assumptions set in section 3.3 for are applicable here. In the next section, we will use the above equations to investigate the changes in the impedance of the reader loop.

5.2.2.1 The impedance variation of a single loop reader antenna when varying tag's load impedance

Using (5.1) and (5.2), we evaluate the effect of R_{modul} on the impedance of the single loop reader antenna by varying the value of R_{modul} from 0 to 1K Ohm. We also vary the C_{modul} so that it reactive impedance X_{Cmodul} takes the values from ≈ 0 to 1K Ohm. This extreme range is purposefully chosen to see how R_{modul} and C_{modul} influence the impedance of a single loop reader antenna. When evaluating the effect of R_{modul}, the value of X_{Cmodul} is set to be very large so that the resulting impedance is mainly due to

the parallel combination of R_L and R_{modul}. Similarly, when evaluating the effect of C_{modul}, the R_{modul} is set to be very large. The changes in the impedance of single loop reader antenna are plotted as in **Figure 5-4**.
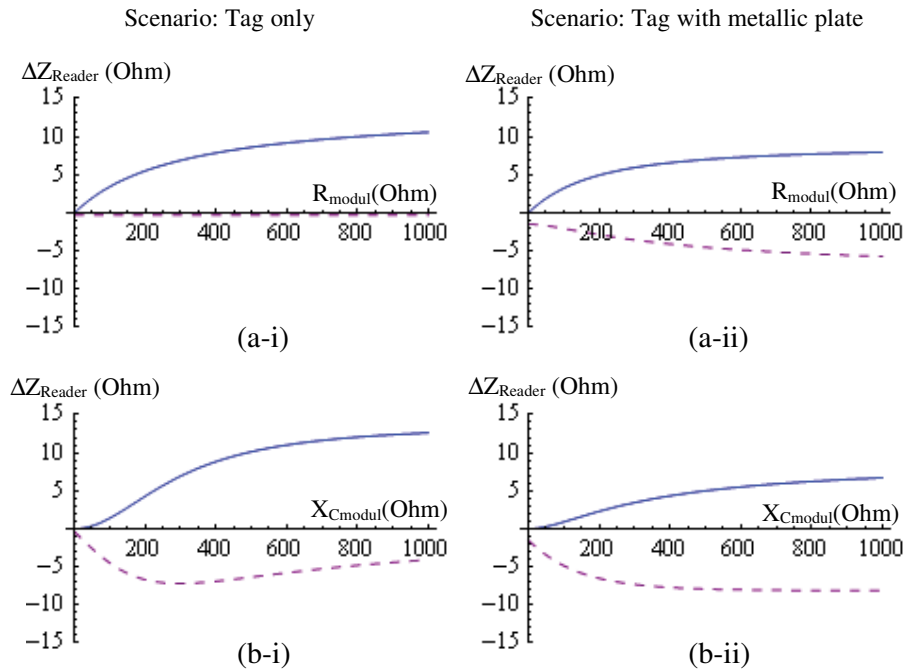
Figure 5-4: The change of input impedance of the single loop reader (h_a=constant)
(a) R_{modul} changes from (0 to 1 KOhm, X_{Cmodul}>>R_L), (b) X_{Cmodul} change from ($\approx$0 to 1 K Ohm, R_{modul}>>R_L). Solid lines represent real components, while the dashed lines represent imaginary components.

The results indicate that the change of the tag's impedance alters the impedance of the single loop reader antenna for both the scenarios. That means, similar patterns occur whether a tag is only present or both the tag and the metallic plate are present. The increase in the tag's impedance 'R_{modul}' or 'X_{Cmodul}' increases the real component of a single loop reader antenna. When the R_{modul} alternately varies between two extreme values, i.e. a low impedance ($R_{modul} << R_L$) and a high impedance ($R_{modul} >> R_L$), as seen in the plots, the impedance of the loop follows the same trend as it varies between low and high impedance states. Similar change can also be observed when the capacitive load changes. Now we will closely examine considering the two extreme cases while varying the separation distance 'h_a'.

5.2.2.2 The impedance variation of a single loop reader antenna due to State of tag's load impedance when varing tag-reader separation

The previous subsection highlights that the change in the impedance of a single loop reader antenna 'ΔZ_{reader}' influenced by the tag's load impedance 'Z_L'. However, the influence of Z_L to the ΔZ_{reader} can be different when the separation between tag and the reader 'h_a' changes. The reason is that, smaller h_a increases the mutual inductance between the tag and the reader. This characteristic can be used to recognise the location of the tag which will be investigated further.

To simplify the analysis, we consider that the tag's load impedance (Z_L) takes only two discrete values corresponding to the state of the switch S_{Rmodul}, i.e. when the S_{Rmodul}=on, then the tag's load impedance = R_L, and when S_{Rmodul}=off, then the tag's load impedance = $R_L \| R_{modul}$. This switching mechanism is illustrated in **Figure 5-1**. Using (5.1) (for the case when only tag is present), and (5.2) (when both tag and metal are present), the resulting ΔZ_{reader} are plotted in **Figure 5-5** (a) and in **Figure 5-5** (b) respectively.
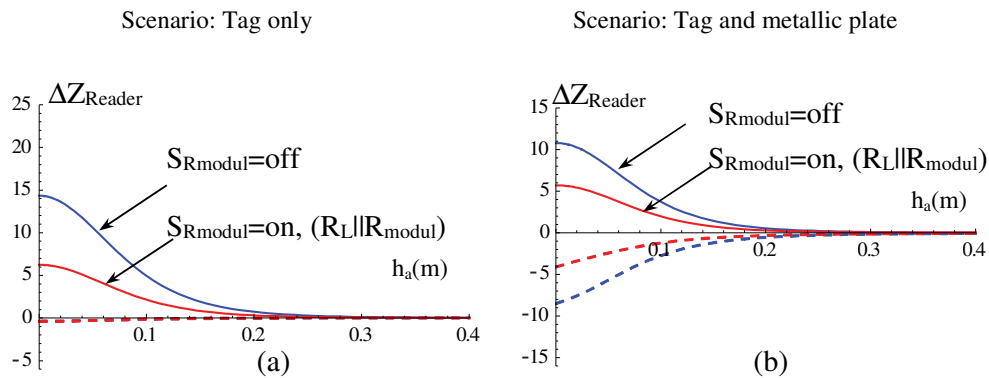
Figure 5-5: The change in impedance at the reader loop when (S_{Rmodul} = on, and off), h_a is varied (a) only tag is present, (b) both tag and metallic plate are present. Solid lines represent real components while dashed lines represent imaginary components.

As expected, the results show that the effect of Z_L on ΔZ_{reader} increases when the tag gets closer to the reader antenna, i.e. with smaller h_a. Two distinct lines pointed in each of the plots of **Figure 5-5** indicate this. As can be seen, the separation between the two solid lines widens as h_a decreases. This characteristic can be useful to indicate separation distance between the reader and the tag. Since bridge signal depends on

ΔZ_{reader}, and hence, they also experience similar characteristics. To verify this, let's repeat similar analysis for the bridge signals.

5.2.3 Effect of tag's load impedance on the bridge signals

To obtain the corresponding variation on the bridge signals, the above changes are applied to the equations of a full bridge loop antenna. The expressions for bridge potentials $V_{\beta1}$ and $V_{\beta2}$ as shown previously in chapters 2 and 3 can be extended to consider multi tags present within its recognition area RRAs. To assist with explanation, we redraw the diagram of a single bridge loop antenna as in **Figure 5-17**.
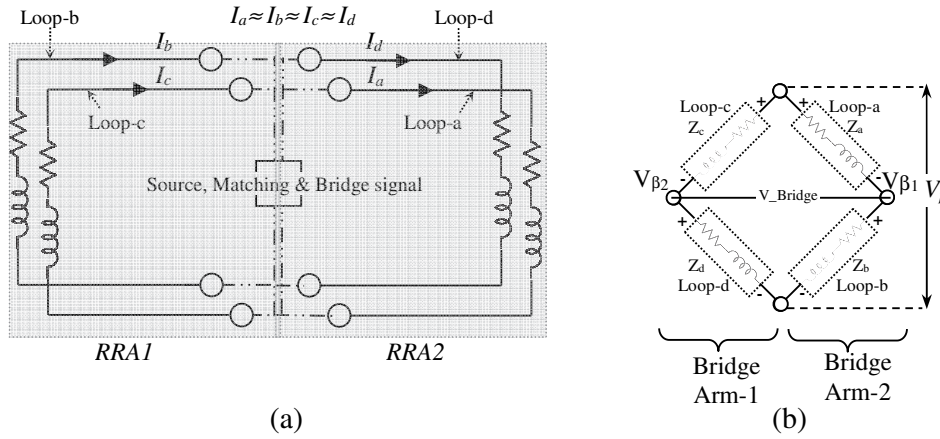
Figure 5-6: Diagram for a single bridge loop antenna

Considering changes on all of the loop elements, more general expressions for the potentials at bridge arm-1 '$V_{\beta1}$' and bridge arm-2 '$V_{\beta2}$' can be written as:

$$V_{1,m} = \left(\frac{Z + (\Delta Z_m^{RRA1})}{2Z + (\Delta Z_m^{RRA2}) + (\Delta Z_m^{RRA1})} \right) V_p, \qquad (5.4)$$

$$V_{2,m} = \left(\frac{Z + (\Delta Z_m^{RRA2})}{2Z + (\Delta Z_m^{RRA1}) + (\Delta Z_m^{RRA2})} \right) V_p. \qquad (5.5)$$

The term ΔZ_m^{RRA1} and ΔZ_m^{RRA2} represent the change in the loop impedance when tags present within the RRA1 and RRA2 respectively. The subscript 'm' indicates two scenarios either: i) the presence of tag only, or ii) the presence of tag and metal, in which $m \in \{Tag, Tag \& Metal\}$.

5.2.3.1 The variation of bridge signal when varying tag's load impedance

We will first look at the influence of changes in tag's load impedance on the bridge signals when a tag present within the bridge loop reader antenna's recognition area RRA. The following bridge signals are considered for analysis:

i)   Imaginary component of the difference between $V_{\beta 1}$ and $V_{\beta 2}$: $\mathrm{Im}(V_{\beta 1} - V_{\beta 2})$

ii)   Phase of ratio between $V_{\beta 1}$ and $V_{\beta 2}$: $\mathrm{Phs}(V_{\beta 1} / V_{\beta 2})$

These two cases are considered here because they can minimise the effect of proximity of metallic objects on the bridge antenna as discussed in chapter 3. The term $V_{\beta 1}$ and $V_{\beta 2}$ do correspond to the potentials at bridge arm-1 and bridge arm-2 as indicated in **Figure 5-6**, and they are calculated using (5.4) and (5.5) respectively.
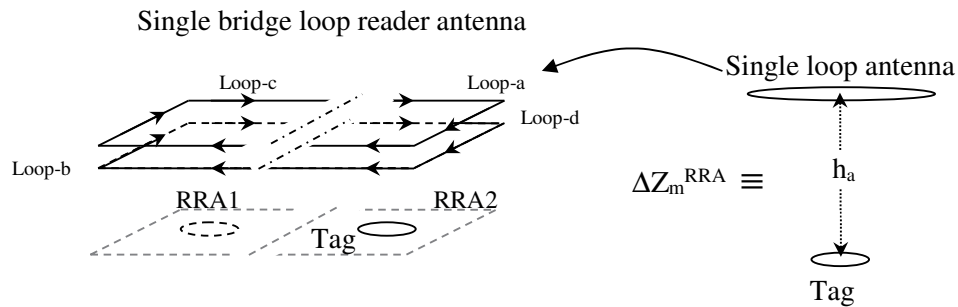
Figure 5-7: Extending characteristics of a single loop reader antenna to a single loop element in a bride antenna

A tag is considered to be located at the centre of RRA1, and then RRA2 as illustrated in **Figure 5-7**. For each case the bridge signals are computed while the load impedance at the tag is made to vary linearly. Results from 5.2.2.1 are utilised to represent the changes in the loop impedance associated with the loops of the bridge antenna. When a tag is located on RRA1, then the change in the loop impedance (loop-c and loop-b) is $\Delta Z^{RRA1} = \Delta Z_{\mathrm{Reader}}$. Similarly, when the tag is within RRA2, the change in impedance for loop-a and loop-d is $\Delta Z^{RRA2} = \Delta Z_{\mathrm{Reader}}$. For all the cases, the separation between the tag and the antenna h_a is kept constant. The results for the impedance change due to both resistive and capacitive loads are plotted in **Figure 5-8** and **Figure 5-9** respectively. Both the scenarios viz., for tag only present, and both tag plus metallic objects present are considered.
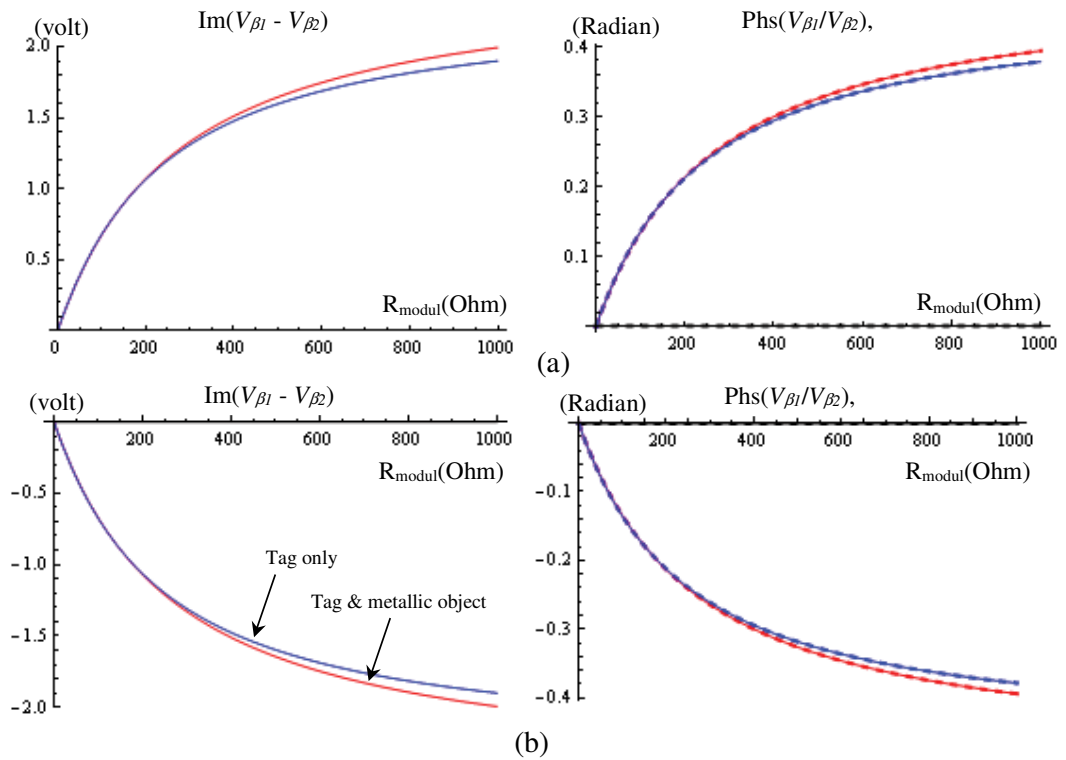
Figure 5-8: Variation of the signals due to change in R_{modul}

(a) the tag located at the RRA2, (b) the tag located at RRA1.
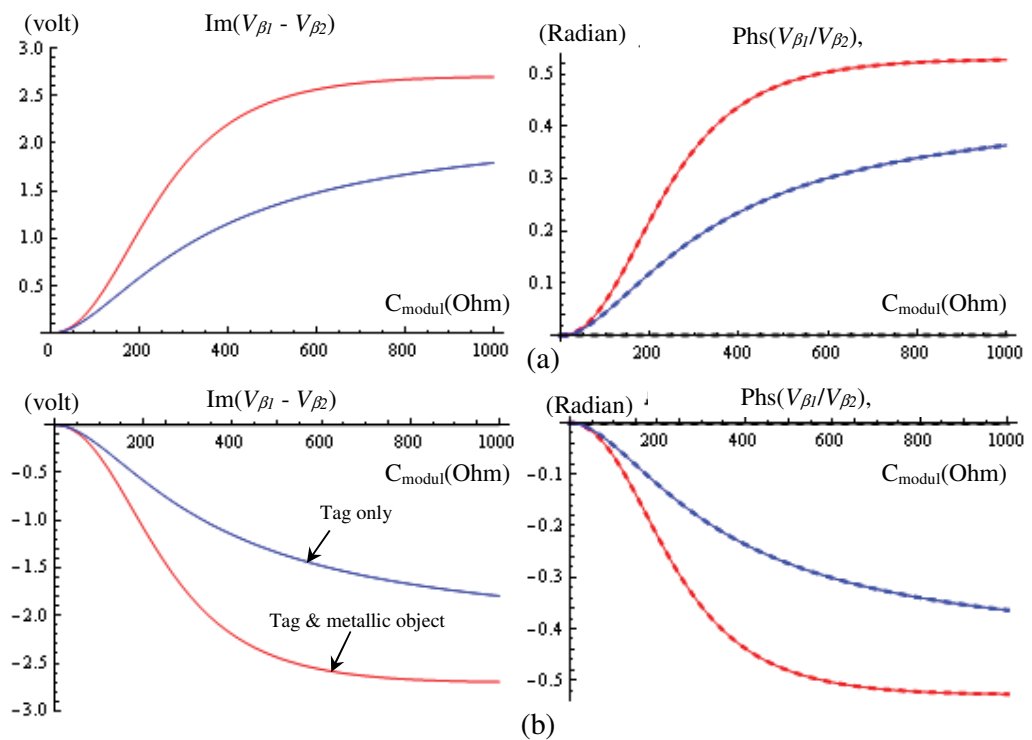
Figure 5-9: Variation of the signals due to change in X_{Cmodul}

(a) the tag located at the RRA2, (b) the tag located at RRA1.

Results in **Figure 5-8** and **Figure 5-9** indicate that the change in the tag's load impedance alters the bridge signals.

Results indicate that the bridge signals change correspondingly with the load impedance when the tag presents in either reader recognition areas RRA1 or RRA2. However, the polarity of the bridge signals change (opposite sign) depending on the location of the tag. When the tag is on RRA2, the bridge signals increase with the increase of tag's load impedance. On the other hand, when the tag is on RRA1 the bridge signals decrease. This difference in polarity as well as the increasing and decreasing trends are important as they can indicate about the position of the tag.

Another important feature is that the expressions derived for bridge signal and used to minimise the effect of metallic interference are also applicable here. Referring to **Figure 5-8** (a) and (b), the lines in the plot whose correspond to both the scenarios (i.e. i. Tag only present, and ii. Tag and metal present) are close together indicating the interference due to metallic object is minimal when applying the proposed method of minimising metallic interference. These occur especially when the tag is operated under ohmic (resistive) load modulation mode. In this modulation mode, R_{modul} is used instead of C_{modul}. We henceforth will be using this ohmic modulation mode.

5.2.3.2 Bridge signals due to State of tag's load impedance (Z_L) at different tag-reader separation (h_a)

Section 5.2.2.2 highlighted that the effect of tag's load impedance (Z_L) can be useful to recognise the location of tag. However, it is not practical for a single loop antenna because it is difficult to obtain the measurable parameters to indicate the changes. Bridge antenna on the other hand can provide practical signals ($V_{\beta1}$ and $V_{\beta2}$) at the bridge terminals.

To investigate whether the characteristics that are present for a single loop reader antenna as indicated in the section 5.2.2.2 are same for a complete bridge antenna, (that involve multiple loops) we perform an analysis of the bridge signal. The method of obtaining the bridge signals as explained in the previous subsection 5.2.3.1 is utilised. The resulting bridge signals ($Im(V_{\beta1}-V_{\beta2})$, and $Phs(V_{\beta1}/V_{\beta1})$) are plotted as in **Figure 5-10**.
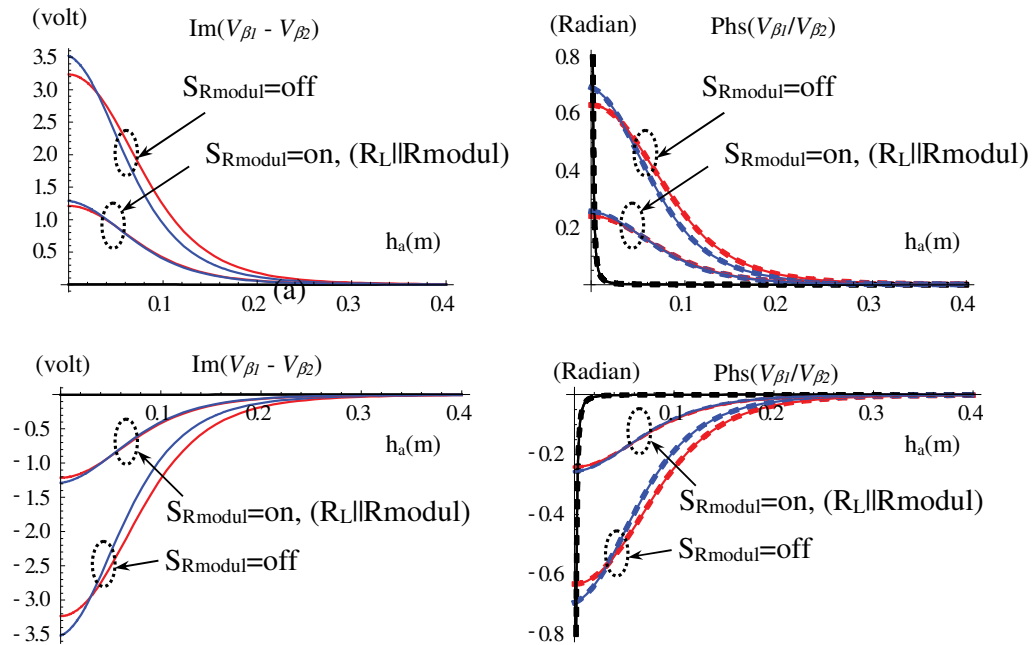
Figure 5-10: Change in bridge signals when (S_{Rmodul} =on, the off) and h_a is varied

(a) the tag is below the loops of RRA2 (b) the tag is below the loops of RRA1.

As expected, in **Figure 5-10** show that the results from the chosen bridge signals follow the trends similar to the results obtained previously in 5.2.2.2 The lines that correspond to states of the switch S_{Rmodul} widens with the distance from the tag to the antenna 'h_a'. This increasing gap is a very promising characteristic to allow localisation when multiple tags are present within the RRA. We will further investigate as to how to utilise this characteristic for the desired application.

5.3 Formation of individual bridge signals to identify the locations of tags

In general, when two or more tags present within RRA of a bridge antenna, the resulting bridge signals are the combined information from all the tags, and hence cannot be directly utilised to obtain position information. However, the use of state of tags (i.e. on or off) due to the change in tag's load impedance (S_{Rmodul}=on, S_{Rmodul}=off) can create variation in the bridge signal which changes with the state of S_{Rmodul}. It is possible to use this information for the separation of the bridge signal and thus locate the locations of the tags with respect to the antenna.

The signal variation due to state of tag was observed in the results in Figure 5-5 of in section 5.2, in which the loop impedance taking different values depending on the state of the detected tag (i.e. the state of S_{Rmodul} either on or off). In addition, the difference between the two values of loop impedance which correspond to S_{Rmodul} gets larger when the detected tag gets closer to the loop antenna.

Similar characteristics also occur for the bridge signals shown in Figure 5-10. The gap between the signals that correspond to the state of the detected tag increases with the increase in relative position 'h_a'. The increase in 'h_a' indicates the reduction of coupling between the tag and the loop antenna.

Reduction in coupling will also occur when the tag is moved away horizontally. For the sake of simplicity, let us only evaluate the change in relative distance by varying the vertical displacement h_a so as to satisfy the assumption made in using (5.4) and (5.5).

To further elaborate this, consider **Figure 5-11**, where a single bridge rectangular loop antenna with two tags present within RRA1 and RRA2. The distances h_1 and h_2 indicate how far the tags are displaced from the centre of the antenna. This is appropriate because when the tag is located away from the centre of the RRA, the level of coupling gets reduced. The same effect can be observed even when the distances h_1 and h_2 are increased. The main aim of this approach is to simplify the problem and demonstrate its usefulness while at the same time still be able to study the changes occur in bridge signal when (more than a single) tags move within the RRAs.

5.3.1 Change in Bridge signals in the presence of two tags

We will begin by first considering that both two tags (TagA and TagB) are located at positions in such a way the level of mutual inductance between each tag and the loop antennas of the bridge are similar. Assume that TagA moves within RRA1 while TagB moves within RRA2 as illustrated in **Figure 5-11** (a). We then create a situation where both of the tags no longer has equal mutual inductance by letting $h_1 \neq h_2$ as illustrated in **Figure 5-11** (b).
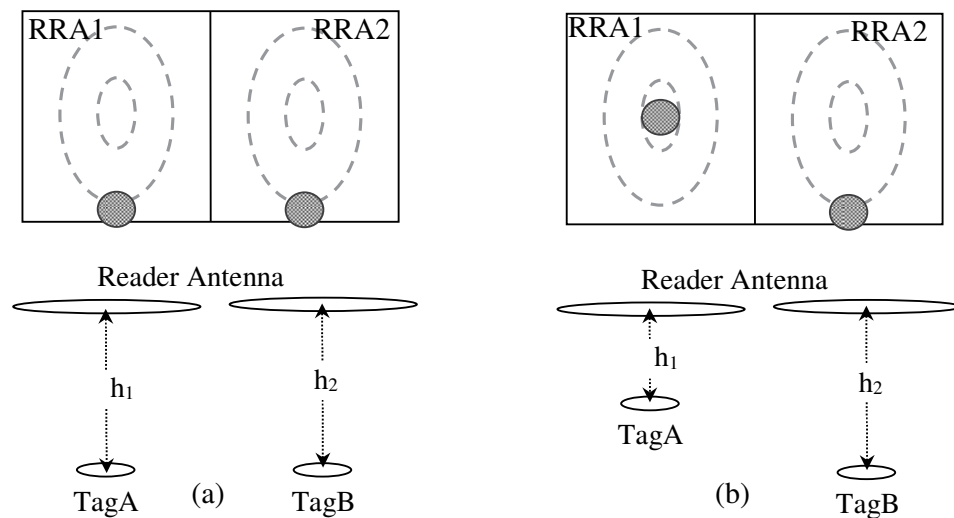
Figure 5-11: (a) TagA and TagB have equal mutual inductance w.r.t the loops of the bridge antenna, (b) TagA and TagB have unequal mutual inductances.

Throughout the previous analysis on the bridge antenna, there is consistent evidence on the influence of tag's load impedance on all the chosen expressions for bridge signals i.e. $Im(V_{\beta 1}-V_{\beta 2})$ and $Phs(V_{\beta 1}/V_{\beta 2})$. Therefore, in this section we will only consider one of the bridge signals that is $Im(V1-V2)$.

In the presence of two tags, the bridge signal can be considered to vary between three values corresponding to the current state of the tags. The possible combination of the state of the tag and the corresponding identification symbol designated for the bridge signal is indicated in the **Table 5-1**.

Table 5-1: Bridge signal due to state of tag

Designation for the bridge signal	State of tag or State of the tags' modulation switch 'S$_{Rmodul}$'	
	TagA or Tag1	TagB or Tag2
v_i	On	Off
v_{ii}	Off	On
v_{iii}	Off	Off

For the scenario in **Figure 5-11** (a), where both the distances h_1 and h_2 are equal, their values are made to increase from 0 to 0.4m, and the resulting bridge signals are shown in **Figure 5-12** (a). As for situation shown in **Figure 5-11** (b), when the distances h_1 and h_2 are made to be not equal (i.e. h_1 is let to increase by 0.03m as compared to h_2), the results are shown in **Figure 5-12** (b-c).
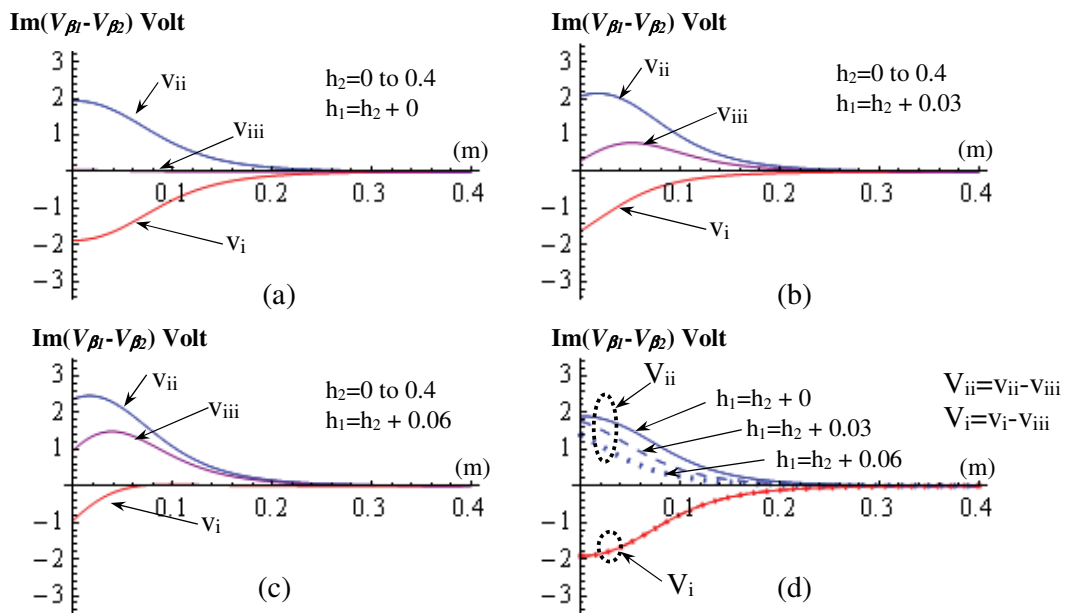
Figure 5-12: Bridge signals when two tags are present under the bridge loops

In the **Figure 5-12**, the terms (v_i, v_{ii}, and v_{iii}) are defined in **Table 5-1** , and the terms (V_{ii} and V_{iii}) defined in **Table 5-2**.

Referring to the results in Figure 5-12 (a), the signals v_{ii} and v_{iii} has equal amplitudes but with different polarity. The reason for this is that both the tags are equally coupled to the loops of the bridge antenna (i.e. they have similar levels of

mutual inductance) but located on different sides of the RRA. This can be regarded as the simplest case when two tags are present. The location of the tags can be directly obtained by examining the polarity and the level of the signal. In other words, we are able to recognise within which RRAs, the tags are located by merely using the polarity of the bridge signals that correspond to the state of tags, and the magnitudes of the bridge signals further refine the location of the tags within those RRAs.

Utilisation of the bridge signal will become complicated when the level of mutual inductances on the tags are different i.e., by letting h1≠h2. In this case, we let h1>h2, the signals start to have offsets with respect to positive y-axis (see Figure 5-12 (b)). Further increase in the difference between h_1 to h_2, increases the offset in the signals (see Figure 5-12 (b)). The offset in the signals can further complicate the recognition the location of the tags. To overcome this problem, we can take 'v_{iii}' as a reference signal and use this reference in obtaining a more stable signal. The 'v_{iii}' is chosen because when this signal occurs, both the tags are in the same state, hence, the amount off offset during this state can be utilised to correct the signal. Designations for offset free bridge signal, which depend on the states of the tags, are indicated below in **Table 5-2**.

Table 5-2: Offset free bridge signal

Designation for the offset free bridge signal	State of tag or State of the tags' modulation switch 'S_{Rmodul}'	
	TagA or Tag1	**TagB or Tag2**
$V_i = v_i - v_{iii}$	On	Off
$V_{ii} = v_{ii} - v_{iii}$	Off	On

A more general expression for the **offset free bridge signal** can be written as

$$V_{tagi\_on} \; = \; v_{tagi\_on} \; - \; v_{tag\_all\_off} \qquad\qquad (5.6)$$

where 'v_{tagi_on}' represent the bridge signal when only S_{Rmodul} of tagi is 'on'. As for the term '$v_{tagi\_all\_off}$', the load modulation switch S_{Rmodul} for all tags are in the 'off' state. Note that we use capital 'V' for offset free signals as opposed to the small letter 'v' for signals having offset. For brevity, we will use 'V_{tagi}' as the short form of 'V_{tagi_on}'.

Applying the offset removal, we obtain signals as indicated in Figure 5-12 (d), which are more stable. Results in this figure show the combination of all the results taken from Figure 5-12 (a-c), which are obtained by substituting the signals from their offsets obtained from their respective 'v_{iii}'. The results in Figure 5-12 (d) do clearly indicate correlation between the level of bridge signals to the location of tags, i.e. the signals are now well correlated with variation in h_1 and h_2. On the next section, we utilise these results to estimate the location and the orientation of the antenna or the moving object when more than one tag is present.

5.4 Verification using realistic models

We verify the above findings using realistic models. The model consists of a single bridge triangular loop HF RFID reader antenna, with tags having characteristics similar to that of commercial tags. The reader antenna is positioned cantered with respect to x-y plane and the tags are positioned below the reader antenna at z=-6cm as illustrated in the **Figure 5-13**. The tag located in RRA1 is denoted as tagA and the other tag which is located in RRA2 is denoted as tagB. The parameter l_A and l_B indicate the distances from the centre of tagA and tagB to the projected x-axis on the overall RRA. These parameters are varied and the resulting bridge signals are computed using FEKO. A 200mW input power is fed to the antenna which is typical of a conventional HF RFID reader. At any instance, three sets of bridge signals are recorded namely v_i, v_{ii} and v_{iii} which correspond to the state of tags as tabulated in **Table 5-1**.
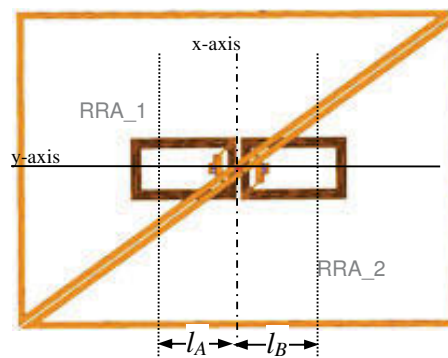
Figure 5-13: Model of tags and the bridge antenna arranged to evaluate the effect on the bridge signals

The control of the state of tags and the change in the distance parameters l_A and l_B are performed using Matlab prior to computation using FEKO. This integration allows the overall computation to be performed effectively.

To see the behaviour of the bridge signal due to the presence of two tags, we vary the parameters in our simulation in the following ways:

i)   The parameters l_A and l_B are increased equal steps so that the tags are away from the central line symmetrically.

ii)   Step (i) is repeated but l_A is offset by 2.4cm.

iii)   Step (i) is repeated but l_A is offset by 4.0cm.

iv)   Step (ii) and (iii) are repeated but the offset is set for l_B instead of l_A.

Results for vi, vii, and viii for the above scenarios are plotted as in Figure **5-14**. Using these results, we then apply offset removal similar to the one we proposed in 5.3.1, the new results are plotted in **Figure 5-15**.
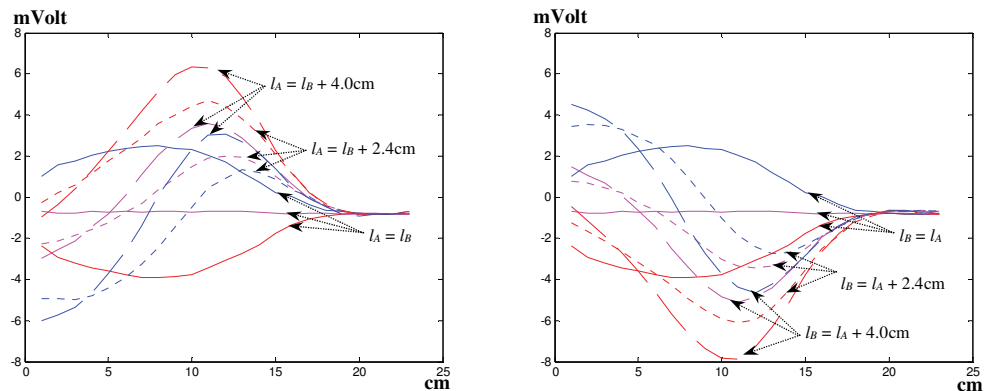
Figure 5-14: Bridge signals before offset removal
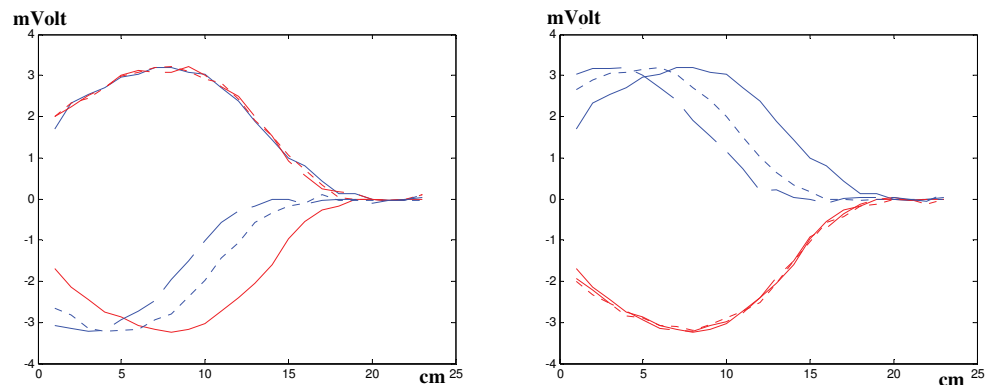
Figure 5-15: Bridge signals after offset removal

Referring to the results shown in Figure **5-14** (a-b), when the tags are equidistant with respect to loops, the bridge signals have a symmetrical variation. When tagA or

tagB are offset, the results in the same figure indicate the whole set of signals shift. This shift makes it difficult to estimate positions as it create positioning errors. The use of offset removal overcomes this problem as clearly indicated by the plots in **Figure 5-15**.

In general, the above results are consistent with the results from the equivalent circuits on thin wire bridge antenna model as discussed previously in 5.3.1. This confirms the veracity of our model and analysis. The removal of offset from the bridge signal improves localisation when there are multiple tags present within the reader recognition area.

5.5 Acquisition of Bridge signals during load modulation

THIS FIGURE IS EXCLUDED DUE TO COPY RIGHT

(a)

(b)
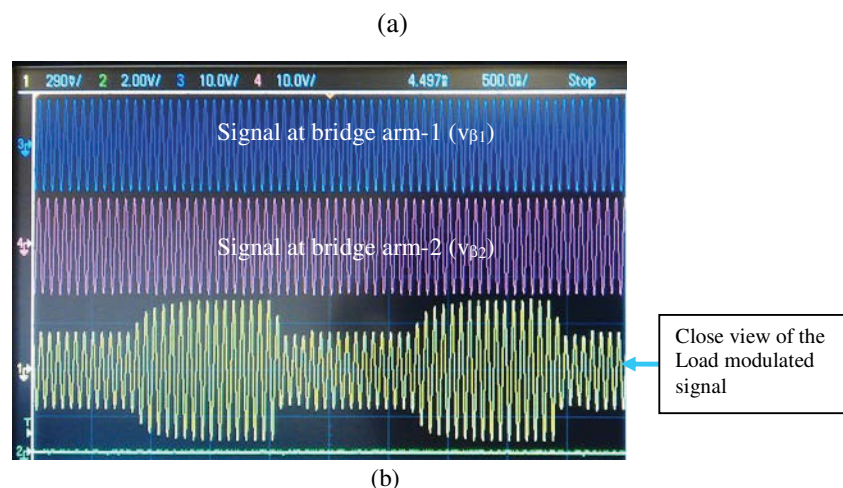
Figure 5-16: Bridge signal during load modulation

(a) The signals from reader and transponder/tag during tag interrogation (reproduce from [106]),

(b) Close view of the load modulated signal.

During ohmic load modulation, the switch S_{Rmodul} is alternately switched 'on' and 'off' that corresponds to the bit stream from the tag, which may contain information to be transferred to the reader. The time instant at which we record the signal is important so that it corresponds to the state of S_{Rmodul} i.e. whether it is on or off. This can be achieved by using an interrupt signal typically accessible from a standard reader. The signals corresponding to tag's load modulation occurs between the interrupt windows as illustrated in Figure 5-16 (a). A close view of the load modulated signal along with the bridge potentials $v_{\beta1}$ and $v_{\beta2}$ is illustrated in Figure 5-16 (b).
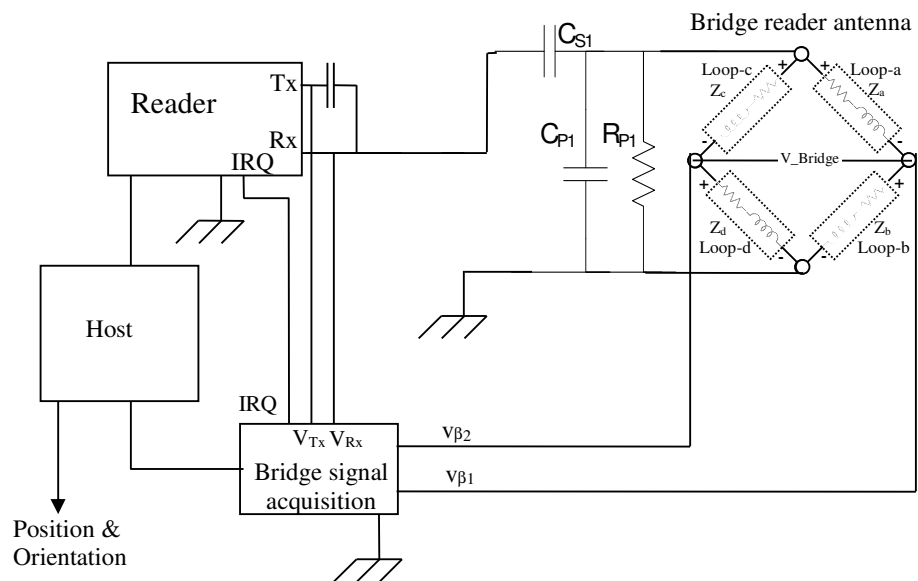
Figure 5-17: Block diagram illustrating the connections to acquire bridge potentials $v_{\beta1}$ and $v_{\beta2}$ along with the signalling to obtain the timing for load modulated signal.

It is important to know the correct time instance to acquire signals $v_{\beta1}$ and $v_{\beta2}$. Referring to **Figure 5-16**, the interrupt signal can only provide the window at which the load modulation can occur. To identify as to when the tag starts sending its load modulated signal, we need to monitor the modulated signal at the reader. The signal is obtainable from receiver (Rx) terminal at the reader. However, the load modulated signal at Rx terminal is extremely weak as compared to the carrier that is available at Rx. To overcome this problem, a comparator can be employed to subtract the signal at R_X from the carrier that is radiated by the transmitter. The output from the comparator is then amplified so that it provides a proper level of load modulated signal. The diagram illustrating the schematic representation of the system for acquiring the bridge signal is illustrated in **Figure 5-17**.

5.6 Algorithm to determine the location and the orientation using state of tag load modulation

To obtain the location of the antenna/object we firstly need to estimate the location the tags with respect to the RRA of the antenna. To simplify explanation, we consider that two tags are detected for any given location. The measured Bridge signals corresponding to the detected tags are denoted as V_{tagA} and V_{tagB}. These are the offset free bridge signals obtained using method described in the previous section. The polarity of the V_{tagi} will indicate under which RRA zones the tagi is located. Depending on the state of the object and the number of measurements, the accuracy of the estimations for position and orientation can be improved.

5.6.1 Position and orientation with limited measurements

Consider that a bridge antenna is used to localise a moving vehicle where the antenna is fixed at its base. To simplify the discussion, let us consider the bridge antenna is in the form of 'single bridge rectangular loop'. When the vehicle is at rest or in motion in its initial state, only one set of measurements are available i.e. V_{β_tagA} and V_{β_tagB}. With these, the orientation and the position of the antenna/object can be roughly estimated. Specifically, upon obtaining the potential $V_{\beta\_tagi(i \in A,B)}$, we can determine under which RRA zone the tags are located by using the polarity of the signal of V_{β_tagi}. Negative polarity indicates that the tag_i is within RRA1 and vice versa (refer to Figure 5-12 (d)). The specific locations of the tags within the RRAs are then determined by using the magnitude of the potentials as illustrated in **Figure 5-18**.

Since there exist multiple solutions that can satisfy the locations of the tags, we apply the following restrictions: i) the separation between the two tags must satisfy $d_{A,B}$, and ii) the tags are assumed to be located within the positive X_β-axis. The distance between tags ($d_{A,B}$) is calculated from the coordinates of the tags obtained from the database of the floor tag infrastructure. Once the locations of the tags within the RRA are identified, the bridge correction factors r_β and θ_β can be estimated. The r_β is calculated as in (5.7) and the angle θ_β is taken as the angle between the central vertical axis (X_β-axis) of the antenna and the line representing r_β (refer to **Figure 5-18**).

$$r_\beta = |l_A - d_{A,B}| \qquad\qquad (5.7)$$
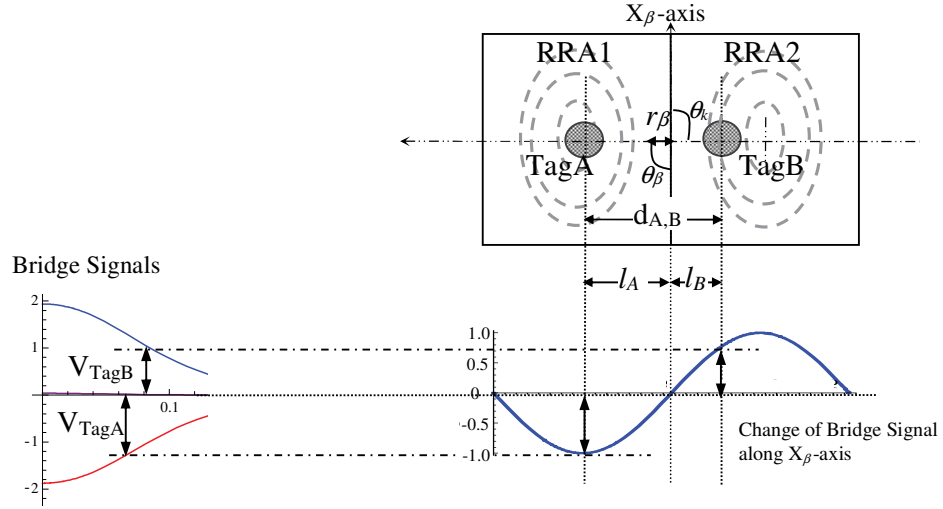
Figure 5-18: Estimate the locations of tags and the relative position

The parameters l_A and l_B are correlated with V_{TagA} and V_{tagB} respectively as indicated by the results in section 5.3 and 5.4. We can write

$$\frac{l_A}{l_B} = \frac{V_{TagA}}{V_{TagB}} \tag{5.8}$$

and

$$l_A = \frac{V_{TagA}}{V_{TagB}} \times l_B \tag{5.9}$$

The θ_β is obtained from

$$\theta_\beta = \begin{cases} \pi/2 \; ; \text{ for } l_A \geq l_B, \\ -\pi/2; \text{ for } l_A < l_B. \end{cases} \tag{5.10}$$

The position of the object then is estimated using

$$P_{TLB}(t) = \begin{bmatrix} mean(x_{Tag_i}) - r_\beta \cos(\theta_k + \theta_\beta) \\ mean(y_{Tag_i}) - r_\beta \sin(\theta_k + \theta_\beta) \end{bmatrix}. \tag{5.11}$$

The term θ_k is the heading angle. It is estimated between the line connecting the estimated coordinates of the tags and the X_β-axis as illustrated in see **Figure 5-18**. The overall flow diagram explaining how to obtain position and orientation is illustrated as in **Figure 5-19**.
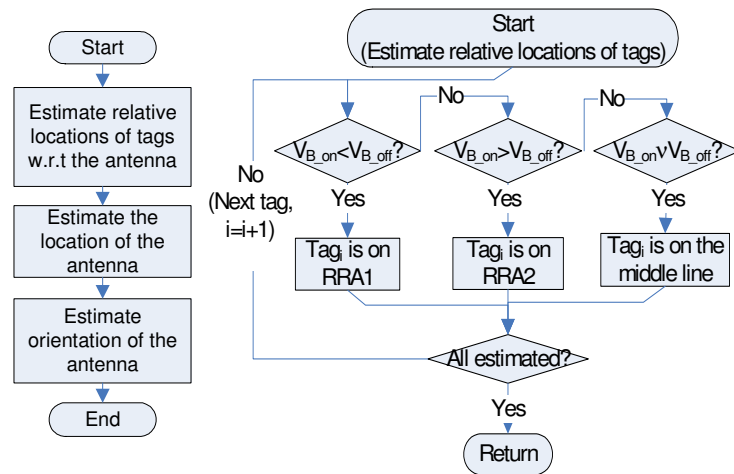
Figure 5-19: Algorithm to determine location and orientation of the antenna

5.6.2 Algorithms to acquire bridge signals during tag load modulation

An algorithm is required to ensure that set of bridge signals are acquired in a proper manner so that the signals correspond to the states of modulation switch (S_{Rmodul}) of the detected tags. We propose two types of algorithms: the first algorithm acquires the bridge signals immediately during reader-tag interrogation period. In other words, the bridge signals associated to the state of S_{Rmodul} of the detected tag are acquired right away when detected tags sending their information to the reader. This algorithm is therefore works relatively faster; however, it may require relatively higher speed components to cope with the high-speed signals.

Our second proposed algorithm is an alternative to the first one. It acquires bridge signals after all the tags within the RRA of the bridge reader antenna are identified. This algorithm uses 'silent' command to communicate with a single tag while acquiring a set of bridge signals that correspond to the state of S_{Rmodul} of the tag. This is performed until the set of bridge signals for all the tags are obtained. Both the algorithms are presented in flow charts as shown in **Figure 5-20**.
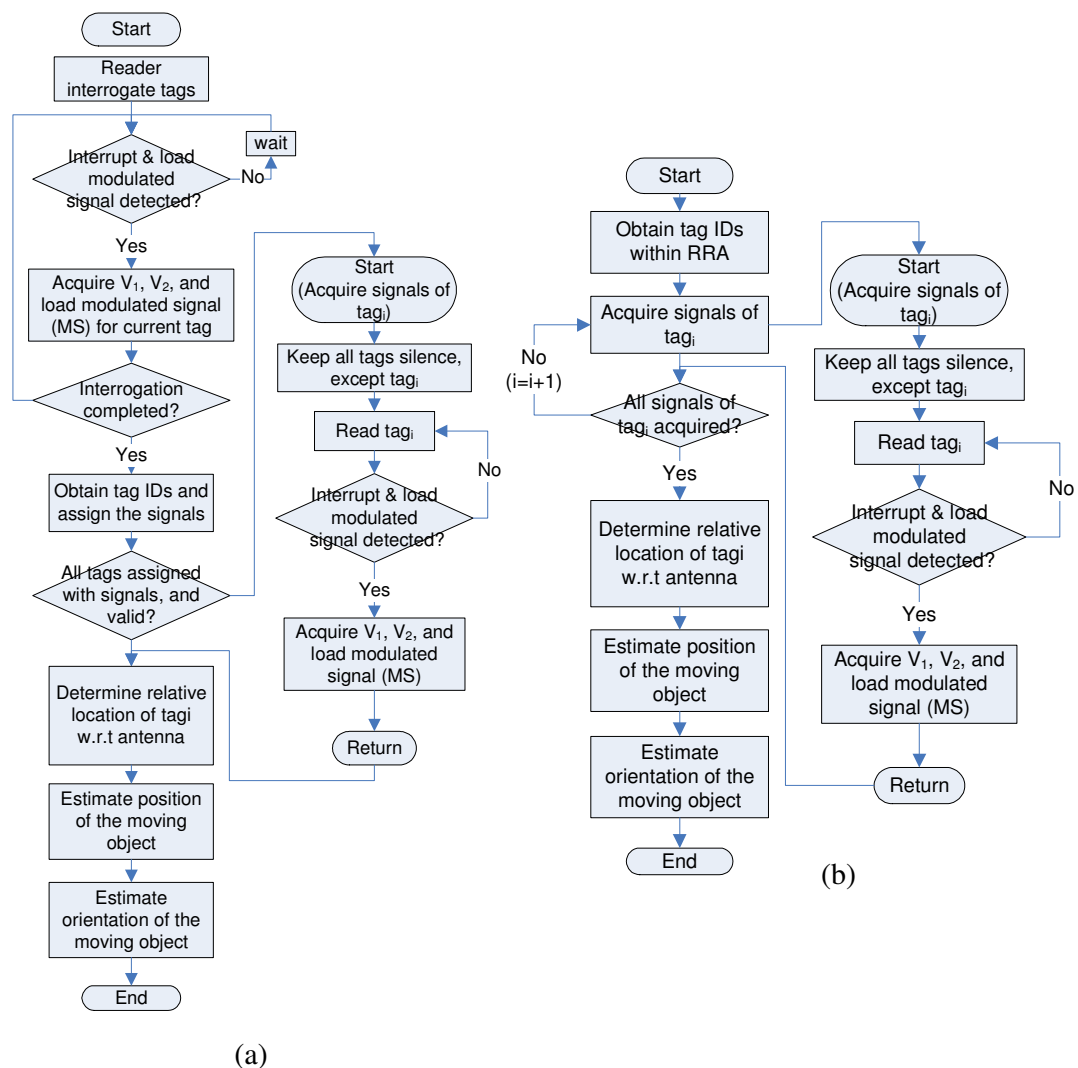
Figure 5-20: Algorithms to acquire information to localise under multi tags;
(a) Algorithm-1: acquire immediately, (b) Algorithm-2: acquire with 'silent mode'.

Some procedures in our first algorithm are similar to the second algorithm. The purpose is to ensure all sets of bridge signals can be acquired if failed in the first attempt.

The 'silent mode' used in the above algorithm is a standard command with most of the commercially available readers and most tags have capability to interact with that command. Our system is designed to work with the commonly used RFID standard that is ISO 15693. If one desires to extend our method with other standards, the above algorithm can be easily modified to suit any HF RFID standard and application. In the next section, we demonstrate use of our second algorithm for performing bridge signal acquisition for our experimentation.

5.7 Experimentations

Series of experimentations are performed to validate the proposed method. Our first aim in this section is to validate whether the bridge signal varies with the state of the modulation switch S_{Rmodul} of the detected tag. The second aim is to verify whether the state of tags from two tags can be utilised to recognise within which RRA zones the tags are located. Finally, we aim to verify the observation that the gap between bridge signals associated with states of S_{Rmodul} (on and off) increases when the tag get closer to the centre of the RRA zones.

Experimental setup as shown in the **Figure 5-21** is considered. We utilised triangular bridge antenna along with commercial RFID tags and reader from Texas Instruments. The reader is connected to a desktop computer running windows based program to interact with the reader. We utilise the algorithm proposed in the previous section to acquire the bridge signals associated with the states of the S_{Rmodul} of the tags. We use magnetic field probes along with an oscilloscope for the signal acquisition so that the modulated signals from the tags, as well as the signals associated with bridge-arm1 and bridge-arm2 of the bridge reader antenna during data acquisition stage can be easily visualised.

For the first experiment, we let both the tags to be positioned at 5cm above plane of the antenna and they are equally spaced from the centre of the antenna. We denote the first and the second tag as tagA and tagB respectively. TagA is positioned at RRA1 while tagB is in RRA2 as indicated in the **Figure 5-21**. Using our second proposed algorithm as described previously, we acquire the bridge signals associated with the state of modulation switches of tagA and tagB.

Next, we position the tags with same elevation as in our first experiment, but now the tags are positioned above a line diagonal crossing two zones of the RRA. This line is indicated as dashed-grey in the **Figure 5-21**. The distances from the centre of the antenna to the tags are set to be equal. While varying these distances, we acquire bridge signals using our algorithm as described in the previous section.

Note that, in both the experiments, we utilise the proposed algorithm that is shown in **Figure 5-20** (b) and we use it until all the bridge signals associated with the states of tag load impedance are fully acquired, so that we can record these signals for post

processing. The acquired bridge signals are in the form of raw signals from bridge arm-1 ($v_{\beta 2}$) and bridge arm-2 ($v_{\beta 1}$), which need further processing.

(a)   (b)
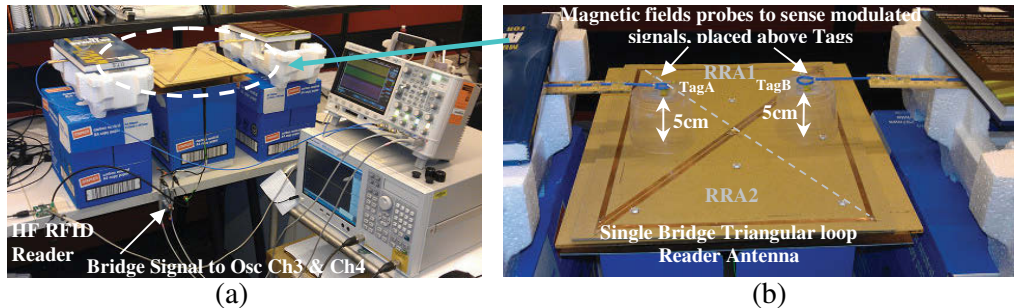
Figure 5-21: Experimental setup to investigate tag load modulation for localisation

Signals due to tag's load modulation

Ch1   Ch2

Modulation Signal from TagA   Modulation signal from TagB

(a)

Signal at bridge arm-1 (Osc Ch3)

(Load $=R_L \| R_{modul}$)   (Load $=R_L$)

(b)

Signal at bridge arm-1 (Osc Ch4)

(Load $=R_L \| R_{modul}$)   Ch4 (Load $=R_L$)

(c)
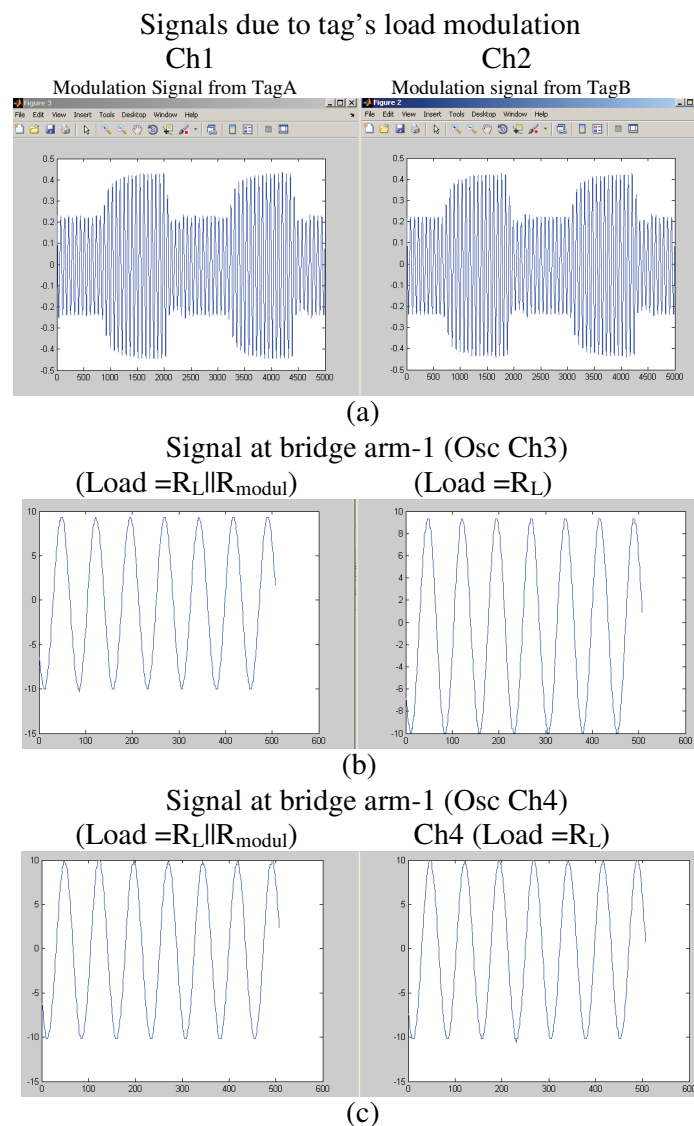
Figure 5-22: Modulated signals from tags and the raw signals at bridge arm-1 and arm-2

The modulated signals due to tag load modulation captured by the probes are indicated in the **Figure 5-22** (a). As can be seen, the modulated signals vary between two levels correspond to the states of the switch S_{Rmodul} viz., 'on' or 'off'. Within these two intervals of switching, signals at bridge arm-1 and arm-2 are recorded when the carrier reaches its steady state. It is important to acquire signals during the steady state (i.e. stable) period as to minimise errors.

Raw signals at arm-1 and arm-2 are also indicated as in **Figure 5-22** (b-c), to show that the acquired signals are stable. Note that bridge signal are obtained from these raw signals of bridge arm-1 ($v_{\beta1}$) and arm-2 ($v_{\beta2}$) using the expressions discussed earlier. These signals will be associated with ith detected tag, which is denoted as ($v_{\beta(1\ or\ 2)\_tagi}$) before offset removal, and denoted as ($V_{\beta(1\ or\ 2)\_tagi}$) after removing the offset.

5.7.1 Results

5.7.1.1 Bridge signal levels due to states of tagA and TagB
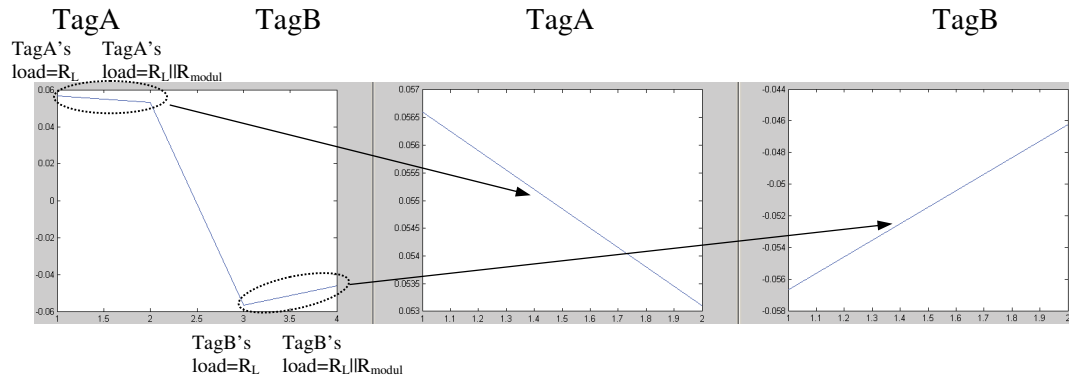
Figure 5-23: Variations in bridge signal due to states of tags

In **Figure 5-23**, it can be observed that the bridge signal due to the transition of the state of TagA (off to on) shows decreasing trend. This shows that the bridge signal moves from higher level to lower level when the S_{Rmodul} of tagA switched from 'off' state to 'on' state. On the other hand, the bridge signal for tagB shows increasing trend when the corresponding state $S_{Rmodule}$ of tagB transitions from 'off' state to 'on' state. This behaviour is consistent with our findings using equivalent circuit which is presented in section 5.3 as well as the results obtained from FEKO simulations

presented in section 5.4. It must be emphasised that FEKO simulation employ rigorous electromagnetic theory for the prediction.

In addition, these characteristics allow us to recognise whether the tag is located within RRA1 or RRA2. A tag whose bridge signal has a decreasing trends deemed to be located within RRA1 and vice versa. Our experimentation confirms this hypothesis that the bridge signals for tagA are showing decreasing trend, that tag is located within RRA1. On the other hand, when the bridge signal due to a tag shows an increasing trend, that tag should be located within RRA2, which is confirmed by our experimentation for tagB. These results, therefore reaffirm our initial hypothesis that the states of tags and their corresponding bridge signals can be useful to recognise the location of the tags with respect to their RRAs.

5.7.1.2 Refining the location of tag using the gap between states of tag

Results in Figure 5-24 show offset free bridge signals associated with tagA and tagB obtained using states of S_{Rmodul} of the corresponding tags. The bridge signals are derived from expression '$V_{\beta\_tagi} = Im(V_{\beta1\_tagi}/ V_{\beta1\_tagi})$'. Note that, this expression is considered because it can reduce the effect of proximity of surrounding metallic objects as shown previously.
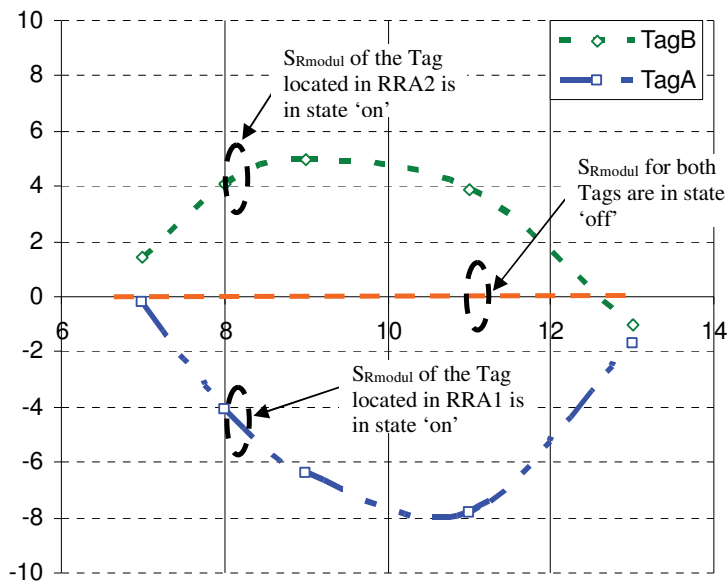
Figure 5-24: Offset free bridge signals that correspond to tagA and tagB

(Obtained using states of S_{Rmodul} of the corresponding tags)

The trend of the signals shows a useful feature that is comparable to those previously discussed in sections 5.3 and 5.4 using equivalent circuits and FEKO simulations. This, serves to validate our findings. In particular, it is stated that, the gap or difference in bridge signals between states of tags would increase when the tags get closer to the loop elements of the bridge antenna (i.e. to the centre of the loop element). This behaviour is indicated in the above experimental results for both the tagA and tagB as plotted in Figure 5-24. One can also find another useful pattern that allows one to determine the location/zone of RRA within which the tags are located from polarity of the signals. Bridge signal from tagA always has its signals that correspond to S_{Rmodul}=on is lower than when S_{Rmodul}=off (i.e. it has negative sign, or decreasing trend). On the hand, on an average, the bridge signal from tagB when its S_{Rmodul}='on' is always at higher level relative to its reference signal when S_{Rmodul}='off' (i.e. it has positive sign or increasing trend). Thus, the overall results from equivalent circuits, FEKO simulations and experimentations point towards the same conclusions as clearly discussed within this chapter.

5.8 Summary

In this chapter, we have discussed the characteristics of the impedance changes of a single loop as well as bridge reader antenna. The behaviour of the bridge signal due to tag's load modulation has also discussed. We have identified methods to effectively breakdown the bridge signals associated with multiple tags. Simple algorithms that can be used to obtain location and orientation using information from each tag are also presented.

Chapter 6

Conclusions

6.1 Overview

In this chapter, major conclusions based on the contribution made from this thesis are presented. Firstly, a summary of the work reported in chapters of the thesis is given. It is then followed by key of contributions that are brought out by each chapter. Finally, ideas for possible future extensions of the thesis are highlighted.

6.2 Summary of the thesis

This thesis presents a novel method to improve positioning and localisation of any moving object using HF RFID by introducing a new concept of bridge loop reader antennas. The key issue in question is as to how the reader recognition area (RRA) can be manipulated to improve HF RFID based positioning of moving autonomous wheelchair in indoor environments. For addressing various aspects of this issue, the relevant analysis and experimentations are divided into four main chapters (chapter-2 to chapter-5).

Chapter2

The concept of bridge antenna for HF RFID reader and how it can make changes to the reader recognition area is introduced in this chapter. The possible variations of bridge reader antenna configurations are identified, and both electromagnetic simulations and measurements on prototypes are carried out with the results plotted for analysis. The model used in electromagnetic simulations using FEKO are discussed. The practical issues in the design and fabrication of prototypes are presented. The bridge antenna performance in term of the induced H-Fields is evaluated at a plane on which tags are positioned and the resultant results of bridge potential signal are analysed. The comparison between simulation and measured results have shown good agreement confirming the usefulness of the concept of proposed bridge antenna. It is identified that the main aim of the proposed bridge

antenna is to split the reader recognition area into multiple zones without the need of multiple readers or switches so as to make the resultant system simple and cost effective.

Chapter3

This chapter describes the effect of proximity of metallic objects on the magnetic field produced by the bridge loop reader antenna. Equivalent circuits for induced magnetic fields for various scenarios that may occur in the localisation are proposed and methods to overcome the effects of metallic object on the bridge signals are suggested. The proposed techniques to improve the performance of the proposed bridge loop antenna have been validated using experimental campaigns and full wave electromagnetic simulations. The findings of this chapter help to improve the application of proposed bridge loop reader antenna for positioning and localisation of moving object even in the presence of metallic obstruction.

Chapter4

This chapter focuses on techniques of localisation of an autonomous wheelchair using HF RFID reader. Methods to improve the positioning when floor tags are sparse placed in a grid is investigated. Novel position and orientation algorithms are proposed which gain fully employ the bridge potential. The proposed system allows sparser floor tag infrastructure leading to lower cost and flexible tag deployment that can adapt to any indoor localisation scenarios. Simulation and experimental results and the comparison with existing techniques show significant improvement in positioning accuracy even for large tag separations, thus ensuring tag-grid sparcity. Our studies also indicate that for HF RFID based positioning, a larger reader recognition area may not necessarily cause higher uncertainties when the bridge antenna is employed.

Chapter5

In this chapter, the variation of the impedance due to tag's load modulation for a single loop reader antenna as well as the bridge loop antenna is investigated. Methods have been proposed to effectively identify the bridge signals associated with the tags when multiple tags are detected by the reader. Algorithms that can be

used to obtain location and orientation are presented for scenarios when tag-grid is not sparse. The findings in this chapter further improve the capability of HF RFID based positioning to quickly estimate the position and orientation of a moving object when it requires to be navigated while moving along a constrained indoor path without the need of additional sensors.

In general, all the chapters have addressed the applicability of the concept of bridge loop antenna for HF RFID based positioning of moving objects such as wheelchairs etc. that is useful for indoor positioning. The key design issues as well as methods for improvement have been investigated which resulted in novel algorithms that can effectively utilise the available information to provide navigation. In a nutshell, the proposed system overcomes the limitations of the existing techniques reported in literatures.

6.3 Summary of Original Contributions

The following are the summary of the contributions resulted during the period of PhD candidature.

1. *Manipulation and characterisation of the reader recognition area (RRA)*

Intensive analysis has been carried out considering the region of reader recognition area (RRA) that is able to reduce uncertainty in HF RFID based positioning. Our study on magnetic fields from various loop antennas that are employed in readers, has established that the RRA can be confined within a more stable and consistent area by inputting proper excitation current to the reader. This ensures that an optimum level of magnetic field is produced to interrogate the chosen floor tags that are located within the desired RRA. This original contribution has led to many other contributions as described below.

2. *The use of bridge potential for finding the position*

This is one of the key contributions of this thesis. For the first time in the open literature, a bridge potential and its realisation using bridge loop antennas for improving localisation is reported in this thesis. This concept brings significant improvement for HF RFID based positioning and localisation as demonstrated by various measurements and simulations in this thesis. In addition, methods for

increasing the positioning accuracy in terms of estimation of position as well as orientation of an object using RFID tags are also proposed in this thesis. Use of bridge potential allowed the use of lesser number of floor tags (by increasing the inter tag separation) while at the same time not reducing the levels of positioning accuracy. The use of lesser number of tags (sparse tag grid) simplifies the deployment, which contributes to easier expansion of the tag infrastructure.

3. *Investigation of different types of bridge antennas*

In this thesis, we have also proposed different types of bridge antennas for obtaining the bridge potential. The bridge antennas are classified in terms of the number of bridges used as well as the shape of the individual loop elements. Three types of bridge antenna models and their prototypes have been presented, they are: i) Single bridge rectangular loop reader antenna; ii) Single bridge triangular loop antenna; and iii) Multi bridge loop antenna in the form of (dual bridge rectangular loop). Their performances in term of the levels of magnetic fields radiated and the bridge signal produced have also been evaluated.

4. *Equivalent circuits to study the performance of the bridge antenna*

We proposed equivalent circuits for the study of bridge antenna. The equivalent circuits are significantly useful to study the behaviour of loop antennas and bridge potential. In particular, they help to simplify the understanding of the bridge signal produced by bridge loop antennas, and avoid complex computations. Our results show that the equivalent circuits agree well with full-wave electromagnetic simulations on realistic models and environments using the commercial simulation tool known as FEKO.

5. *Methods to improve bridge antenna performance to reduce interference from surrounding metallic objects*

For indoor localisation of moving objects, the interference due to surrounding metallic objects is of concern. We proposed methods to identify and remove interference from metallic structures have resulted in well help to produce the usable bridge potential signal even in the presence of interferences. This interesting finding helps to make positioning and localisation more reliable in realistic indoor environments where metallic objects are usually present.

6. *Algorithms for Position and orientation estimations*

Algorithms for position and orientation estimations using information from RFID reader and the bridge potential signal from bridge antenna have been proposed to perform with either densely or sparsely placed tags. The proposed algorithms have been tested using measurements made in a real indoor environment. Detailed comparison with the existing techniques in literature demonstrates the superiority of our proposed methods in localisation. As indicated in the table below, the proposed method offers 79% improvement in positioning accuracy as compared to 52% and 65% achieved by recently published methods in [13] and [23] respectively. In addition to that, the proposed technique is advantageous as it can work with sparser floor tag grid in which larger inter-tag separation. A comparison with existing methods reveal that the technique can work even when inter tag separation is 130cm as indicated in the table. The main reason for the significant improvement is that the proposed technique utilises the bridge potential signal. This comparison indicates that the proposed technique can be highly useful in improving HF RFID based localisation and positioning especially in indoor environments.

Table 6-1: Performance comparison between the proposed method versus methods in recent literature.

Positioning Methods	Tag separation (d_{tag} cm)	Improvement over maximum uncertainty using min-max method (Equations 1-2) in [11]. (%)
Sunhong's [13]	34	52
Choi et al [105] repeated in [23] at sparser tag separation, (RFID system + Encoder)	50	65
Our proposed method presented in chapter-4	**130**	**79**

7. *Methods to incorporate object dynamics with HF RFID measurement*

We proposed methods to incorporate the information on object dynamics (which is derived from wheel encoders of a moving vehicle) to further optimise the

performance of the system. The implementation of this technique does not require additional hardware. When a moving object to be localised is equipped with a wheel encoder, the proposed algorithm has the capability to utilise the information from wheel encoder to further improve the positioning accuracy of the object. The algorithm is unique as compared to any existing techniques in literature because of the utilisation of temporal potential bridge signals. The algorithm uses the recently recorded position by the RFID reader, and the wheel encoder data is taken for a short travelled distance i.e. about the distance between current and previous detected tags. Thus, the errors associated with wheel encoder data are minimised. Improvements in orientation estimation using the proposed technique as compared to the recently published method in literature [12] is indicated in table below.

Table 6-2: Comparison for estimation of heading angle/orientation between the proposed method versus conventional method

Estimation methods	Average values
	Orientation Error (Degree)
Method by S. Park [12]	14.80
Proposed method with bridge-loop antenna	4.51

8.   *Improving HF RFID based positioning using tag's load modulation*

We have shown that tag's load modulation can be useful to improve positioning with HF RFID with bridge loop antenna when multiple tags are present within RRA of the bridge reader antenna. In particular, we have shown that, the difference between two levels of bridge signals associated with the states of tags is useful for identifying the location of the detected tags, either they are within RRA1, or within RRA2. Methods to acquire bridge signals under this mode of operation are also presented.

9.   *Methods to separate bridge signals when multiple tags are detected*

When multiple tags are present, the positioning with bridge antenna gets complicated because information from all tags is available simultaneously which prevents use of the resultant bridge signal directly. Our proposed method separates the bridge potential signals from each tag which helps to extend the capability of the

HF RFID based system. It then allows instantaneous position estimation to be obtained with much better accuracy and more importantly, it also improves the orientation estimation. This can be useful when the object has to move within a constrained path (such as narrow corridor etc.) where accurate positioning is required.

10. Validation of the techniques through experimentations

Significant efforts have been devoted to design and fabricate experimental prototypes to validate the proposed concepts. The techniques and the algorithms have been validated using measurements in realistic metal floored indoor environments.

6.4 Scope for future work

The works reported in this thesis can be further extended as below:

1. Investigation for arbitrary shaped loops for use with either a single bridge or multiple bridges for HF RFID reader antennas

In this thesis, we only consider rectangular and triangular shapes for the loop elements. It is interesting to investigate other loop shapes (which can be arbitrary in shape) and at the same time considering using them with multiple bridges. This can be useful if one wants to maximise the size and shape of the reader recognition area (RRA).

2. Evaluate the concept of bridge antenna for higher frequencies such as UHF

This is another interesting topic to be considered. It possesses great challenges because the current within the loop need to be almost constant at any instant of time which is relatively easier to achieve at lower frequencies than UHF.

3. Integration of both short range and long range RFID for positioning systems

The combination of HF RFID and UHF RFID can bring improvements to the system since the two technologies could complement each other's limitations and strengths.

4. Investigate the use of bridge antenna for specific design applications such as portals, conveyers, item sorting systems, etc

The proposed concept of bridge antenna is novel and has not yet been fully investigated on other areas of localisations. In this thesis we highlighted the general concept and demonstrated using application in positioning. It however can be extended for other areas which can benefit from the concept.

References

[1]   T. Taleb, D. Bottazzi, M. Guizani *et al.*, "Angelah: a framework for assisting elders at home," *IEEE Journal on Selected Areas in Communications,* vol. 27, no. 4, pp. 480-494, 2009.

[2]   N. Min-Young, Z. Al-Sabbagh, K. Jung-Eun *et al.*, "A Real-Time Ubiquitous System for Assisted Living: Combined Scheduling of Sensing and Communication for Real-Time Tracking," *IEEE Transactions on Computers,* vol. 57, no. 6, pp. 795-808, 2008.

[3]   L. Hyo-nam, L. Sung-hwa, and K. Jai-hoon, "UMONS: Ubiquitous monitoring system in smart space," *IEEE Transactions on Consumer Electronics,* vol. 55, no. 3, pp. 1056-1064, 2009.

[4]   F. Dramas, B. Oriola, B. G. Katz *et al.*, "Designing an assistive device for the blind based on object localization and augmented auditory reality." pp. 263-264.

[5]   J. Symonds, D. Parry, and J. Briggs, "An RFID-based system for assisted living: Challenges and Solutions," *The Journal on Information Technology in Healthcare,* vol. 5, no. 6, pp. 387-398, 2007.

[6]   D. Parry, and J. Symonds, "RFID and Assisted Living for the Elderly," *Auto-Identification and Ubiquitous Computing Applications*, J. Symonds, J. Ayoade and D. Parry, eds., pp. 119-136: Hershey, PA : Information Science Reference, 2009.

[7]   L. Chung-Chih, L. Ping-Yeh, L. Po-Kuan *et al.*, "A Healthcare Integration System for Disease Assessment and Safety Monitoring of Dementia Patients," *IEEE Transactions on Information Technology in Biomedicine,* vol. 12, no. 5, pp. 579-586, 2008.

[8]   C. Byoung-Suk, and L. Ju-Jang, "Mobile robot localization scheme based on RFID and sonar fusion system." pp. 1035-1040.

[9]   L. Hyun-Jeong, K. Moon Sik, and L. Min Cheol, "Technique to correct the localization error of the mobile robot positioning system using an RFID." pp. 1506-1511.

[10]   K. Sungbok, "RFID tag arrangement for mobile robot localization." pp. 621-624.

[11]   S. Han, H. S. Lim, and J. M. Lee, "An efficient localization scheme for a differential-driving mobile robot based on RFID system," *IEEE Trans. Ind. Electron.,* vol. 54, no. 6, pp. 3362-3369, Dec., 2007.

[12]   S. Park, and S. Hashimoto, "Autonomous mobile robot navigation using passive RFID in indoor environment," *IEEE Trans. Ind. Electron.,* vol. 56, no. 7, pp. 2366-2373, Jul., 2009.

[13]   S. Park, and S. Hashimoto, "An intelligent localization algorithm using read time of RFID system," *Adv. Eng. Inform., Elsevier,* vol. 24, no. 4, pp. 490-497, Oct., 2010.

[14]   D. McGookin, M. Gibbs, A. Nivala *et al.*, "Initial Development of a PDA Mobility Aid for Visually Impaired People," *Human-Computer Interaction–INTERACT*, pp. 665-668, 2009.

[15]   J. D. Griffin, and G. D. Durgin, "Complete Link Budgets for Backscatter-Radio and RFID Systems," *IEEE, Antennas and Propagation Magazine,* vol. 51, no. 2, pp. 11-25, 2009.

[16]   W. Gueaieb, and M. S. Miah, "An Intelligent Mobile Robot Navigation Technique Using RFID Technology," *IEEE Transactions on Instrumentation and Measurement,* vol. 57, no. 9, pp. 1908-1917, 2008.

[17]   V. Renaudin, O. Yalak, P. Tomé *et al.*, "Indoor navigation of emergency agents," *European Journal of Navigation,* vol. 5, no. 3, pp. 36-45, 2007.

[18]   D. Rose-Marie, M. Maurice, N. Chris *et al.*, "Healthcare Systems and Other Applications," *Pervasive Computing, IEEE,* vol. 6, no. 1, pp. 59-63, 2007.

[19]   P. Peom, and M. Kyongpil, "Development of the Wellbeing Life Support System in Ubiquitous." pp. 1108-1115.

[20]   O. Matsumoto, K. Komoriya, T. Hatase *et al.*, "Intelligent Wheelchair Robot "TAO Aicle"," *Service Robot Applications, Yoshihiko Takahashi (Ed.)*, 2008.

[21]   S. P. Levine, D. A. Bell, L. A. Jaros *et al.*, "The NavChair assistive wheelchair navigation system," *IEEE Transactions on Rehabilitation Engineering,* vol. 7, no. 4, pp. 443-451, 1999.

[22]   R. C. Simpson, D. Poirot, and F. Baxter, "The Hephaestus smart wheelchair system," *IEEE Transactions on Neural Systems and Rehabilitation Engineering,* vol. 10, no. 2, pp. 118-122, 2002.

[23]   B. S. Choi, J. W. Lee, J. J. Lee *et al.*, "A hierarchical algorithm for indoor mobile robot localization using RFID sensor fusion," *IEEE Trans. Ind. Electron.,* vol. 58, no. 6, pp. 2226-2235, Jun., 2011.

[24]   W. Gueaieb, and M. S. Miah, "A Modular Cost-Effective Mobile Robot Navigation System Using RFID Technology," *Journal of Communications,* vol. 4, no. 2, pp. 89, 2009.

[25]   T. Asakawa, K. Nishihara, and T. Yoshidome, "A Detection System of Location and Direction Angle by a RF Tag Reader Using a Rotary Antenna," *Journal of Robotics and Mechatronics,* vol. 20, no. 1, pp. 189-195, 2008.

[26]   E. DiGiampaolo, and F. Martinelli, "A Passive UHF-RFID System for the Localization of an Indoor Autonomous Vehicle," *IEEE Trans. Ind. Electron.,* vol. 59, no. 10, pp. 3961-3970, Oct., 2012.

[27]   R. Siragusa, P. Lemaitre-Auger, A. Pouzin *et al.*, "RFID tags localization along an axis using a tunable near-field focused circular-phase array antenna." pp. 1-4.

[28]   L. M. Ni, Z. Dian, and M. R. Souryal, "RFID-based localization and tracking technologies," *Wireless Communications, IEEE,* vol. 18, no. 2, pp. 45-51, 2011.

[29]   Y. Senta, Y. Kimuro, S. Takarabe *et al.*, "Self-localization for mobile robots using RFID tags without layout information," *Electrical Engineering in Japan,* vol. 172, no. 4, pp. 19-30, 2010.

[30]   H. Sanming, Z. Yuan, L. Choi Look *et al.*, "Study of a Uniplanar Monopole Antenna for Passive Chipless UWB-RFID Localization System," *IEEE Transactions on Antennas and Propagation,* vol. 58, no. 2, pp. 271-278, 2010.

[31]   T. Jingwangsa, S. Soonjun, and P. Cherntanomwong, "Comparison between innovative approaches of RFID based localization using fingerprinting techniques for outdoor and indoor environments." pp. 1511-1515.

[32]   A. Almaaitah, K. Ali, H. S. Hassanein *et al.*, "3D Passive Tag Localization Schemes for Indoor RFID Applications." pp. 1-5.

[33]   P. Vorst, and A. Zell, "Semi-autonomous learning of an RFID sensor model for mobile robot self-localization," *European Robotics Symposium 2008*, Springer Tracts in Advanced Robotics H. Bruyninckx, L. Přeučil and M. Kulich, eds., pp. 273-282: Springer Berlin Heidelberg, 2008.

[34]   C. L. Huang, P. C. Chung, M. H. Tsai *et al.*, "Reliability improvement for an RFID-based psychiatric patient localization system," *Computer Communications,* vol. 31, no. 10, pp. 2039-2048, 2008.

[35]   W. Ching-Sheng, and W. Shyh-Shyan, "An adaptive RFID localization mechanism supporting 3D virtual tour system." pp. 219-224.

[36]   C. Byoung-Suk, L. Joon-Woo, and L. Ju-Jang, "An improved localization system with RFID technology for a mobile robot." pp. 3409-3413.

[37]   M. Bouet, and A. L. dos Santos, "RFID tags: Positioning principles and localization techniques." pp. 1-5.

[38]   Yimin Zhang, Moeness G. Amin, and and Shashank Kaushik, "Localization and Tracking of Passive RFID Tags Based on Direction Estimation," *International Journal of Antennas and Propagation* vol. 2007, pp. 1-9, 2007.

[39]   S. Schneegans, P. Vorst, and A. Zell, "Using RFID snapshots for mobile robot self-localization." pp. 241-246.

[40]   X. Huang, R. Janaswamy, and A. Ganz, "Scout: Outdoor Localization Using Active RFID Technology." pp. 1-10.

[41]   T. Deyle, N. Hai, M. S. Reynolds *et al.*, "RFID-Guided Robots for Pervasive Automation," *Pervasive Computing, IEEE,* vol. 9, no. 2, pp. 37-45, 2010.

[42]   Harvey Lehpamer, *RFID Design Principles*, Boston, London,: Artech House, 2008.

[43]   American National Standard, "RFID HIBC for Product Identification," 2009.

[44]   Y. Senta, Y. Kimuro, S. Takarabe *et al.*, "Machine learning approach to self-localization of mobile robots using RFID tag." pp. 1-6.

[45]   J. W. Lee, D. H. T. Vo, Q. H. Huynh *et al.*, "A fully integrated HF-band passive RFID tag IC using 0.18-um CMOS technology for low-cost security applications," *IEEE Trans. Ind. Electron. ,* vol. 58, no. 6, pp. 2531-2540, Jun., 2011.

[46]   Y. H. Kim, Y. C. Choi, M. W. Seo *et al.*, "A CMOS transceiver for a multistandard 13.56-MHz RFID reader SoC," *IEEE Tran. Ind. Electron. ,* vol. 57, no. 5, pp. 1563-1572, May, 2010.

[47]   Y. Li, J. Liu, and H. Lee, "Ground Switching Load Modulation With Ground Isolation for Passive HF RFID Transponders," *IEEE Trans. Very Large Scale Integrat. Syst. ,* Future Issue., 2011.

[48]   C. Angerer, and M. Rupp, "Advanced synchronisation and decoding in RFID reader receivers." pp. 59-62.

[49]   Y. Li, J. Liu, and H. Lee, "Ground switching load modulation with ground isolation for passive HF RFID transponders," *IEEE Trans. Very Large Scale Integrat. Syst.,* vol. 20, no. 8, pp. 1443-1452, Aug., 2012.

[50]   J. Bing, J. R. Smith, M. Philipose *et al.*, "Energy Scavenging for Inductively Coupled Passive RFID Systems," *IEEE Transactions on Instrumentation and Measurement,* vol. 56, no. 1, pp. 118-125, 2007.

[51]   K. Finkenzeller, *RFID handbook: fundamentals and applications in contactless smart cards and identification*: John Wiley & Sons Inc, 2003.

[52]   K. Jikon, K. Hyunsik, K. Jaewhan *et al.*, "13.56MHz RFID reader SiP with embedded antenna." pp. 186-189.

[53]   G. Antonelli, S. Chiaverini, and G. Fusco, "A calibration method for odometry of mobile robots based on the least-squares technique: theory and experimental validation," *IEEE Trans. Robot.,* vol. 21, no. 5, pp. 994-1004, Oct., 2005.

[54]   A. R. Jimenez Ruiz, F. Seco Granja, J. C. Prieto Honorato *et al.*, "Accurate pedestrian indoor navigation by tightly coupling foot-mounted IMU and RFID measurements," *IEEE Trans. Instr. Measurements.,* vol. 61, no. 1, pp. 178-189, Jan., 2012.

[55]   G. Antonelli, S. Chiaverini, and G. Fusco, "A calibration method for odometry of mobile robots based on the least-squares technique: Theory and experimental validation," *IEEE Transactions on Robotics,* vol. 21, no. 5, pp. 994-1004, 2005.

[56]   J. Borenstein, and L. Feng, "Gyrodometry: A new method for combining data from gyros and odometry in mobile robots." pp. 423-428.

[57]   S. Jia, J. Sheng, and K. Takase, "Obstacle recognition for a service mobile robot based on RFID with multi-antenna and stereo vision." pp. 125-130.

[58]   A. Milella, P. Vanadia, G. Cicirelli *et al.*, "RFID-based environment mapping for autonomous mobile robot applications." pp. 1-6.

[59]   K. Chawla, and G. Robins, "An RFID-based object localisation framework," *Int. J. Radio Freq. Ident. Tech. Appl.,* vol. 3, no. 1/2, pp. 2-30, 2011.

[60]   A. Milella, D. Di Paola, G. Cicirelli *et al.*, "RFID tag bearing estimation for mobile robot localization." pp. 1-6.

[61]   M. Z. Buehrer, Seyed A., *Handbook of Position Location: Theory, Practice and Advances.*: Wiley-IEEE Press, 2012.

[62]   S. S. Saad, and Z. S. Nakad, "A Standalone RFID Indoor Positioning System Using Passive Tags," *IEEE Trans. Ind. Electron.,* vol. 58, no. 5, pp. 1961-1970, May, 2011.

[63]   S. Park, and H. Lee, "Self-recognition of Vehicle Position using UHF Passive RFID Tags," *IEEE Trans. Ind. Electron. ,* Future Issue., 2012.

[64]   J. L. M. Flores, S. S. Srikant, B. Sareen *et al.*, "Performance of RFID tags in near and far field." pp. 353-357.

[65]   L. W. Mayer, and A. L. Scholtz, "A Dual-Band HF / UHF Antenna for RFID Tags." pp. 1-5.

[66]   P. Yang, W. Wu, M. Moniri *et al.*, "Efficient Object Localisation Using Sparsely Distributed Passive RFID Tags," *IEEE Trans. Ind. Electron.,* vol. -, no. - Future Issue, pp. -, 2013.

[67]   J. Bohn, and F. Mattern, "Super-distributed RFID tag infrastructures," *Ambient Intelligence*, pp. 1-12, 2004.

[68]   J. Bohn, "Prototypical implementation of location-aware services based on a middleware architecture for super-distributed RFID tag infrastructures," *Personal and Ubiquitous Computing,* vol. 12, no. 2, pp. 155-166, 2008.

[69]   P. Youngsu, L. Je Won, K. Daehyun *et al.*, "Mathematical formulation of RFID tag floor based localization and performance analysis for tag placement." pp. 1547-1552.

[70]   K. Kodaka, H. Niwa, and S. Sugano, "Reader placement design for two wheeled robots on floor-installed RFID system - Extracting backward sensing problem." pp. 204-210.

[71]   D. S. Seo, D. Won, G. W. Yang *et al.*, "A probabilistic approach for mobile robot localization under RFID tag infrastructures." pp. 1797-1801.

[72]   S. Han, J. Kim, C. H. Park *et al.*, "Optimal detection range of RFID tag for RFID-based positioning system using the k-NN algorithm," *Sensors,* vol. 9, no. 6, pp. 4543-4558, Jun., 2009.

[73]   C. A. Balanis, *Antenna theory analysis and design*: Wiley New York, 2005.

[74]   B. Levin, "Field of a rectangular loop," *IEEE Transactions on Antennas and Propagation,* vol. 52, no. 4, pp. 948-952, 2004.

[75]   L. W. Li, C. P. Lim, and M. S. Leong, "Near fields of electrically small thin square and rectangular loop antennas," *Progress In Electromagnetics Research,* vol. 31, pp. 181-193, 2001.

[76]   L. Le-Wei, L. Mook-Seng, K. Pang-Shyan *et al.*, "Exact solutions of electromagnetic fields in both near and far zones radiated by thin circular-loop antennas: a general representation," *Antennas and Propagation, IEEE Transactions on,* vol. 45, no. 12, pp. 1741-1748, 1997.

[77]   C. T. Tai, *Dyadic Green functions in electromagnetic theory*: IEEE press New York, 1994.

[78]   M. R. Abdul-Gaffoor, H. K. Smith, A. A. Kishk *et al.*, "Comments on Exact solutions of electromagnetic fields in both near and far zones radiated by thin circular loop antennas: a general representation & [and reply]," *Antennas and Propagation, IEEE Transactions on,* vol. 49, no. 5, pp. 845-847, 2001.

[79]   C. Cho, J. Ryoo, I. Park *et al.*, "Design of a novel ultra-high frequency radio-frequency identification reader antenna for near-field communications using oppositely directed currents," *Microwaves, Antennas & Propagation, IET,* vol. 4, no. 10, pp. 1543-1548, 2010.

[80]   "FEKO EM Software & Systems S.A., (Pty) Ltd: 32 Techno Lane, Technopark, Stellenbosch, South Africa."

[81]   C. A. Balanis, "Antenna theory: a review," *Proceedings of the IEEE,* vol. 80, no. 1, pp. 7-23, 1992.

[82]   D. H. Werner, "An exact integration procedure for vector potentials of thin circular loop antennas," *IEEE Transactions on Antennas and Propagation,* vol. 44, no. 2, pp. 157-165, 1996.

[83]   P. L. Overfelt, "Near fields of the constant current thin circular loop antenna of arbitrary radius," *IEEE Transactions on Antennas and Propagation,* vol. 44, no. 2, pp. 166-171, 1996.

[84]   W. Aerts, E. De Mulder, B. Preneel *et al.*, "Dependence of RFID reader antenna design on read out distance," *IEEE Trans. Antennas Propag.,* vol. 56, no. 12, pp. 3829-3837, Dec., 2008.

[85]   X. Qing, and Z. N. Chen, "Characteristics of a metal-backed loop antenna and its application to a high-frequency RFID smart shelf," *IEEE Antenna Propag. Magazine.,* vol. 51, no. 2, pp. 26-38, Apr., 2009.

[86]   M. Y. Ahmad, and A. S. Mohan, "Multi-loop Bridge HF RFID Reader Antenna for Improved Positioning." pp. 1426-1429.

[87]   M. Y. Ahmad, and A. S. Mohan, "Multiple-bridge-loop reader antenna for improved positioning and localisation," *Electronics Letters,* vol. 48, no. 16, pp. 979-980, Aug., 2012.

[88]   M. Ahmad, and A. Sanagavarapu, "Novel Bridge-Loop Reader for Positioning with HF RFID under Sparse Tag Grid," *IEEE Transactions on Industrial Electronics*, no. Future Issue, 2013.

[89]   M. Y. Ahmad, and A. S. Mohan, "Multi-Loop-Bridge Antenna for Improved Positioning Using HF-RFID." pp. 1-2.

[90]   R. Pallas-Areny, J. G. Webster, and R. Areny, *Sensors and signal conditioning*: Wiley New York, 2001.

[91]   T. Instruments, *Tag-it™ HF-I Pro Transponder Inlays Reference Guide*.

[92]   International Standard, "ISO15693-2."

[93]   *13.56 MHz RFID systems and antennas design guide*, Melexis Microelectronic Integrated System, , 2004.

[94]   K. D'Hoe, A. Van Nieuwenhuyse, G. Ottoy *et al.*, "A New Low-Cost HF RFID Loop Antenna Concept for Metallic Environments." pp. 1-5.

[95]   X. Qing, and Z. N. Chen, "Proximity Effects of Metallic Environments on High Frequency RFID Reader Antenna: Study and Applications," *IEEE Transactions on Antennas and Propagation,* vol. 55, no. 11, pp. 3105-3111, 2007.

[96]   L. Ukkonen, L. Sydanheimo, and M. Kivikoski, "Effects of metallic plate size on the performance of microstrip patch-type tag antennas for passive RFID," *IEEE Antennas and Wireless Propagation Letters,* vol. 4, pp. 410-413, 2005.

[97]   J. Koh Wee, H. Tan Joo, and K. C. H. Ernest, "High frequency (HF) suppression with a shielded fence." pp. 638-641.

[98]   "Tata Steel Europe," Ref: http://www.tatasteelconstruction.com/.

[99]   C. Reinhold, P. Scholz, W. John *et al.*, "Efficient antenna design of inductive coupled RFID-systems with high power demand," *Journal of Communications,* vol. 2, no. 6, pp. 14-23, 2007.

[100]   M. N. O. Sadiku, *Elements of electromagnetics*: Oxford university press, 2001.

[101]   D. K. Cheng, *Field and wave electromagnetics*, 2 ed.: Addison-Wesley, 1989.

[102]   H. Hirayama, N. Kikuma, and K. Sakakibara, "A new scheme to avoid null zone for HF-band RFID with diversity combining of loop antennas," *IEICE Trans. Comm.,* vol. 93, no. 10, pp. 2666-2669, Oct., 2010.

[103]   K. Kodaka, H. Niwa, Y. Sakamoto *et al.*, "Pose estimation of a mobile robot on a lattice of RFID tags." pp. 1385-1390.

[104]   Texas_Instruments, "TRF7960 Evaluation Module ISO 15693 Host Commands," http://www.ti.com/lit/an/sloa141/sloa141.pdf, 2008)].

[105]   B. S. Choi, J. W. Lee, and J. J. Lee, "Localization and map-building of mobile robot based on RFID sensor fusion system." pp. 412-417.

[106]   K. A. Josh Wyatt, Andre Frantzke, Peter Reiser, *TRF7960A Reference Firmware Description*, TEXAS INSTRUMENTS, 2011.